DEPARTMENT OF NEUROSCIENCES, BIOMEDICINE AND MOVEMENT SCIENCES

Ph.D. Life and Health Sciences School
Biomolecular Medicine Program

Cycle XXX

S.S.D. BIO/10

Thesis:

Chronic hypoxia induces dormancy in breast cancer cell line MDA-MB-231

Coordinator: Prof.ssa Lucia De Franceschi

_____

Tutor: Prof.ssa Sofia Giovanna Mariotto

_____

Co-tutor: Dr.ssa Elena Butturini

_____

Candidate: Dr. Michele Rossin

_____

INDEX

SOMMARIO

Il microambiente tumorale, ossia l'insieme di cellule e componenti extracellulari che si sviluppano attorno ad un tumore solido, non solo partecipa attivamente alla progressione del tumore stesso, ma anche contribuisce allo sviluppo della chemioresistenza e alla comparsa di metastasi. A causa della struttura anomala dei vasi sanguigni e della rapida proliferazione delle cellule tumorali, l'ambiente tumorale è in alcune parti caratterizzato da zone di parziale o totale ipossia. Sebbene gran parte delle cellule tumorali non sopravviva in queste condizioni ipossiche, una parte di esse si adatta, entrando in uno stato di dormienza, una particolare fase della progressione del tumore, in cui le cellule presentano un basso flusso metabolico e sono bloccate nella fase G0/G1 del ciclo cellulare. Queste cellule possono restare quiescenti per molto tempo senza dare sintomi clinici, sfuggire alle terapie e in condizioni ambientali appropriate ricominciare a proliferare dando origine a metastasi.

Sebbene molti dati sperimentali e clinici individuino nella dormienza uno dei principali responsabili della formazione di metastasi e del fallimento di alcune chemioterapie, tale fenomeno rimane un processo non ancora completamente chiarito in quanto sono presenti pochi modelli cellulari *in vitro* che permettono di definire le risposte biologiche delle cellule dormienti.

In questo lavoro, esponendo la linea cellulare umana di tumore al seno MDA-MB-231 ad almeno 3 cicli di ipossia (1% O_2) e successiva riossigenazione, abbiamo selezionato una sub-popolazione di cellule resistenti all'ipossia. Tali cellule, chiamate chMDA-MB-231, coltivate in ipossia per lungo tempo sopravvivono, entrando in uno stato di dormienza.

La trasformazione delle cellule MDA-MB-231 in chMDA-MB-231 è legato alla diminuzione del rapporto p-ERK/p-p38, uno dei principali *switch* molecolari della dormienza in un microambiente avverso descritti in letteratura. Questo stato di dormienza è reversibile poiché, una volta rimesse le cellule in normossia, la proliferazione riprende in 2 settimane.

Inoltre, i risultati ottenuti dimostrano che lo stress indotto da diversi cicli di ipossia e riossigenazione ha selezionato cellule con un fenotipo staminale $CD24^-/CD44^+/ESA^+$ e caratterizzate dalla capacità di formare sferoidi.

Infine, le cellule chMDA-MB-231 sopravvivono in queste condizioni di dormienza attivando il processo autofagico in quanto presentano alti livelli di autofagolisosomi e della proteina LC3-II.

In conclusione, il modello presentato rappresenta un valido approccio sperimentale per selezionare cellule dormienti caratterizzate da marcatori di staminalità tumorale utile per lo sviluppo di nuovi agenti chemioterapici che possano colpire tali cellule, impedendo loro di formare metastasi, o renderle maggiormente sensibili ai chemioterapici.

ABSTRACT

The tumor microenvironment (TME) is recognized as a key factor in multiple stages of disease progression, local resistance, immune-escaping and metastasis. TME is the product of developing crosstalk between different cells types and components, which provide an essential communication network through the secretion of growth factors and chemokines, and induce oncogenic signals enhancing cancer-cell proliferation and invasion.

The rapid proliferation of tumor cells and the aberrant structure of the blood vessels within tumors result in a marked heterogeneity in the perfusion of the tumor tissue with regions of low oxygen or hypoxia. Although most of the tumor cells die in these hypoxic conditions, a part of them can adapt and survive for many days or months in a dormant state. Dormant tumor cells are characterized by cell cycle arrest in G0/G1 phase as well as low metabolism and, are refractive to common chemotherapy giving rise to metastasis. Despite these features, the cells retain their ability to proliferate when conditions improve.

Exposing human breast cancer cell line exposure MDA-MB-231 to at least three cycles of 1% O_2 hypoxia and reoxygenation, we select a subpopulation of hypoxia resistant cells. These cells, designed as chMDA-MB-231, stably survive under 1% O_2 hypoxia condition by entering in dormant state. The reprogramming of cells into tumor dormancy results from the low p-ERK/p-p38 ratio that is described as the molecular switch of tumor dormancy in restrictive environment. This dormant state is reversible since once replaced in normoxia the cells recover the

proliferation rate in 2 weeks. Moreover, the data in this thesis demonstrate that cycling hypoxic/reoxygenation stress selects dormant MDA-MB-231 cells that present the cancer stem-like phenotype characterized by $CD24^{-}/CD44^{+}/ESA^{+}$ expression and spheroid forming capacity.

Different reports recognize autophagy as a mechanism activated by microenvironment stresses that may contribute to survival of cells in tumor dormancy. Interestingly, we found that chMDA-MB-231 cells have a high level of autophagy, as measured by the detection of autophagolysome and LC3-II expression, suggesting that autophagy may be the survival mechanism of dormant chMDA-MB-231 cells.

We believe that the proposed experimental approach to select dormant breast cancer cells could provide a rationale for the development of novel agents to target dormant tumor cells population.

1. INTRODUCTION

1.1 Tumor microenvironment

For many years, cancer has been considered a complex disease driven by genetic mutations and genomic instability. It is now clear that cancers are not just masses of malignant cells but also intricate organs, to which cells are recruited and interaction between malignant and non-transformed cells contributes to the development and progression of cancer itself.

Tumor microenvironment (TME) is comprised of a complex network of components that are not mere bystanders, but regulate tumor initiation, malignant progression and metastasis and has profound effects on therapeutic efficacy (1). These elements can be widely classified into three main groups: (*i*) cells of haematopoietic origin, (ii) cells of mesenchymal origin and (*iii*) non-cellular components (Figure 1) (2). First, cells of haematopoietic origin arise in the bone marrow and can be subdivided into cells of lymphoid lineage consisting of T cells, B cells, natural killer cells, and those of the myeloid lineage, which include macrophages, neutrophils and myeloid-derived suppressor cells. The different subsets of cells have either positive or negative effects on the outcome of the tumor. Importantly, interactions between cell types within the stroma can also have a major role in tumor progression, as has been shown, for example for $CD4^+$ T cells and macrophages (3).

Then, cells of mesenchymal origin derive from the mesenchyme and include fibroblasts, myofibroblasts, mesenchymal stem cells, adipocytes and endothelial cells. Myofibroblast and mesenchymal stem cells directly support cancer stem cells (CSCs) by creating a favorable niche and facilitating tumor progression, while endothelial cells constitute the walls of blood vessels and have a major role in vascular functionally and angiogenesis. So far, adipocytes were thought only as energy storage houses; however, recent studies have revealed the importance of factors secreted by adipocytes in tumor progression (1).

Finally, the extracellular matrix, the major non-cellular component of the TME, is involved in the formation of a stem cell niche. Although it acts to maintain tissue

architecture and prevent cancer cells formation, an abnormal ECM has been shown to promote tumor growth and angiogenesis (4).

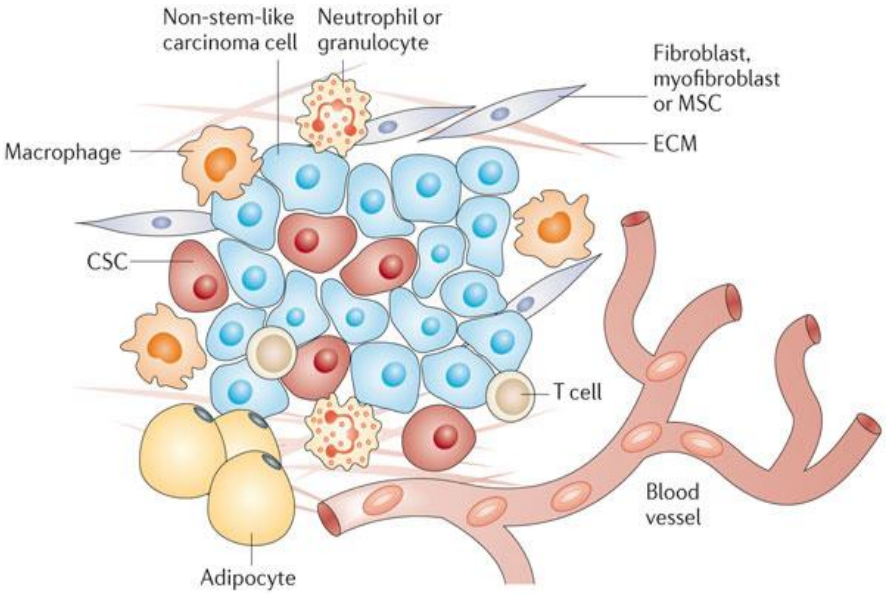

Figure 1. Components of tumor microenvironment. In TME there are *cells of hematopoietic origin* (T-cells, B-cells and NK-cells), *cells of myeloid lineage* (macrophages, neutrophils and myeloid-derived suppressor cells), *cells of mesenchymal origin* (fibroblasts, myofibroblasts, mesenchymal stem cells –MSCs-, adipocytes, endothelial cells and extracellular matrix (ECM). *Image taken from: "What constitutes the tumor microenvironment: Tackling the cancer stem cells - what challenges do they pose? Pattabiraman et al., Nat Rev Drug Discov, 2014".*

Many hallmarks of cancer are related to TME, including the ability to induce proliferation and inhibit apoptosis, to reprogram metabolism, to increase factors that support cancer invasion and metastasis and to promote angiogenesis and avoid hypoxia.

Because the rapid proliferation of the cells requires an accelerated production of basic cellular building blocks, differences in cellular metabolic programs occur within the cells of TME and some proteins, such as HIF-1α, P13K, AKT, p53, PTEN, known as crucial components in the metabolic pathways, can be differently regulated in cancer cells (6). Although recent studies have revealed the importance of fatty acids and proteins as fuel sources for cancer cells, aerobic glycolysis (Warburg effect) remains the major fuel source for tumor cells (7). It is well described that cancer cells can metabolize 10-fold more glucose to produce

lactate than normal tissues. Despite enhanced glycolysis, most cancer cells also maintain mitochondrial respiration to produce a significant fraction of ATP. The metabolic switch of cancer cells toward a more glycolytic phenotype increases the concentration of protons [H^+], causing the acidification of cytoplasm. To overcome low intracellular pH (pHi), cancer cells employ a large redundancy of mechanisms, such as the activation of plasma membrane proton pump ATPase (V-ATPase), carbonic anhydrases (CAIXs) and Na^+/H^+ exchangers or anion exchangers that determine a slow increase of pHi. In response to H^+ efflux, the pH of tumor extracellular space (pHe) becomes acidic, forming a reversed pH gradient. The acidosis of TME promotes cancer progression and induces migration and invasion (8).

Moreover, TME is characterized by disorganized blood vessels that are immature, tortuous and hyperpermeable. The tumor vasculature is typically a complex labyrinth of vessels in which arterioles, capillaries, and venules are not clearly identifiable. Furthermore, tumor vessels are more permeable than normal ones because they are poorly invested with smooth muscle cells, and have a discontinuous endothelial cell lining with an abnormal basement membrane. Increased vessel permeability results in aberrant osmotic forces, leading to accumulation of vascular contents and elevated interstitial fluid pressure. As result, the irregular vasculature system leads to impaired blood flow of tumor, where vessels cannot supply nutrient to cells and remove waste products. In addition, the aberrant geometry of vessels causes an inadequate oxygen supply to tumor cells with micro-regional hypoxia. These particular characteristics of tumor vasculature lead to adverse micro-environmental conditions that obstruct traditional therapeutic anti-cancer strategies (9,10).

Overall, the manipulation of TME could be used as a valid approach to formulate new therapeutical cancer treatment and identifying the most important molecular players in TME represents the first step toward this goal.

1.1.1 Hypoxia in tumor microenvironment

O_2 is an important factor in cells metabolism and the maintenance of O_2 homeostasis is essential for the survival of the cells. Indeed, O_2 is the final electon acceptor during mitochondrial ATP production and other intracellular reactions.

As described above, most of solid tumors are characterized by regions of hypoxia, which result from structural abnormalities of vasculature network, rapid growth of tumor cells and high interstitial pressure. In this microenvironment cells undergo genetic and adaptive changes that allow them to survive and even proliferate. Tumor tissues are characterized by 1-2% O_2 levels or below; these concentrations depend on the initial oxygenation of the tissue, the size and the stage of the tumor as well as on the methods of measurements and in which part of the measurement is performed.

The two most frequently described and investigated subtypes of tumor hypoxia are acute and chronic. These two subtypes can lead to completely different hypoxia-related responses within the tumor, which could have a direct effect on tumor development and response to treatment. In order to accurately assess the specific biological consequences, it is important to understand which time frames best define acute and chronic hypoxia. The discrepancy and lack of clear description about the time frames and the biological consequences of acute and chronic hypoxia are often considered a great problem in oncology (11,12).

Generally, it is accepted that acute hypoxia is an abrupt and brief exposure to hypoxia, which occurs when vessel occlusion lasts for several minutes until hours. It is reversible and often leads to following oxygen fluctuations called cycling hypoxia (13,14). Different *in vitro* models of acute hypoxia are set up by exposing cells to continuous hypoxia between few minutes to 72 hours. Short-term hypoxia allows cells to survive by activating different mechanisms such as autophagy that is achieved by decreasing oxidative metabolism. Furthermore, it has been described that high level of reactive oxygen species (ROS) induced by acute or cycling hypoxia may contribute to tumor cells survival (13,15). Conversely, enduring changes in blood flow and low oxygen availability, which are especially pronounced in larger tumors, result in chronic hypoxia and contribute to long-term cellular changes. In experimental setting, chronic conditions are achieved

incubating the cells in hypoxia between few hours and as long as several weeks. Longer exposure to hypoxia is associated with high frequency of DNA breaks, accumulation of DNA replication errors since hypoxia hampers DNA repair systems leading to genetic instability and mutagenesis. Moreover, chronic hypoxia induces metabolic switch from oxidative phosphorylation to anaerobic glycolysis that leads to continuous lactate production from pyruvate resulting in acidosis (16). Even if both acute and chronic hypoxia can increase resistance to therapy, chronic hypoxia is associated with more aggressive tumor phenotype through the development of micro-niches of quiescent cells and induction of spontaneous metastasis (11,17,18). In any case, cycling hypoxia/reoxygenation represents the oxygenation state that better reflects *in vivo* situation. The biological responses activated by reoxygenation can instigate continuous adaptive mechanisms that contribute to increase the aggressiveness of the cancer cells. Thus, the chemoresistance, the radio-resistance and the ability to proliferate or metastasize are extensively enhanced during hypoxia/reoxygenation cycles.

Although different hypoxic stimuli within tumors makes it difficult to generalize the real effects on tumor biology, and metabolism, it is now well known that the biology of hypoxic cancer cells is the product of the interplay between the prevailing oxygen tension, hypoxia-induced signaling, and cellular damage by ROS (13).

1.1.2 Signaling pathways in hypoxic tumor microenvironment: hypoxia inducible factors

Hypoxia inducible factors (HIFs) are heterodimeric transcription factors consisting in a stable and constitutively expressed β-subunit (HIF-1β) and an oxygen sensitive α-subunit (HIF-1α). To date, three isoforms of HIF-α subunit (HIF-1α, HIF-2α and HIF-3α) have been described, from which HIF-1α and HIF-2α are the best characterized. While HIF1α is expressed ubiquitously, HIF2α is expressed in more restricted number of cell types such as hepatocytes and endothelial cells.

HIF activation is a multi-step process involving HIF-α stabilization, nuclear translocation, heterodimerization with HIF-1β and transcriptional activation of

genes that function in angiogenesis, tumor vascularization and chemoresistance.

The key regulation of HIF-1 signaling is orchestrated by two types of oxygen-sensor proteins: prolyl hydroxylase (PHDs) and asparaginyl hydroxylase (FIH), known as factors inhibiting HIF-1α through hydroxylation under normoxic condition. Specifically, PHDs hydroxylate two conserved prolyl residues in HIF-1α allowing a rapid interaction with the von Hippel-Lindau tumor-suppression protein (VHL), a component of E3 ubiquitin ligase complex. Subsequently, HIF-1α becomes marked with polyubiquitin chains that drive them to destruction by the proteasome system.

Another oxygen-dependent major mechanism for negative regulation of HIF-1α pathway does not involved VHL protein. In this case, FIHs hydroxylate an asparagine residue in the carboxy-terminal transcriptional activation domain (C-TAD) of HIF-α and block the cooperative interaction with the co-activator CBP/p300 impairing HIF-1α gene transcription (19). Thus, PHDs and FIHs ensure full repression of the HIF pathway under normoxia condition by controlling both the degradation and inactivation of HIF-1α subunit.

On the other hand, when the oxygen level drops, the hydroxylases lose their activity and HIF-1α is stabilized , translocates to the nucleus where dimerize with the constitutively expressed HIF-1β subunit. HIF complex binds to DNA in the hypoxia-response elements (HRE) region and promotes transcription of genes involved in angiogenesis, metabolic adaptation, survival, apoptosis and cells migration (20).

Figure 2 is a schematic representation of HIF-1α signaling pathway under normoxia and hypoxia.

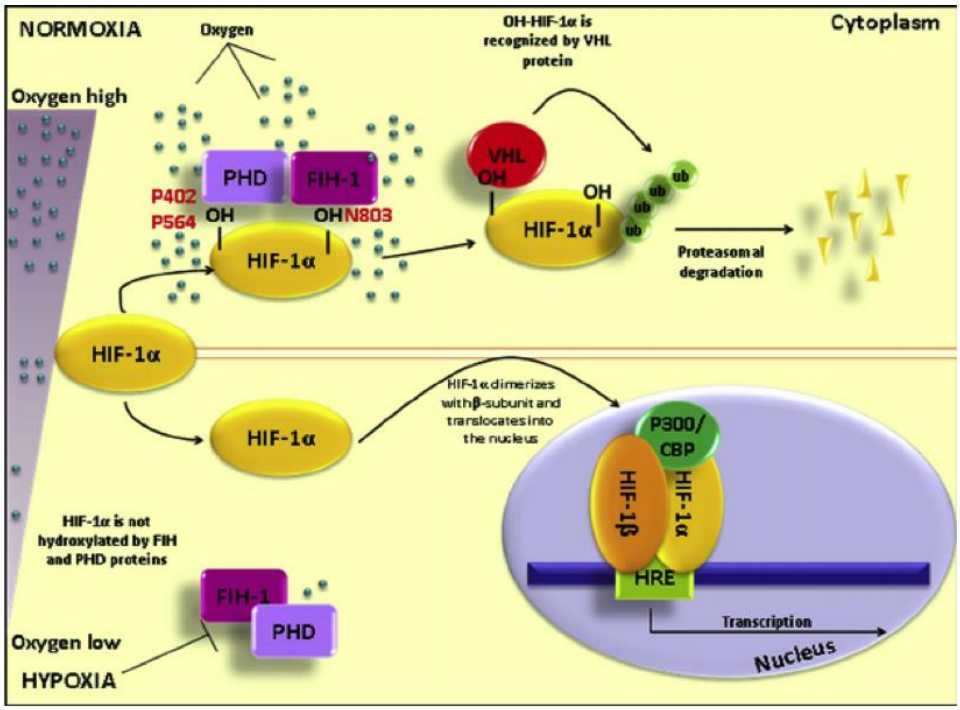

Figure 2. HIF-1α oxygen-dependent regulation. HIF-1α protein is oxygen-sensitive and its stability depends on O_2 level. In normoxic conditions, PHD enzymes hydroxylate proline 402 and 564 in HIF-1α allowing a rapid poly-ubiquitylation and subsequently proteasome degradation. Furthermore, FIH-1 hydroxylates asparagine 803 in HIF-1α impairing its DNA binding. Under hypoxic conditions, the rate of asparagine and proline hydroxylation decreases and HIF-1a that is not prolyl-hydroxylated is not degradated. HIF-1α dimerizes with the β-subunit and translocates to the nucleus. P402 and P564, proline residues; N803, asparagine residue; HIF-1a, hypoxia-inducible factor 1 alpha; FIH, factor inhibiting HIF; PHD, prolyl-hydroxylase domain; VHL, von Hippel-Lindau; CBP, CREB binding protein; HRE, hypoxia responsive enhancer elements. *Image taken from: "Therapeutic targeting of hypoxia and hypoxia-inducible factor 1 alpha in multiple myeloma, Borsi E., Translational Research, 2014".*

In most *in vitro chronic* hypoxia studies, HIF-1α subunit levels are increased and stabilized within few hours, but after few days decrease to lower expression levels. This is likely due to the HIF-1-mediated upregulation of PHD2, which retains enough activity to hydroxylate HIF-1α, resulting in its renewed degradation (21). Instead, cycling hypoxia results in an enhanced activity and stabilization of HIF-1α, which is at a much greater level than that in chronic hypoxia (22). This damaging phenotype, where HIF-1α is accumulated, is also associated with an increased resistance to radiotherapy and chemotherapy as well as increased metastatic potential (16).

During hypoxia, HIFs supports and even enhances the metabolic reprogramming

of glycolysis through the upregulation of almost all glycolytic genes and the monocarboxylate transporters that export lactate. It has been shown to upregulate the expression of genes encoding glucose transporters 1 and 3, glycolytic enzymes such as hexokinase 1 and 3, aldolase A and C and glyceraldehyde-3-phosphate dehydrogenase-6.

HIF transcription factors have also been shown to affect the function and stability of some oncogenes and tumor suppressor genes. Although one of the most studied oncogenes linked to HIF is p53, the relationship between HIF and p53 remains still discussed. Hypoxia has been shown to induce p53 stability in some conditions but the molecular mechanism is unclear (23). It appears that severity and duration of the hypoxic stimulus influence the hypoxia-induced differences in metabolism that are dependent on HIF during acute hypoxia, but engages p53-mediated gene expression changes during chronic hypoxia (16).

HIFs proteins, in particular HIF-1, also regulate a set of genes involved in extracellular matrix remodeling, migration and digestion of the basement membrane. This group includes vimentin, fibronectin, keratins, matrix metalloproteinase 2, cathepsin D that is associated with a concomitant loss of E-cadherin, a crucial feature of epithelium mesenchyme transition (EMT). In this regard, the first evidence linking HIF to decreased expression of E-cadherin was demonstrated in ovarian carcinoma in 1999 when immunolocalization of nuclear HIF-1α showed a strong topological correlation with loss of E-cadherin (24).

1.1.3 ROS production in tumor microenvironment

ROS are a broad class of oxygen radical species that are produced in cells as a normal byproduct of metabolic processes. They are characterized by heterogeneous properties and have a plethora of downstream effects, depending on their concentrations. Under physiological conditions the continuous production and detoxification of cellular ROS lead to a tightly controlled and well-balanced redox status. On the other hand, an imbalance between ROS production and removal results in the accumulation of ROS in the cells and leads to oxidative stress. In order to maintain the redox balance, cells activate some ROS scavenging systems, mainly composed of antioxidant

enzymes and non-enzymatic ROS scavengers. Common enzymes that are involved in the detoxification process of ROS are superoxide dismutase, catalase, peroxiredoxins and glutathione peroxidases. For their reducing power, glutathione and NAD(P)H are the most well-known electrons donators (25).

ROS and associated oxidative stress have been historically considered harmful to the cell as they can damage cellular DNA, oxidize fatty acids and aminoacids. The effects of these oxidation lead to tissue destruction associated with various diseases.

Consequences of ROS production in cancer biology are pleiotropic and complex. Although higher ROS levels are related to cancer cell growth, angiogenesis and metastasis, their role in cancer cells is still disputed. It has been shown that ROS have mainly dual functions, cytotoxic or tumorigenic, depending on different types and levels of ROS (25). At low concentration, ROS seem to increase cell proliferation and survival through the post-modification of some kinases and phosphatases. Conversely, excessive ROS levels irreversibly damage the cellular macromolecular components and result in cell death. Furthermore, high ROS levels can mediate mobility and invasive properties of cancer cells, contribute to extracellular matrix remodeling, increase neo-angiogenesis and induce metabolic reprogramming of both cancer and stromal cells.

TME is characterized by elevated ROS levels that trigger oxidative stress, deeply affecting tumor progression and metastasis. This condition can result from increased basal metabolic activity, mitochondrial dysfunction, peroxisome activity, uncontrolled growth factor of cytokines signaling, and oncogene activity, as well as from enhanced activity of known ROS sources as NADPH oxidase (NOXs), cyclooxygenases (COXs), or lipoxygenases (LOXs) (26,27).

It is well accepted that ROS levels strongly increase during hypoxic exposure, mainly in chronic hypoxia ranges and reoxygenation periods that follow hypoxia (22). These events partially justify the different impacts of continuous and cycling hypoxia on a variety of parameters, such as angiogenesis, metastatic behavior and treatment responses. Mechanisms that mediate adaptation to burst of ROS lead to activate the detoxification systems with an increase of hypoxia-induced glutathione and NAD(P)H synthesis. These signaling pathways in TME,

contribute to render cancer cells even more resistant to a variety of stresses including anticancer drug exposure or mechanical forces when entering the bloodstream (13). Thus, within TME, both ROS production and detoxification are known to be critical to maintain the redox balance for the cancer cells viability (28).

1.2 Tumor dormancy and the interplay with tumor microenvironment

The development of metastasis rather than tumor itself is one of the major causes of death among cancer patients. In some instances, this occurs shortly after primary tumor detection and treatment because tumor cells are already expanding at the moment of the diagnosis. However, in many types of tumors, metastatic diseases occur years or decades after tumor resection. The appearance of tumor relapse after prolonged time is explained by the survival of disseminated tumor cells (DTCs) in a dormant state. These cells survive in a quiescent state and remain undetected for long periods, explaining the prolonged asymptomatic residual disease and treatment resistance.

The period between primary tumor detection and metastatic relapse is often defined as *tumor dormancy*, a poorly understood stage in cancer progression in which cells are characterized by mitotic cycle arrest in G0/G1 phase and low metabolism (29). This state is reversible and under certain conditions, such as induction by growth factors, cytokines, nutrients, or chemical agents, the cells can re-enter in the cell cycle to proliferate again.

Tumor dormancy results by tumor cell growth arrest (*cellular dormancy*) and by mechanisms that antagonize the expansion of a dividing tumor cell population (*tumor mass dormancy*) (Figure 3). The first one can occur when tumor cells enter a state of quiescence. In this regard, the absence of proliferation in dormant cells has been attributed to the up-regulation of cell cycle inhibitors such as p21 and p27. In contrast to single cell dormancy, in *tumor mass dormancy*, the cells usually divide but the micrometastatic lesion does not expand beyond a certain size because of either limitations in blood supply or an active immune system. It seems to be caused by a balance of cells proliferation and apoptosis, regulated by pro-angiogenic proteins and angiogenic inhibitors produced by tumor and stromal

cells, as well as immunological switches. This phenomenon is also termed *angiogenic dormancy* (30). According to this definition, Naumov *et al*. sustain that a failure to activate the angiogenic switch contributes to maintain a group of cells in a dormant state (31). Indraccolo *et al*. reported that a short-term perturbation in a transient angiogenic burst could be sufficed to interrupt tumor dormancy (32). In this regard, therapeutic strategies to target tumor vasculature, such as anti-VEGF drugs, are the current approaches to oppose dormant cells.

Tumor mass dormancy can be also maintained by the immune system that controls and does not completely eliminate malignant tumor growth. This process is termed *immunologic dormancy* and given that tumor cells are inherently genetically unstable, the strong immune pressure placed on tumor cells in equilibrium makes them susceptible to acquire mutations that may allow for immune evasion. These adapted tumors frequently defects in antigen presentation, processing or both, through loss of MHC class I or latent membrane protein (LMP)-family molecules, rendering them undetectable by the adaptive immune system. They are also capable of establishing a global immunosuppressive state in the TME by secreting some cytokines, such as TGF-β and VEGF, or by recruiting immunosuppressive cell type, including T regulatory cells and myeloid-derived suppressor cells (MDSCs). These recruited cells contribute to the anti-inflammatory cytokine production and suppress the anti-tumorigenic capacities of the other immune cell types. Once micrometastases overcome dormancy, they become receptive to signals and cell types within the TME to support their expansion. Thus, controlled immune activation, marked by an induction of T cells, is a promising avenue to force tumor dormancy (Figure 3) (30).

To date, little is known regarding tumor dormancy and the biology of dormant cells. Nevertheless, it is clear that one major driving force for tumor dormancy is cellular environment, which poses a challenge to the cells regarding survival and proliferation. Indeed, cells enter or escape dormancy according to restrictive or permissive microenvironment, adapting themselves to better serve its needs. In the restrictive TME, one of the early responses of tumor cells is to reduce growth and the rate of oxygen consumption. Using immunocytochemical techniques, some researchers have demonstrated that hypoxic tumor cells are in a non- or slow-

proliferating state and a majority of these cells are negative for proliferation markers, such as Proliferating Cell Nuclear Antigen (PCNA) or Bromodeoxyuridine (BrdU) (20).

In according to these evidences, the link between cellular dormancy and TME is highlighted by the fact that if the dormant DTCs are originated from the hypoxic niche of the primary tumor, they may be already pre-programmed to be growth-arrested and enter a dormant state before to reach other sites. On the other hand, the inductor of dormancy can be the restrictive microenvironment of the target organs where the DTCs arrive. However, whether hypoxia signaling prepares a "metastatic soil" in distant organs to remain in a prolonged state of dormancy is not well clarified. However, in several different types of cancers, the bone marrow is a common homing organ for DTCs. In most studies, DTCs are detected in the hypoxic regions of bone marrow and persist there over many years with the potential to recirculate into other organs.

In order to find treatments to remove solitary dormant cells or dormant micrometastasis, the researchers need to understand which mechanisms are responsible for metastatic dormancy and what processes trigger dormancy escape. Next paragraph points out some aspects of the knowledge on the mechanisms underlying dormancy in cancer.

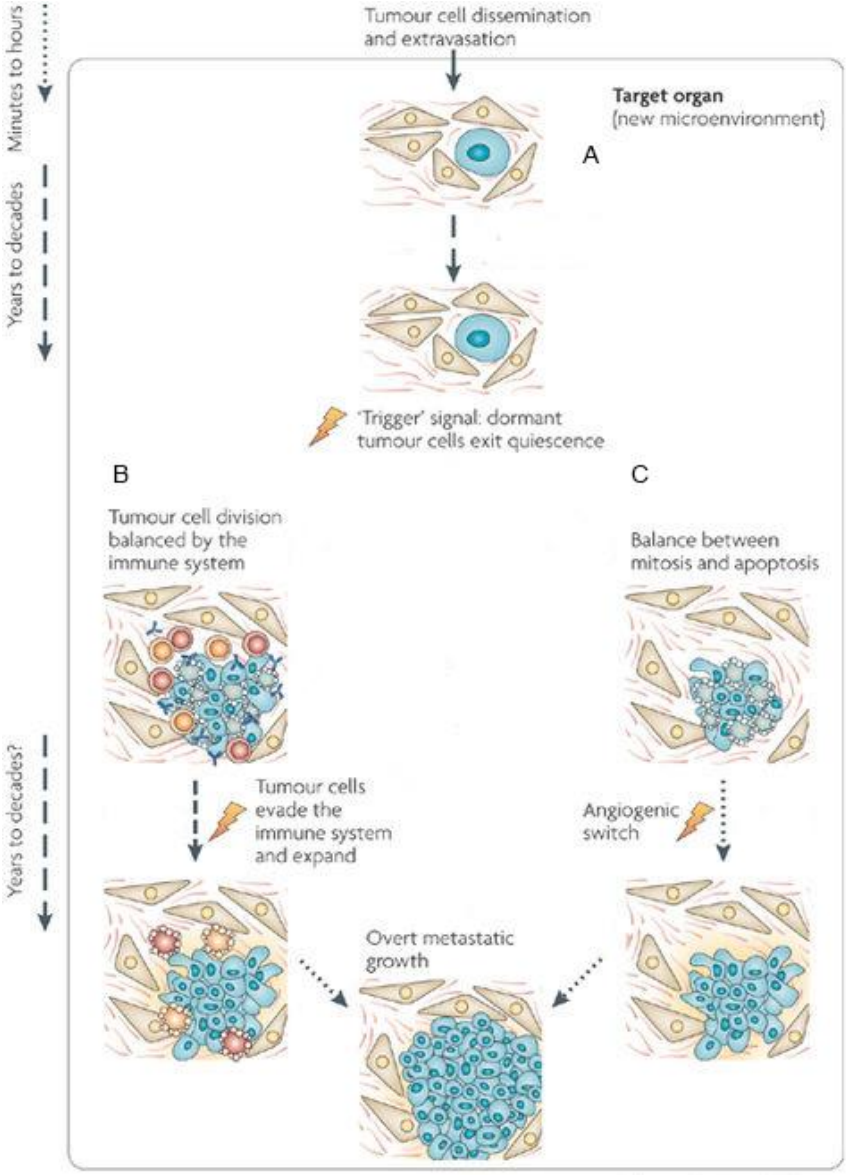

Fig. 3. An integrated view of cancer dormancy. Tumor cells that survive dissemination lodge in the target organ parenchyma. **A**. This new microenvironment most probably determines the fate of the disseminated tumor cells and could account for most of the dormancy time (*cellular dormancy*). If the cells are not genetically progressed it is possible that they are unable to grow autonomously or transduce growth signals from the microenvironment, instead entering a quiescence-like phenotype. Even with genetic alterations, stress and/or microenvironment signals might impose a growth-suppressive program. For tumor cells, a quiescent state might be a natural response to a microenvironment that lacks recruitment signals, tumor cells can fully progress into overt lesions. **B.** It is possible that before becoming overt lesions, dormancy might continue owing to the immune system preventing tumor expansion (*immunologic dormancy*). The immune system might prevent tumor mass expansion for long periods. **C**. Moreover, a tumor cell mass can enter *angiogenic dormancy*. Differentiated tissues can produce angiogenesis inhibitors to maintain tumor vasculature from expanding for long periods. However, it is still unclear how long this mechanism can be maintained in a genetically unstable proliferative tumor cell population, which probabilistically should be prone to accumulating new genetic alterations that activate the angiogenic switch. *Image taken from: "Models, mechanisms and clinical evidence for cancer dormancy, Aguirre-Ghiso JA., Nat. Rev. Cancer, 2007".*

1.2.1 Signaling mechanisms in tumor dormancy

To date, several cancer cell-intrinsic pathways that lead to cellular dormancy have been described. The first signaling mechanism that has been connected with the cells proliferation and DTCs dormancy were the balance between the activities of the mitogen-activated protein kinases (MAPKs) ERK1/2 and p38 (33). In particular, the switch toward phosphorylation of ERK1/2 favors proliferation, while predominant phosphorylation of p38 lead to quiescence. It is now well accepted that in a permissive microenvironment, the interaction between DTCs and extracellular matrix as well as stromal cells results in the in activation of mitogenic signaling (high p-ERK/p-p38) that promote cell growth. Conversely, in restrictive microenvironment, where the activation of stress signaling occurs, low p-ERK/p-p38 ratio represents the molecular switch for induction of a prolonged phase of dormancy (34). The activities of these kinases were found to be driven by the interaction of urokinase-type plasminogen activator receptor (uPAR), α5β1 integrin, fibronectin focal adhesion kinase (FAK) and Src-kinases. It has been demonstrated that proliferating cells are characterized by high expression of uPAR that lead to activation of Src-kinase resulting in the ERK1/2 phosphorylation. Increased level of fibronectine also results in ERK1/2 phosphorylation. Conversely, p38 phosphorylation is favored when uPAR expression is lost and fibronectin is absent (35-37).

Recently, it has been shown that transforming growth factor β2 (TGFβ2) activates p38 in cancer cells disseminated to bone inducing dormancy. This correlates with up-regulation of the proliferation inhibitor p27 and down-regulation of cyclin-dependent kinase 4 (CDK4). In this regard, an up-regulation of TGFβ2 and p27 expression induced by hypoxia has been shown in dormant cancer cells, confirming a key role of hypoxia on dormancy (38).

Moreover, phosphorylation of p38 leads to the activation of the unfolded protein response (UPR) pathway, which promotes cells survival and dormancy. Some studies from Aguirre-Ghiso laboratory highlight that, although all the three sensors of UPR, PERK, ATF6, IRE1 are activated in dormant human epidermoid carcinoma HEp3 cell, only PERK activation contributes towards the growth arrest of cells (35,39-41). This occurs by attenuating translation of G1-S transition

regulators such as cyclin D1, D3 and CDK4. On the other hand, the activation of both ATF6 and IRE1 are required for the basal adaptation and cell survival in restrictive microenvironment. This occurs in part via the ATF6 mediated Rheb induction and a strong inhibition of mTOR signaling (Figure 4) (42).

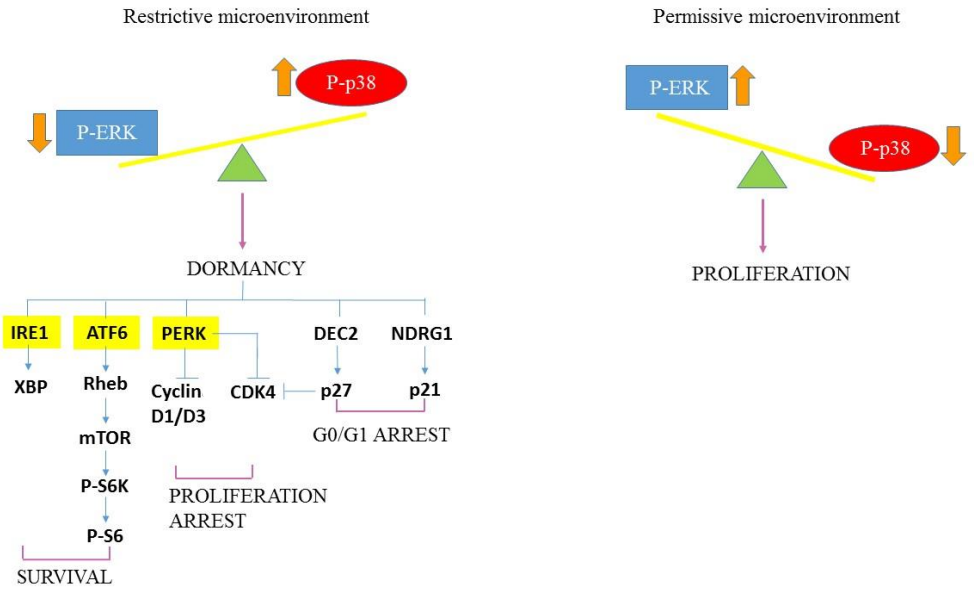

Figure 4. Signaling mechanisms in response to TME. In a permissive microenvironment *(right)*, interactions with the ECM, and stromal cells, allow to DTCs to adapt and integrate growth-promoting signals and activate the mitogenic signaling (high p-ERK/low p-p38 ratio). Conversely, in restrictive microenvironment *(left)*, the loss of surface receptors or the interaction with non-growth-permissive ligands result in activation of stress signaling (low p-ERK/high p-p38 ratio) inducing both dormancy and survival signals. Activation of p38 induces G0/G1 arrest that is mediated by DEC2 e NDRG1, which control the expression of regulators of the cell cycle such as p21 and p27. Furthermore, phosphorylated p38 induces an ER stress response that coordinates growth arrest and survival through the activation of PERK. It leads to the downregulation of cyclin D1/D3 and CDK4 and to the induction of dormancy. ATF6 and IRE1 contribute to DTCs dormancy by promoting survival. ■ Three yellow squares indicate UPR. *Image modified from: "Regulation of tumor cell dormancy by tissue microenvironmentsand autophagy", Sosa M.S. et al., Adv. Exp. Med. Biol., 2013.*

Recently, it has been demonstrated the key role of the suppression of PI3K/AKT pathway in the induction of tumor dormancy as well as in the survival disseminated tumor cells (34). PI3K/AKT signaling regulates cell proliferation, survival and metabolism in cancer cells and it is frequently constitutively activated in multiple human cancers (43). Under prolonged lack of nutrients, the

suppression of AKT activity is necessary for preserving the energy source, decreasing energy demand and activating a strategy of cancer cells to survive in a chronically deteriorated microenvironment (44). The mechanism by which AKT activity is suppressed is not completely understood. It may involve different steps in the PI3K/AKT signaling such as inappropriate activation of receptor tyrosine kinase (RTK), inactivation of upstream kinases, i.e. PI3K, activation of phosphatase PTEN or/and inactivation of mTORC1 (Figure 5). PI3K/AKT axis directly inhibits glycogen synthase kinase 3-beta, which normally suppresses proliferation, and activates the canonical cell cycle pathway. Conversely, the suppression of AKT that occurs in dormant state, allows to activate both CDKs inhibitors p21 and p27 that arrest cell cycle, and the autophagic machinery that protects cells during starvation or stress condition (45).

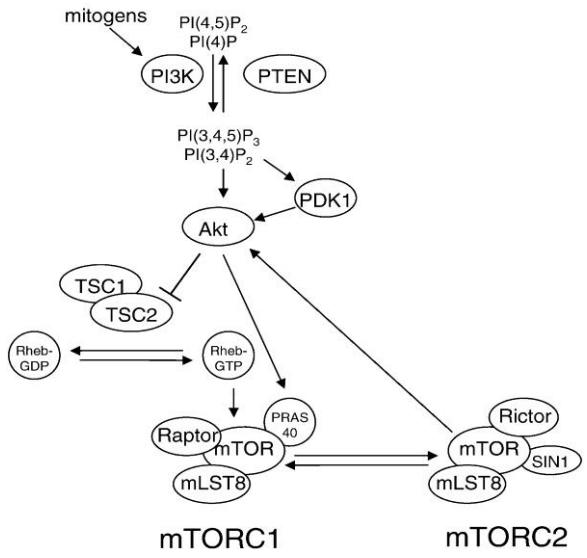

Fig.5 Prototypic mechanisms of Akt regulation. The lipid kinase PI3K is activated in response to mitogenic signals and phosphorylates the phosphoinositides PI(4)P and PI(4,5)P_2 at their D3 position, generating PI(3,4)P_2 and PI(3,4,5)P_3, respectively. The tumor suppressor PTEN opposes this activity of PI3K. PI(3,4)P_2 and PI(3,4,5)P_3 bind to Akt and PDK1, promoting their translocation to the cell membrane. Akt is then activated by sequential phosphorylation of T308 and S473 by PDK1 and mTORC2, respectively. Akt, in turn, activates mTORC1 indirectly by phosphorylation and inactivation of TSC2, which suppresses the activity of the Rheb GTPase, an activator of mTORC1. Akt also directly activates mTORC1 through phosphorylation of PRAS40, a component of mTORC1. *Image taken from: "Akt-dependent and -independent mechanisms of mTOR regulation in cancer, Memmott RM et al, Cell Signal, 2009".*

1.3 Cancer stem cells in tumor microenvironment

Recent studies indicate the presence of a small, intra-tumoral subpopulation of tumor-initiating cancer cells with deregulated stem-cell-like properties that enable them to be resistant to conventional therapies. These tumorigenic cancer cells, called cancer stem cells (CSCs), may be the linchpins of disease recurrence and may significantly contribute to metastasis (2).

Specifically, CSCs exhibit a functional stemness signature comprising self-renewal and ability to differentiate into multiple cancer cells (63). *Self-renewal* is a characterized mitotic cell division in which a stem cell originates one or two undifferentiated cells perpetuating the stem cell pool. On the other hand, the stem cells differentiate into more specialized cell types generating all the diverse cellular phenotypes of the primary lesion (2). Evidences support the vital role of this subset of cells in initiation and maintenance of a tumor in addition to their capability to dictate invasion, metastasis, heterogeneity, and therapeutic resistance. Therefore, the identification and isolation of these CSCs using putative surface markers have been a priority of research in cancer. However, definition of specific CSCs surface markers in all cancer types requires further investigations. It is clear that heterogeneity among tumors renders it difficult to discover unique markers (64).

There are some putative stem cell markers that are in major use for identification and isolation of CSCs from different solid tumors (65-67) Even if every marker shows independent expression, it seems to be a co-expression of surface markers in CSCs, debatable in several cancer types. Indeed, CD44 and CD24 have been used extensively in combination or with other putative markers (CD133, CD166, EpCAM) to isolate CSCs from solid tumors (64). Abraham *et al*. demonstrated that the majority of breast human tumors tissue (78%) displayed ≤10% $CD44^{+}/CD24^{-/low}$ cells and the remainder contained >10%. (68).

CSCs selection and evolution are influenced by TME that provides a breeding ground to maintain a more stem-like and undifferentiated phenotype. For instance, hypoxia exerts a selective pressure on the CSCs population contributing directly to the development of more aggressive cancer cells and resistance to therapies (69,70). Recently, it has been demonstrated that prolonged hypoxia exposure

results in the induction of genes essential for stem cell function such as Oct4, Nanog and c-Myc. These genes are regulated by HIFs, in particular the isoform HIF-2α, which is specifically involved in the self-renewal and multipotency of CSCs. Molecular database analyses revealed that HIF-2α expression correlates with poor outcome of patients with metastasis and represent a promising target for the eradication of CSCs in cancer therapy (71).

1.3.1 Tumor dormancy and cancer stem cells

There is a tight and complex relationship between stemness and dormancy even if the ability of CSCs to proliferate and initiate robust tumor outgrowth, seems to be incompatible with a cancer dormant state. Elegant studies provided strong evidences for the existence of dormant cells as a subpopulation of CSCs in different tumors such as breast, colon, pancreas and ovary (72-77). Nevertheless, it is important to note that not all dormant cells have the stem like properties of self-renewal and differentiation (78).

Unlike dormant tumor cells that can remain quiescent for several years, it is not clear if CSCs undergo so long phase of quiescence (69). However, it is well described that these dormant CSCs exploit phases of cellular dormancy to ensure tumor maintenance and survival in harmful TME, including growth-inhibitory niches and cytotoxic mileus.

It is clear from the previous discussion that hypoxic TME maintains an undifferentiated and quiescent state of CSCs and, since hypoxia promotes tumor dormancy, it could be one of the key links between the dormancy and the stemness. How the hypoxia triggers CSCs populations towards quiescence is still unclear even if some improvements are carried out. It has been demonstrated that slow-cycling CSCs are more likely localized in the low oxygen area of the tumor, away from the blood vessels whereas the fast-cycling cells with limited self renewal capacities, reside in areas much closer to the vasculature (79).

Moreover, several studies have unraveled intriguing parallels between the mechanisms regulating CSCs behavior and angiogenic control of tumor dormancy. While CSCs might survive in the angiostatic environments associated with dormancy, they also promote cancer vascularization in settings of tumor

outgrowth (80,81). Since CSCs own the ability to promote tumor progression by triggering angiogenic responses, they are likely to represent the dormant tumor populations ultimately responsible for delayed cancer recurrences (79).

Another direct link between CSCs and dormant tumor populations is their converging to survive cancer therapy. Indeed, dormant cells are often spared by current treatment modalities, as determined in both animal models and clinical disease (82,83). Similarly, CSCs frequencies are enhanced in metastatic tumor recurrences post-therapy compared to those in pre-therapy samples. Importantly, therapeutic refractoriness of tumor dormant cells is attributable to several resistance mechanisms also intrinsic to the CSCs compartment, including impairment of cancer apoptotic pathways, alterations of cell cycle checkpoints, and reduced drug accumulation. (84).

Taken together these findings highlight the critical importance of TME in the biology of CSCs that creates a strong relationship with tumor dormancy.

However, in light of the intriguing discussion between CSCs biology and the mechanisms controlling tumor dormancy, insights from CSCs biology could help the future research on tumor dormancy.

1.4 Autophagy

Autophagy, or type II programmed cell death, is a catabolic process, evolutionarily conserved and genetically controlled, whereby cells self-digest intracellular organelles to remove those with compromised function and to maintain cell homeostasis. However, autophagy can also be considered a temporary survival mechanism during periods of starvation where self-digestion offers an alternative energy source and may facilitate the disposal of unfolded proteins under stress conditions. The catabolic function provided by autophagy is thereby suppressed once the external nutrient supply is adequate to support cellular metabolism. Besides starvation, autophagy can be also activated by other physiological stress stimuli, such as hypoxia, endoplasmatic reticulum stress, high temperature, hormonal stimulation or pharmacological agents (85) (Figure 6).

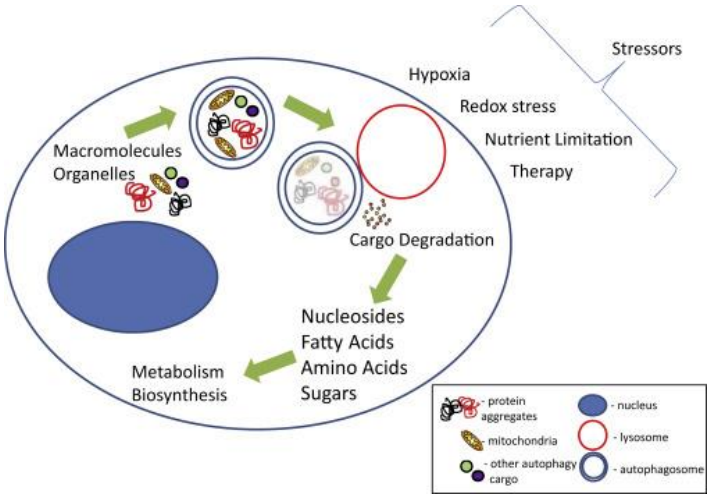

Fig. 6 The process of autophagy leads to the degradation of cargo. The blue double-membraned vesicle, autophagosome; red vesicle, lysosome; blue shaded oval structure, nucleus. Cargo in the autophagosome is represented by the following: mitochondria in yellow, protein aggregates in black and red, and other cargo generally represented in green and purple *Image taken from: "Autophagy and tumor metabolism, Kimmelman AC et al, Cell Metabolism, 2017".*

Depending on the mode of cargo delivery to lysosome, autophagy can be subdivided into three subtypes: chaperon-mediated autophagy, microautophagy and the most studied process named macroautophagy (86). Chaperone-mediated autophagy involves the direct translocation of cytosolic proteins across the lysosomal membrane, by molecular chaperones (e.g., the 70 kDa heat shock cognate protein, Hsc70). Microautophagy involves inward invagination of lysosomal membrane, which delivers a small portion of cytoplasm into the lysosomal lumen. Macroautophagy is the most efficient autophagic clearance mechanism and the most common type of autophagy, therefore, hereafter macroautophagy will be referred to as autophagy. Macroautophagy is a process conserved by yeast to mammals and is mediated by a double-membrane special organelle termed autophagosome. Upon induction, a small vesicle (phagophore) elongates and encloses a portion of cytoplasm, which results in the formation of the autophagosome. Then, the outer membrane of the autophagosome fuses with a lysosome to form an autolysosome, leading to the degradation of the enclosed materials together with the inner autophagosomal membrane (Figure 7). Aminoacids and other small molecules that are generated by autophagic

degradation are delivered back to the cytoplasm for recycling or energy production (87). Specifically, the process of autophagosome formation involves two major steps, nucleation and elongation of the isolation membrane, in which different proteins, such as the products of AuTophaGy-related (Atg) genes and microtubule-associated protein light chain 3 (LC3) are involved (88). LC3 is one of the best characterized protein on autophagosome, and therefore, it serves as widely used marker of autophagy (89). It is expressed in cells as a full-length cytosolic protein that, upon autophagy induction is proteolytically cleaved, to generate LC3-I that is conjugated with phosphatidylethanolamine and forms LC3-II (90-92).

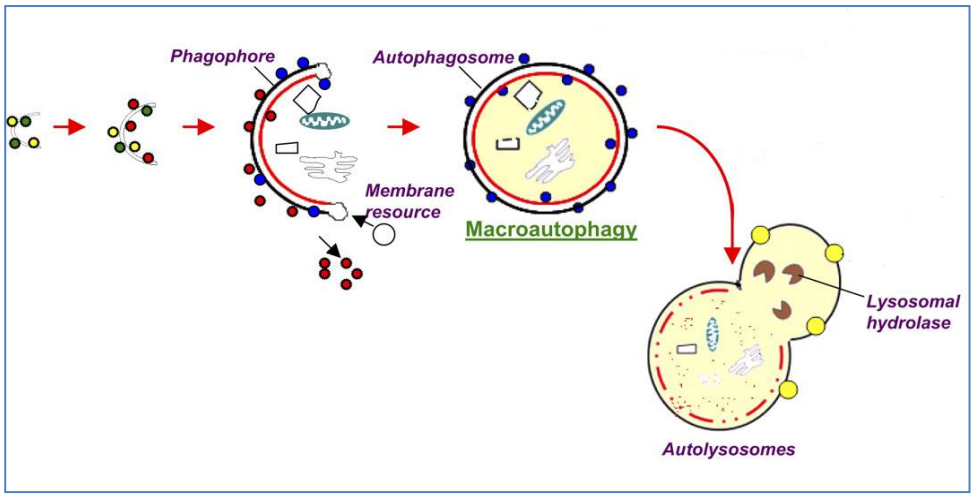

Fig. 7 Macroautophagy steps. Macroautophagy starts with the de novo formation of a cup-shaped isolation double membrane that engulfs a portion of cytoplasm. Colored balls indicate proteins (Atgs, etc) involved in the process. The image is taken from: *"Autophagy: molecular machinery, regulation, and implications for renal pathophysiology", Periyasamy-Thandavan et al, American Journal of Physiology - Renal Physiology, 2009".*

Among the numerous components involved in the regulation of autophagy, the Mammalian Target of Rapamycin (mTOR) is now recorgnized as sensor that coordinately regulates the balance between growth and autophagy in response to cellular physiological conditions and environmental stress (93). mTOR is a serine/threonine protein kinase that belongs to the phosphatidylinositol kinase-

related kinase (PIKK) family. The inhibition of mTOR activity, through Akt and MAPK signaling, under nutrient starvation, induces autophagy as well as negative regulation of mTOR, through AMPK and p53 signaling, promotes it (94).

Under physiological conditions, autophagy has a number of other vital roles such as maintenance of the aminoacid pool during starvation, prevention of neurodegeneration, antiaging function, clearance of intracellular microbes and regulation of innate and adaptive immunity (86,95).

In addition to the physiological roles of autophagy, many reports describe its controversial involvement in the genesis and the progression of cancer (96-98). Indeed autophagy acts either as a tumor suppressor, by preventing the accumulation of damaged proteins and organelles, or as a mechanism of cell survival that promote and maintain the growth of established tumors (99).

1.4.1 Autophagy sustains survival of dormant cancer cells

A potential role of autophagy in dormancy was originally evidenced in *C. elegans* during a dormancy-like state, where larvae are exposed to hostile microenvironment. In this model, *C. elegans* activated autophagy that could promote survival during quiescent states (100).

Since autophagy is activated in response to changes of the microenvironment, it could be interesting to investigate the mechanisms that induce autophagy and allow to the survival and the maintenance of the dormant state in tumor cells. Although the efforts to show through *in vitro* or *in vivo* models, the role of autophagy in dormancy and the mechanisms that are activated during this state remain largely discussed. However, studies in models of breast cancer cells suggest that the decreased mitogenic signaling of β1-integrin in dormancy may stimulate autophagy (101). Moreover, it has been shown that dormant cancer cells activate p27 that is involved in cell cycle arrest and directly induces autophagy to facilitate cells survival in response to growth factor withdrawal (102,103).

It would be critical to determine whether autophagy plays a dormant or survival-inducing role, or both, in quiescence tumor cells. If autophagy induces a pro-survival state, then strategies to block it could eradicate dormant cells. In case that

it contributes to both quiescence and survival, then more detailed analysis of these pathways would be required to reveal ways to inhibit only the survival signals without interrupting quiescence (104).

2. AIM OF THE THESIS

The hypoxic tumor microenvironment has been recognized as a cause of malignancy or resistance to various cancer therapies. However, the effect of a chronic exposure of the cells to hypoxia and the following reoxygenation cycles remain elusive. Although most of the tumor cells die in chronic hypoxia, some of them can survive for more than several days in a quiescent state. This dormant state is reversible, with tumor cells recovering the ability to self-renew once closed vessels reopen or new vasculatures reach the hypoxic area. Because dormant tumor cells may be the founders of metastasis, one hypothesis is that these cells share stem cell-like characteristics that may be responsible for their long half-lives.

An understanding of the regulatory machinery of tumor dormancy is essential for identifying early cancer biomarkers and could provide a rationale for the development of novel agents to target dormant tumor cells population. The lack of established *in vitro* models of tumor dormancy represents the major factor that hampers the understanding of dormant cells response. Indeed, the majority of *in vitro* hypoxia studies have been carried out exposing cell lines to acute hypoxia (3-24 h), whereas only few reports of chronic hypoxia have been published.

Therefore, the aim of the thesis is to establish and characterize a new *in vitro* model of cell dormancy using hypoxia/reoxygenation cycles and culturing the surviving cells in chronic hypoxia condition.

3. MATERIALS AND METHODS

3.1 Cell lines and cells culture

Human breast cancer cell lines MDA-MB-231, MDA-MB-468, T47D, and MCF-7 were purchased from American Type Culture Collection. All the cell lines were cultured in DMEM (LifeTechnologies) supplemented with 10% FBS, 100 UI/mL penicillin, 100 µg/mL streptomycin, and 40 µg/mL gentamycin (Life Technologies) in a 5% CO_2 atmosphere at 37°C. Hypoxic culture was achieved by incubating cells with 1% O_2 and 5% CO_2 in a Multigas Incubator (RUSKINN C300, RUSKINN Technology Ltd) in DMEM without sodium pyruvate and supplemented with 25 mM HEPES, 10% FBS, 100 UI/mL penicillin, 100 µg/mL streptomycin, and 40 µg/mL gentamycin. After some hypoxia/reoxygenation cycles, the surviving cells were cultured under 1%O_2 athmosphere for at least 3 months. The hypoxia-resistant MDA-MB-231 cell line was designed as chMDA-MB-231.

3.2 Morphological analyses of dormant cells and tumorspheres

Approximately 6 x 10^4 MDA-MB-231 and chMDA-MB-231 cells were seeded on a 4-chamber µslide, with 13 mm glass bottom *(IbidiGmbH).* After 24 h, cells were incubated for 5 min with a staining solution made of CellMaskDeep Red *(LifeTechnologies)* 1:1000 cell media without serum. Before the acquisition, the medium was replaced with a special medium without phenol red (DMEM/F12 NoPhenolRED, *LifeTechnologies)* to avoid any interference with the fluorescence signal.

The tumospheres deriving from 60 wells of a coated 96 well-plate were gently collected by a p1000 tip with a cut extremity and seeded on a 4-chamber µslide. After 24 h, cells were incubated for 60 min with a staining solution made of CellMaskDeep Red 1:1000 *(LifeTechnologies)* and Hoescht 1:1000 *(LifeTechnologies)* in DMEM/F12NoPhenolRED. Cell images were captured using a confocal laser-scanning fluorescence microscope Leica SP5 *(Leica*

Microsystem) at 63x magnification and processed using Adobe Photoshop and ImageJsoftwares *(Rasband, W.S., ImageJ, http://rsb.info.nih.gov/ij/, 1997–2008).*

3.3 Cells viability

The viability of MDA-MB-231 and chMDA-MB-231 cells were evaluated with a 0.1% Trypan Blue exclusion test using a Countess Automated Cell Counter *(LifeTechnologies).*

3.4 Immunophenotype

Cells were harvested, washed in phosphate buffer saline (PBS) and stained with anti-human CD326/ESA-FITC, CD24-FITC *(MiltenyiBiotec),* CD44-PE *(BD Pharmingen).* After incubation at room temperature for 15 min, cells were washed in PBS, acquired on aFACScan cytometer (Becton Dickinson) and analyzed by FlowJo9.3.3 software *(Tree Star).* Data were expressed as the difference of Median Fluorescence Intensity (MFI) between stained and unstained cells.

3.5 Cell cycle

Cells were incubated with 10 mM Vybrant DyeCycle orange stain *(LifeTechnologies)* for 15 min and with 1 mM Sytox Blue dead Cell stain *(LifeTechnologies)* for additionally 15 min to exclude dead cells from cytometric analysis.

3.6 Cell proliferation

Cells were labeled with the amine-reactive dye 5,6-carboxyfluor-escein diacetate, succinimidyl ester (CFSE), as described previously (105).This dye is incorporated into cells and divided equally into daughter cells during proliferation. Thus, cells proliferation can be determined by measuring the MFI by flow cytometry on a FACS scan flow cytometer. Briefly, they were resuspended at a final concentration of 10^7cells/mL in PBS-5% FBS and incubated with 5 mM CFSE for 5 min at room temperature. The reaction was stopped by washing twice with PBS-5% FBS. Cells were replated at 10^6 cells/mL in complete medium in normoxic andhypoxic conditions. An aliquot of cells was harvested every 24 h for 3 days,

added with TO-PRO-3 *(LifeTechnologies)* and subjected to flow cytometry analysis.

3.7 Measurement of glucose, pyruvate, and lactate concentration

After 3–5 days of culture under normoxic or hypoxic conditions, the medium of MDA-MB-231 and chMDA-MB-231 cells were harvested and cells were counted. The concentration of glucose and lactate in the media was measured by using the glucose assay kit *(CaymanChemical)* and the lactate assay kit *(Megazyme International)*, respectively, according to the manufacturer's instructions. To measure the amount of pyruvate produced, 5–50 μL of medium were added to 370 mM Tris–HCl pH 8, containing 350 mM NADH and 3 mg of LDH *(Sigma)*, to a final volume of 300 μL. The total change of the absorbance at 340 nm was measured and using the molar extinction coefficient of NADH at 340 nm (6,220 M/cm), the moles of NADH oxidized, that are equal to the moles of pyruvate produced, were calculated.

3.8 Glutathione content quantification

The intracellular GSH concentration was measured by endpoint spectrophotometric titration on a Jasco V/550 spectrophotometer *(JASCO)* using the 5,50-dithiobis(2-nitrobenzoic acid) *(DTNB, Ellman'sreagent)* (106). Briefly, MDA-MB-231 and chMDA-MB-231 cells were lysed by freezing and thawing in 100 mM sodium phosphate buffer, pH 7.5, containing 5 mM EDTA, (KPE buffer), and after centrifugation at 16,000 rpm for 10 min, total protein concentration was determined by Bradford reagent *(Pierce)* using bovine serum albumin as standard (107). The supernatants were deproteinized with 5% trichloroacetic acid. For [GSH] measurement, acidified clear supernatants were neutralized and buffered at pH 7.4 with 200 mM K_2HPO_4, pH 7.5. The reaction was then started by the addition of 60 mM DTNB and the increase inabsorbance at 412 nm was measured until no variation in absorbance was evident. The amount of total GSH was determined by comparison with GSH standard curve.

3.9 Detection of intracellular reactive oxygen species (ROS)

a) CM-H_2DCFDA staining: MDA-MB-231 and chMDA-MB-231 cells were resuspended in HBSS (*LifeTechnologies*) at $3x10^5$ cells/mL and loaded with 2.5 μM of the cell-permeant probe 5-(and-6)-chloromethyl-2'7'-dichlorodihydrofluorescein diacetate acetyl ester (CM-H_2DCFDA; *Molecular Probes*) for 1 h at 37°C, as previously described (108). ROS generation was evaluated in flow cytometry (Becton Dickinson) by measuring the green fluorescence signal (Fl-1) of CM-H_2DCFDA that occurs after removal of the acetate groups by intracellular esterases and oxidation by free radicals. Data were analyzed by FlowJo 9.3.3 software.

b) Mitosox staining: Approximately 6 x 10^4 MDA-MB-231 and chMDA-MB-231 cells were seeded on a 4-chamber μslide, with 13 mm glass bottom (Ibidi GmbH). After 24 h, cells were incubated for 30 min with a staining solution made of Mitosox 1:1000 (*LifeTechnologies*), Mitotracker greenFM 1:5000 (*LifeTechnologies*) and Hoescht 1:1000 (*LifeTechnologies*) in medium without FBS. Before the acquisition, the medium was replaced with a medium without phenol red (DMEM/F12 NoPhenolRED, *LifeTechnologies*) to avoid any interference with the fluorescence signal. Cell images were captured using a confocal laser-scanning fluorescence microscope Leica SP5 at 63× magnification and processed using Adobe Photoshop and ImageJ softwares (*Rasband, W.S., ImageJ, http://rsb.info.nih.gov/ij/, 1997–2008*).

3.10 Western Blot

Cells were homogenized at 4°C in 20 mM HEPES, pH 7.4, containing 420 mM NaCl, 1 mM EDTA, 1 mM EGTA, 1% Nonidet-P40 (NP-40), 20% glycerol, protease cocktail inhibitors *(GE Healthcare, Amersham)* and phosphatase cocktail inhibitors. Protein concentration was measured by Bradford reagent using bovine serum albumin as standard (107). Protein extracts (50 μg/lane) were resolved by SDS PAGE electrophoresis and transferred to PVDF membrane *(Immobilon P, Millipore)*. Immunoblotting assays were carried out by standard procedures using anti-LC3, anti-p(Thr180/182)-p38, anti-p38, anti-p(Ser)-AKT, anti-AKT and anti-P70S6 kinase antibodies *(Cell Signaling Technology)*, anti-STAT1, anti-STAT3,

anti-p53, anti-p(Thr202/Tyr-204)-ERK and anti-ERK antibodies (Santa Cruz Biotechnology), anti-HIF1α antibody *(BD bioscience)* anti-actin antibody (Millipore), anti-HIF2α antibody *(Novus Biologicals)*. After washing, membranes were developed using anti-rabbit or anti-mouse IgG peroxidase-conjugated antibodies *(Cell Signaling Technology)* and chemiluminescent detection system *(Immun-Star™ WesternC™ Kit, Bio-Rad).* Blotted proteins were detected and quantified using the ChemiDoc XRS Imaging System *(Bio-Rad)*.

3.11 Real time PCR

Cellular RNA was extracted by PureLink Total RNA kit *(AmbionTM)* according to the manufacturer's instructions. Total RNA was quantified at 260/280 nm, and the integrity of the samples was checked by 1% agarose gel electrophoresis. Aliquots corresponding to 1μg of total RNA were reverse transcribed by using the SuperScript Vilo cDNA synthesis kit *(InvitrogenTM)* following the manufacturer's protocol. Aliquots of the cDNAs (corresponding to 50 ng of the original RNA) were subjected to real-time PCR with the QuantiTect SYBR Green PCR Kit *(Qiagen,)* following the manufacturer's instructions. Bioinformatically validated primer sets for real-time PCRs were purchased by Qiagen (QuantiTect Primer Assays: Hs_RRN18S_1_SG for 18S, Hs_PGK_1_SG for PGK, Hs_SLC2A1_1_SG for GLUT1 and Hs_GADPH_2_SG for GAPDH). 18S rRNA was used as the housekeeping gene for sample normalization and was amplified in separate tubes within the same run. The PCR was performed with an initial pre-incubation step for 15 min at 95°C, followed by 45 cycles of 94°C for 15 s, annealing at 55°C for 30 s, and extension at 72°C for 30 s. The specificity of the amplified products was monitored performing melting curves at the end of each amplification reaction. All amplicons generated a single peak, thus reflecting the specificity of the primers. Real-time PCR was performed using the Rotor-Gene 6000 *(Corbett Cambridgeshire, UK)* and data analysis was conducted using the Rotor-Gene Software. Data were normalized to 18S and sample expression levels are shown as percentages of the internal control gene. Experiments were repeated at least three times.

3.12 Detection of autophagic markers

a) Acridine orange staining. Approximately 6 x 10^4 MDA-MB-231 and chMDA-MB-231 cells were seeded on a 4-chamber µslide, with 13 mm glass bottom *(ibidi GmbH, Germany)*. After 24 h cells were rinsed in phosphate buffer saline (PBS) and stained with acridine orange (AO) (1:1500 in PBS). Cell images were captured immediately by using a confocal laser-scanning fluorescence microscope Leica SP5 *(Leica Microsystem)* at 63× magnification and processed using Adobe Photoshop and ImageJ softwares (*Rasband, W.S., ImageJ, http://rsb.info.nih.gov/ij/, 1997–2008*).

b) Monodansylcadaverine staining and autophagosome formation assay. MDA-MB-231 and chMDA-MB-231 cells were incubated with the fluorescent probe monodansylcadaverine *(MDC, Sigma)* a selective marker for acidic vesicular organelles, such as autophagic vacuoles. Briefly, cells were seeded in 96-well plates (3 × 10^4 cells/well) and after 24 h were incubated in culture medium containing 50 µM MDC at 37 °C for 15 min. Cells were then washed with Hanks buffer (20 mM HEPES pH 7.2, 10 mM glucose, 118 mM NaCl, 4.6 mM KCl, and 1 mM CaCl2) and fluorescence was measured using a multimode plate reader (Ex_{340nm} and Em_{535nm}) *(GENios Pro, Tecan).* The values were normalized for cell proliferation by Crystal Violet assay.

c) LC3-II. The presence of lipidated LC3-II isoform was analysed by Western Blot as described above using mouse anti-LC3I/II antibody that detects endogenous levels of LC3B isoforms I and II.

3.13 Statistical analysis

Data reported are the means ± S.D. of a least three independent experiment. Statistical analysis were performed by one-way analysis of variance *(ANOVA)* with Bonferroni test. P value ≤ 0.05 was indicated as a statistically significant.

4. RESULTS

4.1 Survival of the cells under chronic hypoxia

In order to establish a new *in vitro* model of breast cancer dormancy, we cultured four human breast cancer cell lines in 1% O_2 atmosphere: MDA-MB-231, MDA-MB-468, T47D and MCF-7. The cells were exposed to hypoxia for 1-7 days and then the surviving cells were reoxygenated for 1-3 weeks depending on the rescue of the cells and their proliferation rate. In our hands, only MDA-MB-231 cells were able to recover their proliferation rate and grow until the confluence. Then, MDA-MB-231 cells were exposed to repetitive cycles of hypoxia/reoxygenation.

We set up the hypoxia/reoxygenation conditions regarding the number of cycles and exposure time.

The optimized procedure included exposure of MDA-MB-231 cells up to 7 days to hypoxia and reoxygenation of the surviving cells for 7-10 days depending on their viability. After reoxygenation and growing, we exposed the cell line again to a second round of hypoxia, and found an increase in viability. After three rounds of hypoxia and oxygenation, the cells, designed as chronic hypoxia resistant MDA-MB-231 (chMDA-MB-231), were able to stably grow in 1% O_2 hypoxia even if with a decreased proliferation rate. ChMDA-MB-231 cells were cultured under hypoxia for at least 3 months.

Cells cycle analysis revealed that the new established hypoxia-resistant chMDA-MB-231 cells were accumulated in G0/G1 phase and the percent in G2/M phase was drastically reduced (Figure 9A).

Analysis of CFSE dilution showed a lesser decrease of fluorescence corresponding to higher concentration of the probe in chMDA-MB-231 after 24, 48, and 72 h of culture under hypoxia respect to MDA-MB-231 in normoxia conditions. These data indicate that chMDA-MB-231 cells have a lower proliferation rate than the parental ones (Figure 9B).

The arrest in G0/G1 phase and the low proliferation rate were reversible. Indeed, once replaced into fresh medium and re-oxygenized the cells, designed as reverted chronic hypoxia resistant MDA-MB-231 (RchMDA-MB-231), showed a recovery of the proliferation rate in 2 weeks (Figure 9).

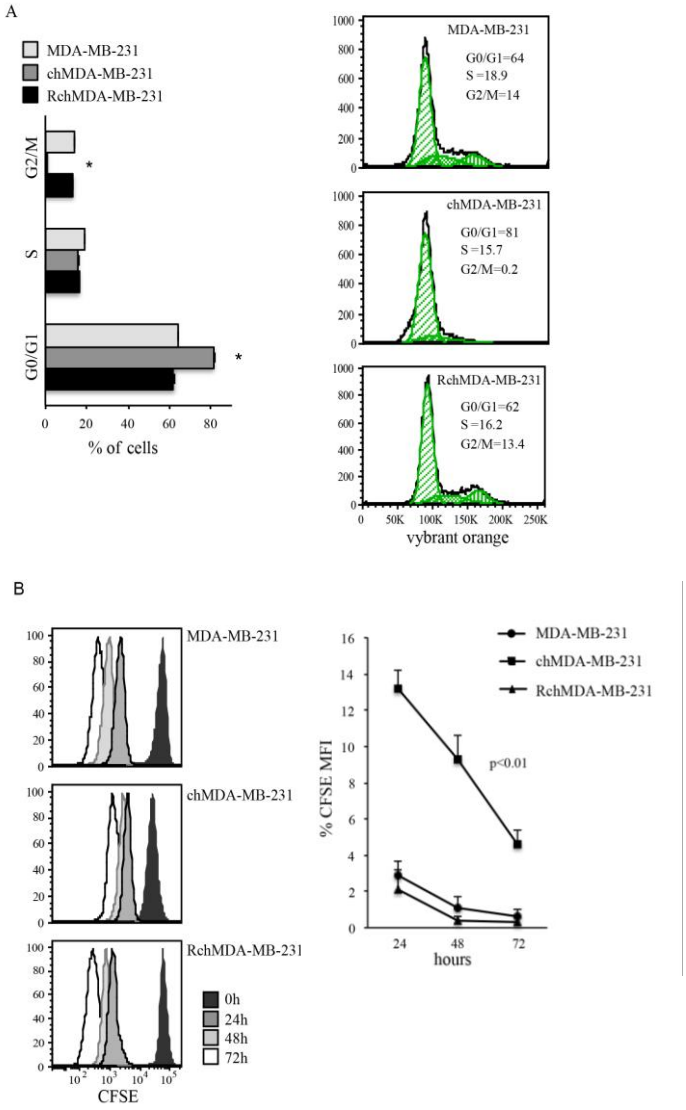

Fig. 9 MDA-MB-231 cell line can survive chronic hypoxia entering into dormant state (A) *Right*. Flow cytometry analysis of cell cycle in MDA-MD-231 cells and in chMDA-MB-231. The cells were stained with 10 μM Vybrant DyeCycle orange and with 1 μM Sytox Blue (to exclude died cells from analysis). The cell cycle of chMDA-MB-231 reoxygenated in fresh medium (RchMDA-MB-231) was analyzed too. *Left*. Statistical analysis of the cell cycle phases. *$P < 0.01$ **(B)** *Right*. Overlay histogram of the daily CFSE fluorescence intensity in the TO-PRO-3neg population. In MDA-MB-231 cells, CFSE is diluted among the daughter cells and fluorescence intensity decreases day by day. In chMDA-MB-231 cells, a lesser dilution of CFSE indicates decreased cell division. In RchMDA-MB-231 cells, the pattern of CFSE dilution is similar to that of MDA-MB-231 cells. *Left*. Plot of the daily percentage of CFSE fluorescence intensity as respect to time 0 in each condition (MFI ± SE, $P < 0.01$).
Representative results or means ± SE of at least four experiments are depicted.

Furthermore, a morphologic analysis of chMDA-MB-231, stained with the plasma CellMask dye, was performed by live confocal microscope. These cells displayed

a longer and a more fibroblastoid shape and higher cellular volume than the parental cells (Figure 10).

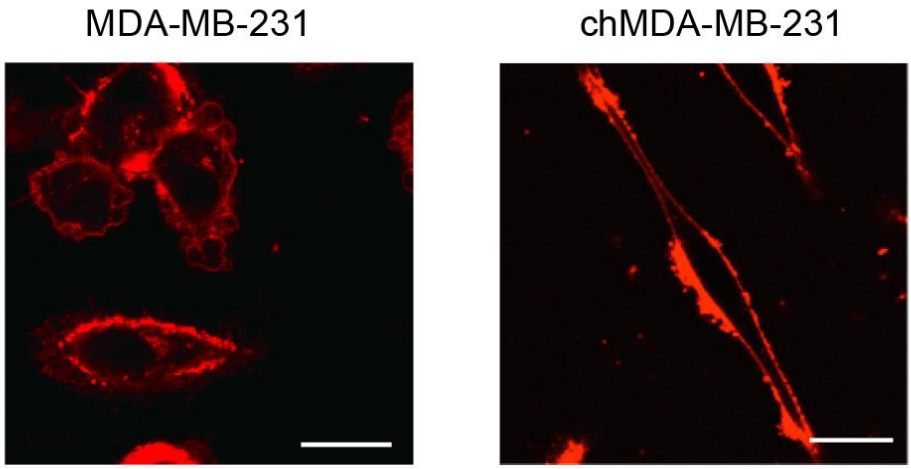

Fig. 10 Confocal microscopy of MDA-MB-231 and chMDA-MB-231 after CellMaskDeep staining. Scale bar 10 μm.

Differently from the parental cells, chMDA-MB-231 cells viability was less affected by doxorubicin, one of the most effective agents in the treatment of breast cancer patients (Figure 11).

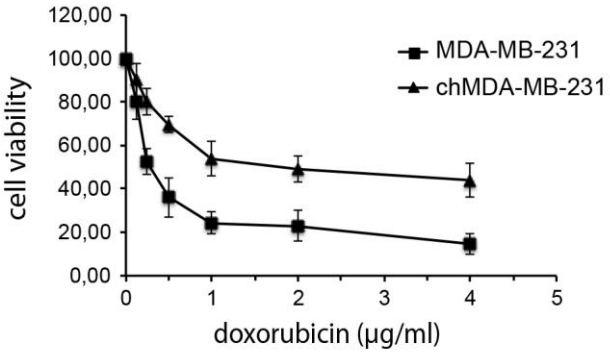

Fig. 11 Cell viability of MDA-MB-231 and chMDA-MB-231 cells after 24 h treatment with doxorubicin. ChMDA-MB-231 cells show a higher chemoresistance than the parental cells (EC_{50} = 0.25 μg/ml ± 0.05, MDA-MB-231; EC_{50} = 2.00 μg/ml ± 0.15, chMDA-MB-231). Representative results or means ± SE of at least four experiments are depicted.

All together, these results indicated that chMDA-MB-231 cells reversibly entered a dormant status under prolonged hypoxia.

In order to investigate the molecular switch of dormancy induction in MDA-MB-231 under hypoxia, we cultured cells in 1% O_2 until 7 days. Western Blot analysis of the phosphorylation state of p38 and ERK1/2 revealed that p-p38 increased after 3 days of culture in hypoxia reaching high after 7 days while p-ERK level remained stable at all time points examined. The densitometric analysis showed that the ratio of p-ERK/p-p38 in MDA-MB-231 cells cultured in hypoxia was reduced as compared to MDA-MB-231 cells in normoxia starting from 7 days (Figure 12).

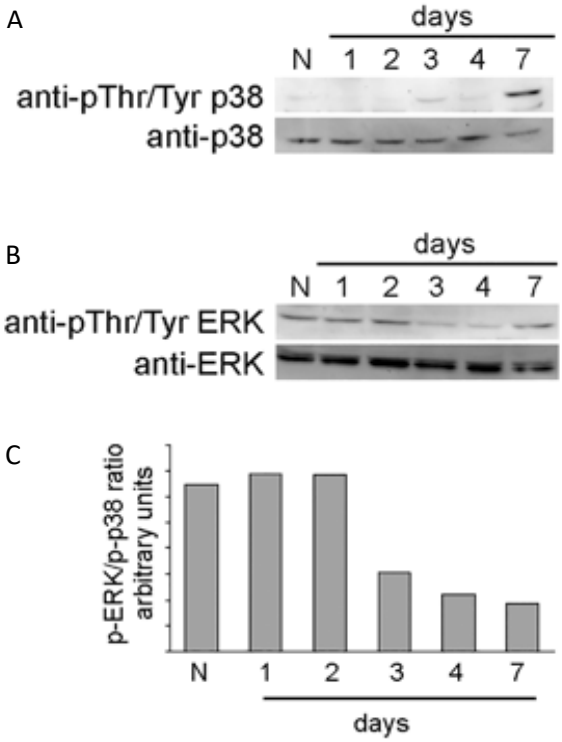

Fig. 12. Effect of chronic hypoxia on phosphorylation of ERK and p38 in MDA-MB-231. (A) Western Blot analysis shows that chronic hypoxia time-dependently triggers Thr/Tyr phosphorylation of p38. This protein was not phosphorylated when cells were cultured under normoxia (N). **(B)** ERK phosphorylation state is not modified in MDA-MB-231 cells cultured under 1% O_2 at all the indicated time. **(C)** The densitometric analysis of each Western Blot was performed by QuantityOne software. The bars represent the ratio between phosphorylation of ERK, normalized on total ERK protein, and phosphorylation of p38, normalized on total p38 protein. The images are representative of four independent experiments.

4.2 Analysis of redox state under chronic hypoxia

In order to evaluate the redox status of the cells under chronic hypoxia, measure of ROS and GSH production were performed in chMDA-MB-231.

chMDA-MB-231 cells loaded with CM-H_2DCFDA, a specific cell-permanent ROS indicator, exhibited an increase of fluorescence as respect to the parental cell line ($MF_{chMDA\text{-}MB\text{-}231}$= 1344 ± 541 vs $MFI_{MDA\text{-}MB\text{-}231}$= 331 ± 71, Figure 13A). These data indicated an enhancement of intracellular ROS in chMDA-MB-231. Moreover, the intracellular GSH concentration, measured by DTNB staining, was lower in chMDA-MB-231 cells than in parental ones (10,60 ± 2,00 nmoles/mg proteins vs 20,70 ± 1,50 nmoles/mg proteins, Figure 13B)

At the same time, confocal live microscopy analysis revealed a marked increase of mitochondrial ROS production in dormant chMDA-MB-231 cells as indicated by the appearance of a red signal, originated by the oxidation of the MitoSOX red reagent, which co-localizes with that of the mitochondrial marker (MitoTracker) (Figure 13C).

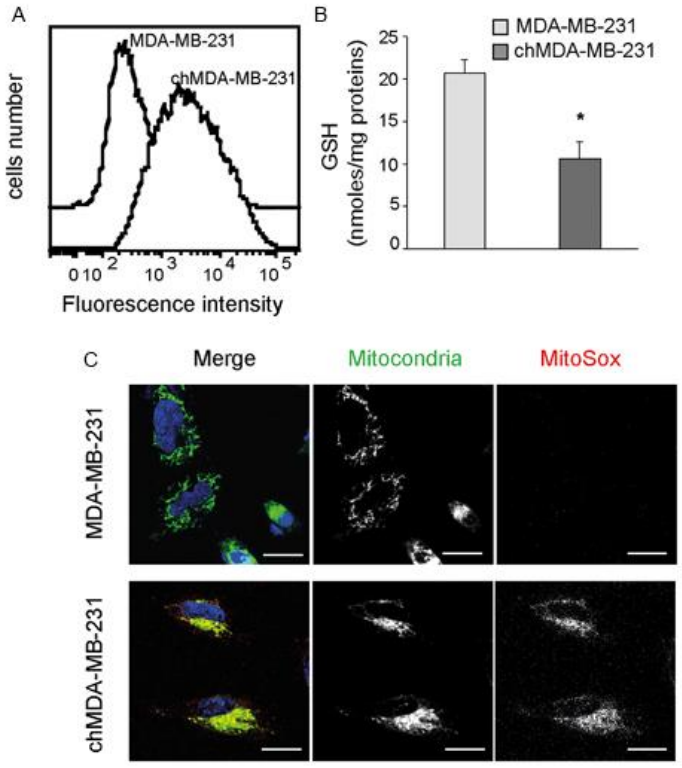

Fig. 13. Evaluation of redox state under chronic hypoxia. (A) Flow cytometry analysis of ROS production in MDA-MB-231 and chMDA-MB-231 cells loaded with CM-H_2DCFDA.The fluorescence increase in chMDA-MB-231 cells indicates a higher ROS production as respect to parental cells. **(B)** Spectrophotometric analysis of intracellular GSH concentration in MDA-MB-231 and in chMDA-MD-231. The decrease of absorbance at 420 nm in chMDA-MB-231 cells indicates a lower GSH concentration as respect to parental cells. Bar graphs represent the mean ± SE. $*P < 0.01$. Representative results of at least four experiments are depicted.
(C) Confocal live microscopy of MDA-MB-231 and chMDA-MB-231 after Mitosox, Mitotracker greenFM, and Hoescht staining. Merge and single channel images come from a single zplane. Scale bar 10 μm. The appearance of red signal in chMDA-MB-231 reveals an increase of mitochondrial ROS production.

4.3 Evaluation of energy metabolism under chronic hypoxia

We further assessed the status of energy metabolism of the cancer cells in the dormant state. We measured glucose consumption and pyruvate and lactate production in the supernatants of chMDA-MB-231 and MDA-MB-231. As expected, the metabolism of dormant cells was deeply attenuated compared to MDA-MB-231, since chMDA-MB-231 presented reduced levels of glucose consumed and pyruvate-lactate produced (Figure 14A). Moreover, under normoxic condition, the amount of lactate produced is 3.3-fold lower than that of pyruvate, while under hypoxic conditions the amounts of lactate and pyruvate are similar. These data suggest that under normoxia cells execute aerobic catabolism of pyruvate, while under hypoxia they change toward anaerobic lactic fermentation.

Next, we analyzed the expression of HIF-1α, a master regulator of energy metabolism under hypoxia. HIF-1α induces the expression of some target genes that promote angiogenesis, glycolysis, cellular proliferation or inhibition and metastasis. In line with another study performed by Wang *et al.*, MDA-MB-231 cells constitutively expressed HIF-1α under normal oxygen conditions (109) while chMDA-MB-231 cells present a lower level of HIF-1α protein (Figure 14B). As expected, the expression of GLUT1, GAPDH, and PGK, three glycolytic genes regulated by HIF-1α, decreased in chMDA-MB-231 as compared to MDA-MB-231 (Figure 14C).

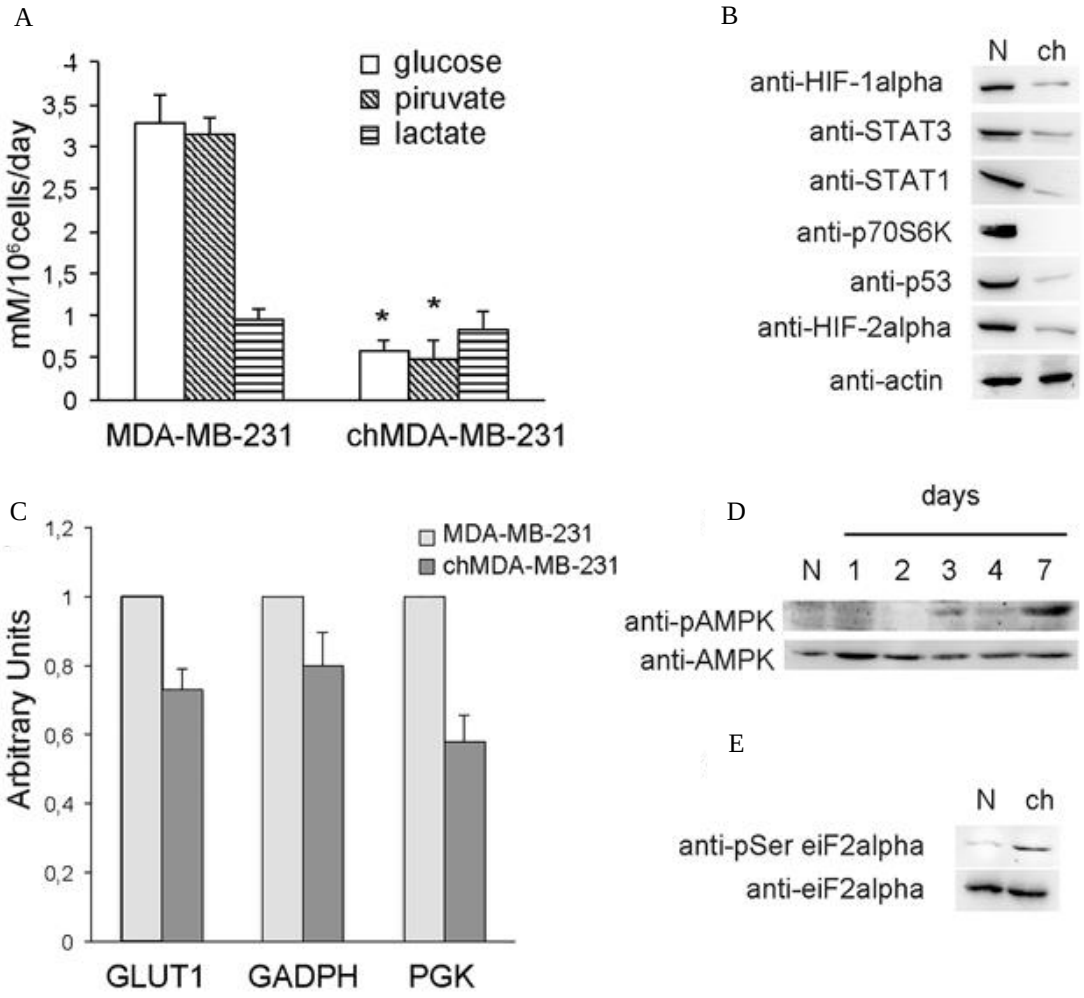

Fig. 14. Effect of chronic hypoxia on energy metabolism and protein expression in MDA-MB-231. (A) Analysis of MDA-MB-231 and chMDA-MB-231 cells metabolism. The media were analyzed to define the amount of glucose consumed (□), pyruvate produced (▧), and lactate produced (▤). Bar graphs represent the means of glucose consumed ± SE of three independent experiments. *$P < 0.01$ versus normoxic condition. **(B)** Western blot analysis of various proteins expression in chMDA-MB-231 (ch) compared to MDA-MB-231 (N). Actin is used as control loading. The images are representative of four independent experiments. **(C)** Histograms of the analysis of GLUT1, GAPDH, and PGK gene expression in MDA-MB-231 in normoxic and hypoxic conditions by RT-PCR. **(D)** Western blot analysis shows that chronic hypoxia up-regulated Thr phosphorylation of AMPK without affecting the total amount of AMPK in MDA-MB-231. MDA-MB-231 cells cultured under normoxic condition were used as control (N). **(E)** Western blot analysis shows that chronic hypoxia up-regulated Ser phosphorylation of eIF2α (ch) without affecting the total amount of eIF2 in chMDA-MB-231. MDA-MB-231 cells cultured under normoxic condition were used as control (N). The images are representative of four independent experiments.

Since it has been described that AMPK inhibits energy-consuming pathways in conditions of starvation and increases energy-producing one, we performed Western Blot analysis in order to evaluate the phosphorylation state of AMPK in cells under hypoxia. As shown in figure 14D, threonine phosphorylation of AMPK increased in MDA-MB-231 after 7 days of hypoxia as compared to cells cultured under normoxia.

All together, the obtained data confirm the lowering of energy metabolism under chronic hypoxia conditions and highlight another characteristic of cancer cells in dormant state.

4.4 Chronic hypoxia induces different protein profile in MDA-MB-231

In order to evaluate protein expression profile of chMDA-MB-231, we performed Western Blot analysis of some proteins crucial for the development of cancer. As shown in Figure 14B, the expression of various proteins was down-modulated in chMDA-MB-231, suggesting a clear difference between the protein expression profile of cells cultured under normoxia and hypoxia. Therefore, we analyzed the phosphorylation state of eIF2α, a key factor in the modulation of global protein synthesis (110). It has been described that different cellular stresses phosphorylate eIF2 on serine 51 resulting in the promotion of a pro-adaptive signaling pathway by the inhibition of global protein synthesis (111). As shown in Figure 14E, the phosphorylation of eIF2α increased in chMDA-MB-231 compared to parental cell line.

4.5 Chronic hypoxia selects cancer stem cells population

As described in the Introduction Section, hypoxic TME exerts a physiological pressure that selects cells with stemness properties. This sub-population promotes tumor invasion, metastasis and overcomes standard therapies. Furthermore, CSCs are able to induce tumorspheres formation (112).

In order to investigate whether chMDA-MB-321 were characterized by stemness markers, we performed a flow cytometry analysis of CD24, CD44 and ESA, that are characteristics markers of breast cancer stem cells (112,113). We found that

chMDA-MB-231 cells were $CD24^-$ (data not shown) and displayed an up-modulation of CD44 and ESA expression in comparison with the parental cell line (Figure 15A).

In order to test the ability of chronic hypoxia to induce tumorspheres formation, the floating cells in the culture medium of chMDA-MB-231 cells (F-chMDA-MB-231), were analyzed by Trypan Blue assay and flow cytometry F-chMDA-MB-231 cells were still viable, $CD24^-$ (data not shown) and express higher level of CD44 and ESA in comparison to parental cells (Figure 15A). The cells were seeded at low density on coated 96 multiwell plates and cultured under hypoxic condition for 10 days. Images of cells were taken at days 1, 3, 5, 7 and 10 to visualize the formation of tumorspheres. After 3 days of hypoxia, the cells were able to form tumorspheres of at least 80 μm that were able to proliferate reaching the diameter of 150 μm after 10 days (Figure 15B). Live cell imaging of tumorspheres after 10 days, stained with a nuclear probe (Hoechst) and a plasma membrane marker (CellMask) are reported in Figure 15C.

Furthermore, chMDA-MB-231 tumorspheres (150 μm diameter) were able to re-differentiate into adherent cells re-acquiring epithelial morphology after 7-10 days of culturing in normoxic condition (Figure 15B).

As expected, parental cell line MDA-MB-231 did not show the formation of tumorspheres under normoxia conditions (data not shown).

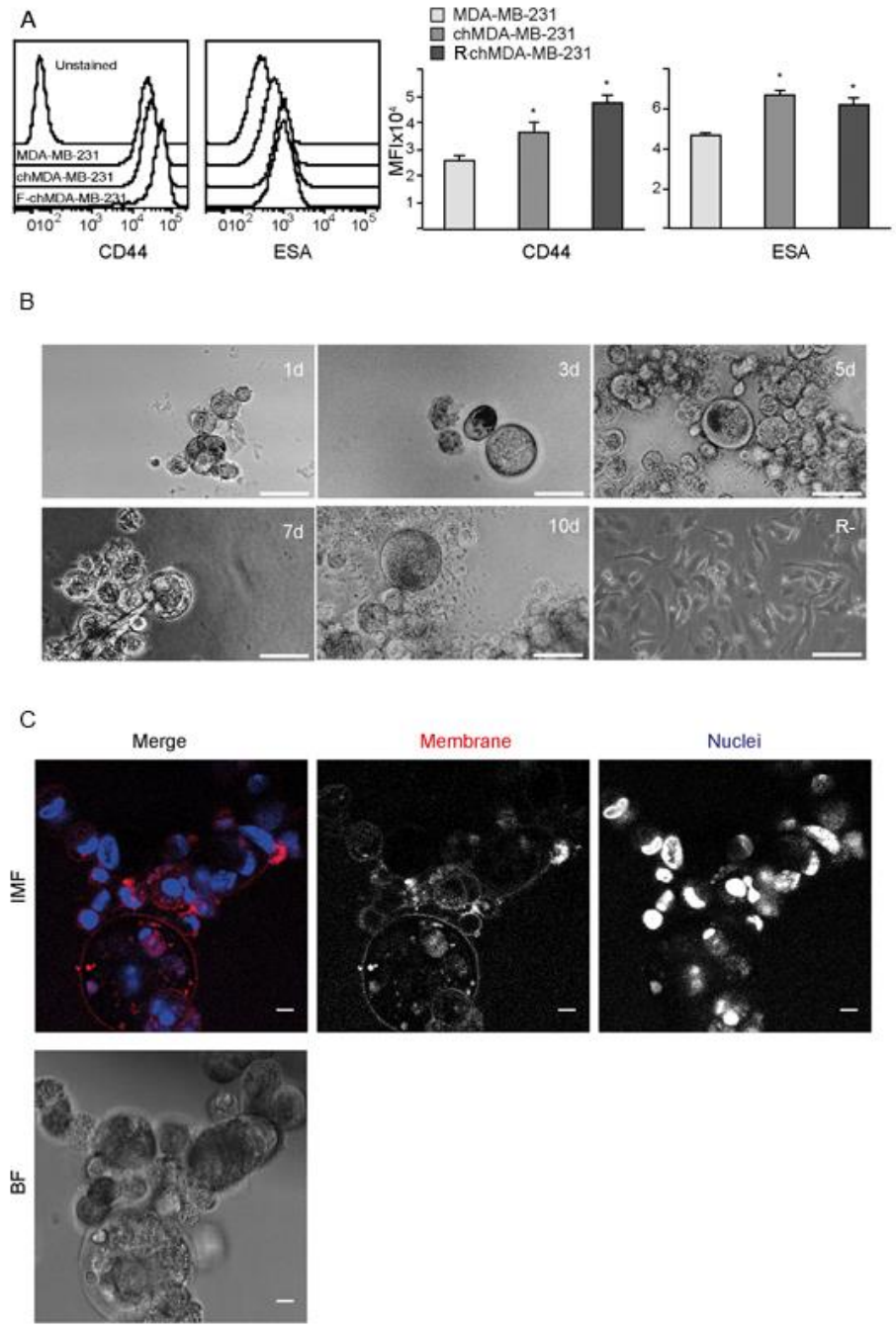

Fig.15 Chronic hypoxia selects cancer stem cells population. **(A)** Cell surface expression of CD44 and ESA in MDA-MB-231 and chMDA-MB-231. Left. Flow cytometry pattern. Right. Quantitative comparison (MFI). Bar graphs represent the mean ± SE of at least four independent $*P < 0.01$ versus normoxic condition. **(B)** Phase-contrast microscopy images of tumorospheres formation starting from the viable floating cells in the culture medium of chMDA-MB-231 on day 1, 3, 5, 7, and 10. The image of RchMDA-MB-231 (150 μm diameter) reoxygenated in fresh medium was analyzed too (R-). Representative images from three separate experiments are shown. Scale bar 50 μm. **(C)** Confocal live cell microscopy of spheroids after 10 days under chronic hypoxia stained with nuclear probe Hoechst and plasma membrane marker CellMaskDeep. Representative images from three separate experiments are shown.

4.6 Autophagy sustains MDA-MB-231 under chronic hypoxia

It is now recognized that autophagy is not only a cellular process that removes damaged cellular components but also promotes cell survival during stress conditions of cancer cells (85). Moreover, it has been reported that autophagy induction may also contributes to tumor dormancy (96).

We examined the activation of autophagic process in chMDA-MB-231 through the formation of autolysosomes (autophagic vesicles fused with lysosomes) using the fluorescent probe AO, which changes fluorescence emission from green to red upon accumulation into lysosomal acidic compartments. Live cell staining with AO revealed a significant increase of red dots in the cytosol of chMDA-MB-231 as compared to MDA-MB-231 cultured under normoxia where AO displayed mainly a diffuse green pattern (Figure 16A). The induction of autophagy was supported by six-fold MDC uptake increase in chMDA-MB-231 cells (Figure 16B).

To confirm the activation of autophagy, we also examined the presence of LC3-II by Western Blot. As described before, during activation of the autophagic process, LC3-I is cleaved and conjugated with phosphatidylethanolamine to form LC3-II. As expected, under chronic hypoxic conditions Western Blot showed increased LC3-II accumulation (Figure 16C).

It has been previously demonstrated that epithelial ovarian cancer cells enter a dormant state and survive through autophagy controlled in part by decreased AKT signaling (114,115). Western Blot analysis showed that serine phosphorylation of AKT was down-regulated in chMDA-MB-231 cells compared to MDA-MB-231cells cultured under normoxia (Figure 16C). The AKT kinase has a crucial role in the PI3K/AKT/mTOR pathway, which phosphorylates numerous targets to regulate cellular functions including growth, proliferation and survival (116). Since the protein level of 70S6K, a downstream target of mTORC1, was decreased in chMDA-MB-231, we could not verify the activation of this protein.

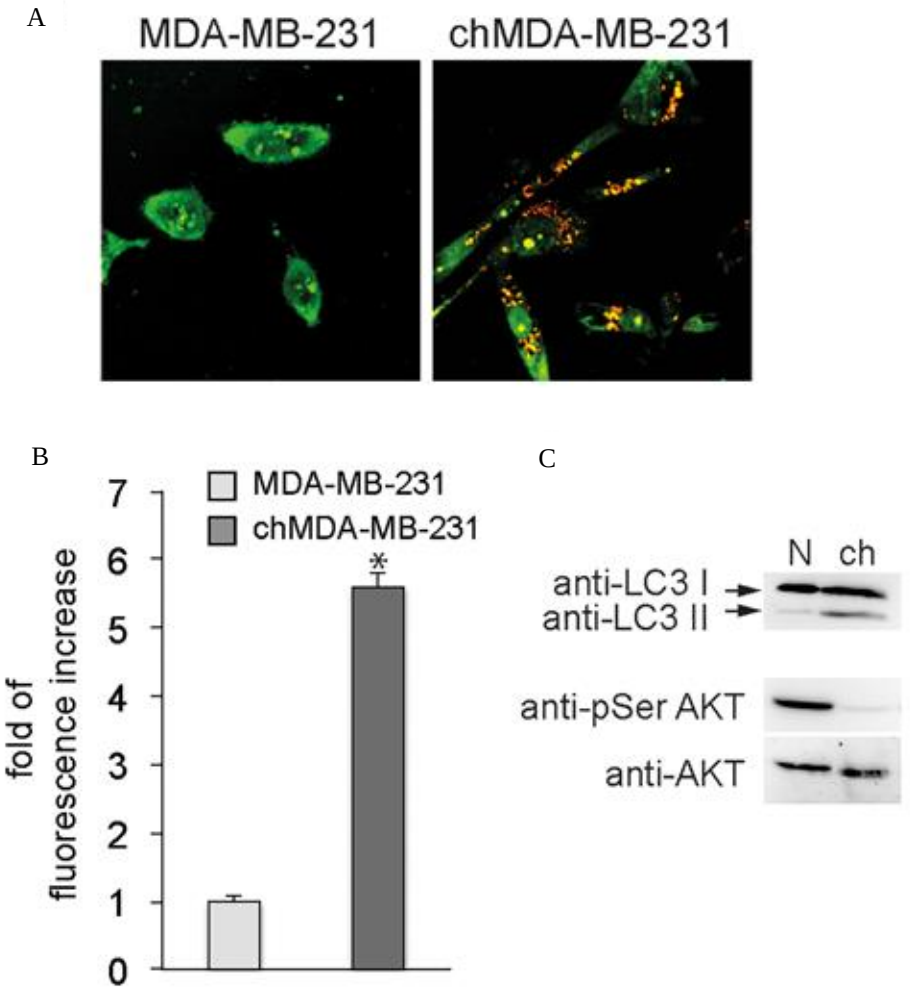

Fig. 16 Analysis of autophagy in chMDA-MB-231. (A) Confocal microscopy of MDA-MB-231 after Acridine Orange staining. Scale bar 10 µm. The image are representative of three biological replicates. The red dots in the cytosol of chMDA-MB-231 indicate the formation of autolysosomes. **(B)** Monodansylcadaverine incorporation assay in MDA-MB-231 and chMDA-MB-231 cells. Bar graphs represent the mean ± SE of at least three independent replicates, each performed using three technical replicates.*$P < 0.05$. **(C)** Western blot of the autophagy-related protein LC3 and of the serine phosphorylation state of AKT in MDA-MB-231 (N) and chMDA-MB-231 (ch). The induction of autophagy was confirmed by the appearance of LC3-II that is downregulated in chMDA-MB-231 cells compared to the parental cells. AKT expression was used as control loading. The images are representative of four independent experiments.

In order to verify the contribute of the autophagic process to chMDA-MB-231 survival under chronic hypoxia, the cells were treated with chloroquine, a well-known inhibitor of autophagy. Once established the non-toxic concentration of chloroquine for the cells, MDA-MB-231 and chMDA-MB-231 were treated with 20 and 40 µM chloroquine for 72 h. The viability of chMDA-MB-231 cells, was more affected than that of MDA-MB-231 cells after treatment with both concentrations of chloroquine indicating that autophagy could contribute to the survival of chMDA-MB-231 under chronic hypoxia (Figure 17).

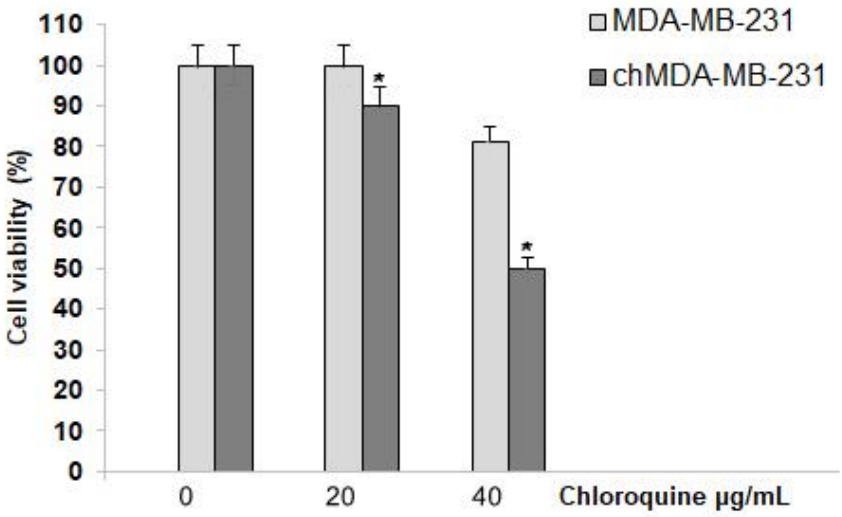

Fig 17. Cell viability after treatment of chloroquine in MDA-MB-231 and chMDA-MB-231. The inhibition of autophagy by treatment with chloroquine in chMDA-MB-231 results in lower cell viability than MDA-MB-231 cells**.** Bar graphs represent the mean ± SE of three independent experiments. **P* < 0.05.

5. DISCUSSION

TME, comprising a network of different components, regulates tumor initiation and development, contributes to metastasis appearance and has profound effects on the efficacy of therapies. TME is characterized by an irregular vasculature, which impairs blood flow in tumors and causes different regions of hypoxia. Some studies show that tumor cells adapt themselves to hypoxia, modifying their growth, metabolism and resistance to chemotherapy. Cells exposed to hypoxia as well as to consecutive cycle of hypoxia/reoxygenation, can enter a quiescent state that induces them to dormancy. Although dormant cancer cells do not directly contribute to tumor growth, they can be a reservoir and a source of tumorigenic cancer stem cells.

The lack of established *in vitro* models of tumor dormancy represents one of the major factors that hamper the understanding of dormant cells responses and a hypoxia-resistant cell line might be useful for the study of cancer dormancy. Herein, we demonstrate that chronic hypoxia conditions, that mimics TME enriche MDA-MB-231 cells for a dormant cells population that is normally under-represented in the parental cell line. We exposed different breast cancer cell lines to repetitive cycle of hypoxia/reoxygenation but most of them did not survive after 1-2 cycles. Only MDA-MB-231 cells were able to adapt to repetitive cycles of hypoxia/reoxygenation and survive under prolonged hypoxic condition.

Disputed data concerning the ability of breast cancer cells to survive in hypoxic conditions are present in the literature. Although some researchers established human breast MCF7 hypoxia-resistant cell line, in our hands, these cells did not survive after two cycles of hypoxia/reoxygenation. These differences may be due to the use of different culture conditions (i.e. cellular density and medium composition) and type of hypoxia induction (i.e. cobalt chloride) in comparison to our model (117,118). It is important to note that triple negative MDA-MB-231 cell line is one of the most aggressive among breast cancer cell lines analyzed and this feature might contribute to survival of the cells in adverse conditions.

The chMDA-MB-231cell line established in this work, shows decreased proliferation, arrest in G0/G1 phase and low metabolic rate that are characteristic features of dormant state. Previous studies from Aguirre-Ghiso laboratory showed

that proliferating human head, and neck carcinoma cell line HEp3, displayed a high p-ERK/p-p38 ratio that favors proliferation in vivo. Reprogramming cells into dormant HEp3 presented a reversion of this ratio that resulted in a prevalence of p-p38 over p-ERK signaling (35,37,41). Accordingly, we demonstrated that p38 phosphorylation was increased in MDA-MB-231 after 7 days of hypoxia, resulting in a lower p-ERK/p-p38 ratio that induced a prolonged phase of dormancy.

When the cells adapt their metabolic activity to TME conditions, AMPK acts as a metabolic checkpoint by activating catabolic process and inhibiting anabolic metabolism. Our study shows that AMPK was activated in MDA-MB-231 starting from 7 days of hypoxia suggesting that AMPK activation could regulate cellular energy homeostasis through the autophagic recycling of intracellular components, as recently described (119,120).

Some works report that hypoxia promotes autophagy as cells survival mechanism in the tumor mass as well as in tumor lines (96). In addition to this, many reports describe that oxidative stress, induced by the ROS increase and GSH depletion, directly correlates with autophagy activation (121-124). Accordingly, we measured an increase of ROS production and decrease of GSH concentration in chMDA-MB-231 cell line. Furthermore, we found that chMDA-MB-231 cells have a high level of autophagy, as analyzed by the detection of autophagolysomes and LC3-II expression, suggesting that autophagy may be the survival mechanism of dormant chMDA-MB-231 cells. As previously described, in chronic hypoxia inhibition of AKT activity is necessary for the activation of autophagy (125) and it is also crucial for the induction of dormancy and survival of cancer cells (44). In accordance with these data, AKT serine phosphorylation was suppressed in chMDA-MB-231 respect to the parental cell line in normoxia, preserving the energy source by decreasing energy demand. Protein synthesis is one of the most energy-demanding process and the initiating factor eIF2α plays an important role in the down regulation of protein synthesis in response to hypoxic stress (110). Our data, consistent with this notion, show an increase of the phosphorylation of eIF2α in chMDA-MB-231 compared to parental cell line, confirming the arrest of the protein synthesis in response to hypoxia.

It is known that hypoxia exposures can drive a reversible phenotype that enhances stem-like properties of cells to ensure survival of the tumor. Moreover, recent evidences reveal a correlation between cell dormancy and stemness, even if the mechanisms underlying these two phenomena remain discussed. The data of this work demonstrate that, different cycles of hypoxia/reoxygenation select a MDA-MB-231 population that presents the characteristics stemness phenotype of CSCs $CD24^{-}/CD44^{+}/ESA^{+}$ and generates tumorspheres. It is widely described that spheroids have a clinical and biological relevance in many tumors (126-128). It is well accepted that spheroids cultures more properly mimic the cell-cell or cell-matrix interactions, metabolic gradients, cellular viability and differentiation of malignant cells within tumor mass than the monolayers cells culture do (129).

We believe that this study describes a valid *in vitro* approach to select dormant cancer cells that own stemness properties using hypoxia /reoxygenation regime. This may represent an area with profound implications for therapeutic developments in oncology.

6. REFERENCES

1. Klemm, F., and Joyce, J. A. (2015) Microenvironmental regulation of therapeutic response in cancer. *Trends in cell biology* **25**, 198-213

2. Pattabiraman, D. R., and Weinberg, R. A. (2014) Tackling the cancer stem cells - what challenges do they pose? *Nature reviews. Drug discovery* **13**, 497-512

3. Zhu, Y., Knolhoff, B. L., Meyer, M. A., Nywening, T. M., West, B. L., Luo, J., Wang-Gillam, A., Goedegebuure, S. P., Linehan, D. C., and DeNardo, D. G. (2014) CSF1/CSF1R blockade reprograms tumor-infiltrating macrophages and improves response to T-cell checkpoint immunotherapy in pancreatic cancer models. *Cancer research* **74**, 5057-5069

4. Lu, P., Takai, K., Weaver, V. M., and Werb, Z. (2011) Extracellular matrix degradation and remodeling in development and disease. *Cold Spring Harbor perspectives in biology* **3**

5. Casey, S. C., Amedei, A., Aquilano, K., Azmi, A. S., Benencia, F., Bhakta, D., Bilsland, A. E., Boosani, C. S., Chen, S., Ciriolo, M. R., Crawford, S., Fujii, H., Georgakilas, A. G., Guha, G., Halicka, D., Helferich, W. G., Heneberg, P., Honoki, K., Keith, W. N., Kerkar, S. P., Mohammed, S. I., Niccolai, E., Nowsheen, S., Vasantha Rupasinghe, H. P., Samadi, A., Singh, N., Talib, W. H., Venkateswaran, V., Whelan, R. L., Yang, X., and Felsher, D. W. (2015) Cancer prevention and therapy through the modulation of the tumor microenvironment. *Seminars in cancer biology* **35 Suppl**, S199-223

6. Kim, J., Kim, J., and Bae, J. S. (2016) ROS homeostasis and metabolism: a critical liaison for cancer therapy. *Experimental & molecular medicine* **48**, e269

7. Warburg O., W. F., Negelein E. (1927) the metabolism of the tumors in the body. *J Gen Physiol* **8**, 519-530

8. Damaghi, M., Wojtkowiak, J. W., and Gillies, R. J. (2013) pH sensing and regulation in cancer. *Frontiers in physiology* **4**, 370

9. Carmeliet, P., and Jain, R. K. (2000) Angiogenesis in cancer and other diseases. *Nature* **407**, 249-257

10. Gee, M. S., Procopio, W. N., Makonnen, S., Feldman, M. D., Yeilding, N. M., and Lee, W. M. F. (2003) Tumor Vessel Development and Maturation Impose Limits on the Effectiveness of Anti-Vascular Therapy. *American Journal of Pathology* **162**

11. Bayer, C., and Vaupel, P. (2012) Acute versus chronic hypoxia in tumors: Controversial data concerning time frames and biological consequences. *Strahlentherapie und Onkologie : Organ der Deutschen Rontgengesellschaft ... [et al]* **188**, 616-627

12. Vaupel, P., and Harrison, L. (2004) Tumor Hypoxia: Causative Factors, Compensatory Mechanisms, and Cellular Response. *The Oncologist* **9**

13. Michiels, C., Tellier, C., and Feron, O. (2016) Cycling hypoxia: A key feature of the tumor microenvironment. *Biochimica et biophysica acta* **1866**, 76-86

14. Martinive, P., Defresne, F., Bouzin, C., Saliez, J., Lair, F., Grégoire, V., Michiels, C., Dessy, C., and Feron, O. (2006) Preconditioning of the Tumor Vasculature and Tumor Cells by Intermittent Hypoxia: Implications for Anticancer Therapies. *Cancer research* **66**, 11736

15. Hsieh, C.-H. (2010) Cycling hypoxia increases U87 glioma cell radioresistance via ROS induced higher and long-term HIF-1 signal transduction activity. *Oncology Reports* **24**

16. Eales, K. L., Hollinshead, K. E., and Tennant, D. A. (2016) Hypoxia and metabolic adaptation of cancer cells. *Oncogenesis* **5**, e190

17. Bellot, G., Garcia-Medina, R., Gounon, P., Chiche, J., Roux, D., Pouyssegur, J., and Mazure, N. M. (2009) Hypoxia-induced autophagy is mediated through hypoxia-inducible factor induction of BNIP3 and BNIP3L via their BH3 domains. *Mol Cell Biol* **29**, 2570-2581

18. Rofstad, E. K., Gaustad, J. V., Egeland, T. A., Mathiesen, B., and Galappathi, K. (2010) Tumors exposed to acute cyclic hypoxic stress show enhanced angiogenesis, perfusion and metastatic dissemination. *International journal of cancer* **127**, 1535-1546

19. Kenneth, Niall S., and Rocha, S. (2008) Regulation of gene expression by hypoxia. *Biochemical Journal* **414**, 19

20. Muz, B., de la Puente, P., Azab, F., and Azab, A. K. (2015) The role of hypoxia in cancer progression, angiogenesis, metastasis, and resistance to therapy. *Hypoxia* **3**, 83-92

21. Ginouves, A., Ilc, K., Macias, N., Pouyssegur, J., and Berra, E. (2008) PHDs overactivation during chronic hypoxia "desensitizes" HIFalpha and protects cells from necrosis. *Proceedings of the National Academy of Sciences of the United States of America* **105**, 4745-4750

22. Dewhirst, M. W., Cao, Y., and Moeller, B. (2008) Cycling hypoxia and free radicals regulate angiogenesis and radiotherapy response. *Nature reviews. Cancer* **8**, 425-437

23. Denko, N. C., Fontana, L. A., Hudson, K. M., Sutphin, P. D., Raychaudhuri, S., Altman, R., and Giaccia, A. J. (2003) Investigating hypoxic tumor physiology through gene expression patterns. *Oncogene* **22**, 5907-5914

24. Pouyssegur, J., Dayan, F., and Mazure, N. M. (2006) Hypoxia signalling in cancer and approaches to enforce tumour regression. *Nature* **441**, 437-443

25. Tong, L., Chuang, C. C., Wu, S., and Zuo, L. (2015) Reactive oxygen species in redox cancer therapy. *Cancer letters* **367**, 18-25

26. Fiaschi, T., and Chiarugi, P. (2012) Oxidative stress, tumor microenvironment, and metabolic reprogramming: a diabolic liaison. *International journal of cell biology* **2012**, 762825

27. Bablor, M. B. (1998) NADPH Oxidase: An Update. *Blood* **93**, 1464-1476

28. Cairns, R. A., Harris, I. S., and Mak, T. W. (2011) Regulation of cancer cell metabolism. *Nature reviews. Cancer* **11**, 85-95

29. Gomis, R. R., and Gawrzak, S. (2016) Tumor cell dormancy. *Molecular oncology*

30. Quail, D. F., and Joyce, J. A. (2013) Microenvironmental regulation of tumor progression and metastasis. *Nature medicine* **19**, 1423-1437

31. Naumov, G. N., Akslen, L. A., and Folkman, J. (2006) Role of angiogenesis in human tumor dormancy: animal models of the angiogenic switch. *Cell cycle* **5**, 1779-1787

32. Indraccolo, S., Favaro, E., and Amadori, A. (2006) Dormant tumors awaken by a short-term angiogenic burst: the spike hypothesis. *Cell cycle* **5**, 1751-1755

33. Sosa, M. S., Avivar-Valderas, A., Bragado, P., Wen, H. C., and Aguirre-Ghiso, J. A. (2011) ERK1/2 and p38alpha/beta signaling in tumor cell quiescence: opportunities to control dormant residual disease. *Clinical cancer research : an official journal of the American Association for Cancer Research* **17**, 5850-5857

34. Sosa, M. S., Bragado, P., and Aguirre-Ghiso, J. A. (2014) Mechanisms of disseminated cancer cell dormancy: an awakening field. *Nature reviews. Cancer* **14**, 611-622

35. Aguirre Ghiso, J. A., Liu, D., Mignatti, A., Kovalski, K., and Ossowski, L. (2001) Urokinase receptor and fibronectin regulate the ERK(MAPK) to p38(MAPK) activity ratios that determine carcinoma cell proliferation or dormancy in vivo. *Molecular biology of the cell* **12**, 863-879

36. Koul, H. K., Pal, M., and Koul, S. (2013) Role of p38 MAP Kinase Signal Transduction in Solid Tumors. *Genes & cancer* **4**, 342-359

37. Aguirre Ghiso, J. A., Ossowski, L., and SK, R. (2004) Green fluorescent protein tagging of extracellular signal-regulated kinase and p38 pathways reveals novel dynamics of pathway activation during primary and metastastic growth. *Cancer research* **64**, 7335-7345

38. Bragado, P., Estrada, Y., Parikh, F., Krause, S., Capobianco, C., Farina, H. G., Schewe, D. M., and Aguirre-Ghiso, J. A. (2013) TGF-beta2 dictates disseminated tumour cell fate in target organs through TGF-beta-RIII and p38alpha/beta signalling. *Nature cell biology* **15**, 1351-1361

39. Aguirre-Ghiso, J. A. (2007) Models, mechanisms and clinical evidence for cancer dormancy. *Nat. Rev. Cancer* **7**, 834-846

40. Aguirre Ghiso, J. A. (2002) Inhibition of FAK signaling activated by urokinase receptor induces dormancy in human carcinoma cells in vivo. *Oncogene* **21**, 2513-2524

41. Aguirre-Ghiso, J. A., Estrada, Y., D. and Ossowsky, L. (2003) ERK (MAPK) Activity as a Determinant of Tumor Growth and Dormancy; Regulation by p38 (SAPK). *Cancer reasearch* **63**, 1684-1695

42. Schewe, D. M., and Aguirre-Ghiso, J. A. (2008) ATF6alpha-Rheb-mTOR signaling promotes survival of dormant tumor cells in vivo. *Proceedings*

of the National Academy of Sciences of the United States of America **105**, 10519-10524

43. Engelman, J. A. (2009) Targeting PI3K signalling in cancer: opportunities, challenges and limitations. *Nature Reviews Cancer* **9**, 550

44. Endo, H., Okuyama, H., Ohue, M., and Inoue, M. (2014) Dormancy of cancer cells with suppression of AKT activity contributes to survival in chronic hypoxia. *PloS one* **9**, e98858

45. Memmott, R. M., and Dennis, P. A. (2009) Akt-dependent and -independent mechanisms of mTOR regulation in cancer. *Cellular signalling* **21**, 656-664

46. Banys, M., Hartkopf, A. D., Krawczyk, N., Kaiser, T., Meier-Stiegen, F., Fehm, T., and Neubauer, H. (2012) Dormancy in breast cancer. *Breast cancer* **4**, 183-191

47. Yeh, A. C., and Ramaswamy, S. (2015) Mechanisms of Cancer Cell Dormancy--Another Hallmark of Cancer? *Cancer research* **75**, 5014-5022

48. Zhang, S., Mercado-Uribe, I., Xing, Z., Sun, B., Kuang, J., and Liu, J. (2014) Generation of Cancer Stem-like Cells through Formation of Polyploid Giant Cancer Cells. *Oncogene* **33**, 10.1038/onc.2013.1096

49. Linde, N., Fluegen, G., and Aguirre-Ghiso, J. A. (2016) The Relationship Between Dormant Cancer Cells and Their Microenvironment. *Advances in cancer research* **132**, 45-71

50. Lu, X., Mu, E., Wei, Y., Riethdorf, S., Yang, Q., Yuan, M., Yan, J., Hua, Y., Tiede, B. J., Lu, X., Haffty, B. G., Pantel, K., Massagué, J., and Kang, Y. (2011) VCAM-1 promotes osteolytic expansion of indolent bone micrometastasis of breast cancer by engaging α4β1-positive osteoclast progenitors. *Cancer cell* **20**, 701-714

51. Malladi, S., Macalinao, D. G., Jin, X., He, L., Basnet, H., Zou, Y., de Stanchina, E., and Massagué, J. (2016) Metastatic Latency and Immune Evasion Through Autocrine Inhibition of WNT. *Cell* **165**, 45-60

52. Box, G. M., and Eccles, S. A. (2011) Simple Experimental and Spontaneous Metastasis Assays in Mice. in *Cell Migration: Developmental Methods and Protocols* (Wells, C. M., and Parsons, M. eds.), Humana Press, Totowa, NJ. pp 311-329

53. Rosol, T. J., Tannehill-Gregg, S. H., Corn, S., Schneider, A., and McCauley, L. K. (2004) Animal Models of Bone Metastasis. in *The Biology of Skeletal Metastases* (Keller, E. T., and Chung, L. W. K. eds.), Springer US, Boston, MA. pp 47-81

54. Lawson, M. A., McDonald, M. M., Kovacic, N., Hua Khoo, W., Terry, R. L., Down, J., Kaplan, W., Paton-Hough, J., Fellows, C., Pettitt, J. A., Neil Dear, T., Van Valckenborgh, E., Baldock, P. A., Rogers, M. J., Eaton, C. L., Vanderkerken, K., Pettit, A. R., Quinn, J. M. W., Zannettino, A. C. W., Phan, T. G., and Croucher, P. I. (2015) Osteoclasts control reactivation of dormant myeloma cells by remodelling the endosteal niche. *Nature Communications* **6**, 8983

55. Hüsemann, Y., Geigl, J. B., Schubert, F., Musiani, P., Meyer, M., Burghart, E., Forni, G., Eils, R., Fehm, T., Riethmüller, G., and Klein, C. A. (2008) Systemic Spread Is an Early Step in Breast Cancer. *Cancer cell* **13**, 58-68

56. Folkman, J. (2002) Role of angiogenesis in tumor growth and metastasis. *Seminars in Oncology* **29**, 15-18

57. Holmgren, L., O'Reilly, M. S., and Folkman, J. (1995) Dormancy of micrometastases: Balanced proliferation and apoptosis in the presence of angiogenesis suppression. *Nature medicine* **1**, 149

58. Naumov, G. N., Bender, E., Zurakowski, D., Kang, S.-Y., Sampson, D., Flynn, E., Watnick, R. S., Straume, O., Akslen, L. A., Folkman, J., and Almog, N. (2006) A Model of Human Tumor Dormancy: An Angiogenic Switch From the Nonangiogenic Phenotype. *JNCI: Journal of the National Cancer Institute* **98**, 316-325

59. Uhr, J. W., and Pantel, K. (2011) Controversies in clinical cancer dormancy. *Proceedings of the National Academy of Sciences* **108**, 12396-12400

60. Weinhold, K. J., Goldstein, L. T., and Wheelock, E. F. (1979) The tumor dormant state. Quantitation of L5178Y cells and host immune responses during the establishment and course of dormancy in syngeneic DBA/2 mice. *The Journal of Experimental Medicine* **149**, 732

61. Aguirre-Ghiso, J. A. (2007) Models, mechanisms and clinical evidence for cancer dormancy. *Nature rewies Cancer* **7**, 834-846

62. Naumov, G. N., MacDonald, I. C., Weinmeister, P. M., Kerkvliet, N., Nadkarni, K. V., Wilson, S. M., Morris, V. L., Groom, A. C., and Chambers, A. F. (2002) Persistence of Solitary Mammary Carcinoma Cells in a Secondary Site. *Cancer research* **62**, 2162

63. Lobo, N. A., Shimono, Y., Qian, D., and Clarke, M. F. (2007) The biology of cancer stem cells. *Annual review of cell and developmental biology* **23**, 675-699

64. Jaggupilli, A., and Elkord, E. (2012) Significance of CD44 and CD24 as cancer stem cell markers: an enduring ambiguity. *Clinical & developmental immunology* **2012**, 708036

65. Botchkina, I. L., Rowehl, R., Rivadeneira, D. E., Karpeh JR, M. S., Crawford, H., Dufour, A., Ju, J., Wang, Y., Yan, L., and Botchkina, G. I. (2009) Phenotypic Subpopulations of Metastatic Colon Cancer Stem Cells: Genomic Analysis. *Cancer Genomics and Proteomics* **6**, 19-30

66. Du, L., Wang, H., He, L., Zhang, J., Ni, B., Wang, X., Jin, H., Cahuzac, N., Mehrpour, M., Lu, Y., and Chen, Q. (2008) CD44 is of functional importance for colorectal cancer stem cells. *Clinical cancer research : an official journal of the American Association for Cancer Research* **14**, 6751-6760

67. Leung, E. L.-H., Fiscus, R. R., Tung, J. W., Tin, V. P.-C., Cheng, L. C., Sihoe, A. D.-L., Fink, L. M., Ma, Y., and Wong, M. P. (2010) Non-Small Cell Lung Cancer Cells Expressing CD44 Are Enriched for Stem Cell-Like Properties. *PloS one* **5**, e14062

68. Abraham, B. K., Fritz, P., McClellan, M., Hauptvogel, P., Athelogou, M., and Brauch, H. (2005) May Not Be Associated with Clinical Outcome but May Favor Distant Metastasis. *Clinical Cancer Research* **11**, 1154-1159

69. Sertil, A. R. (2014) Hypoxia and Tumor Dormancy: Can the Two Tango? , 13-24

70. Bar, E. E., Lin, A., Mahairaki, V., Matsui, W., and Eberhart, C. G. (2010) Hypoxia increases the expression of stem-cell markers and promotes clonogenicity in glioblastoma neurospheres. *The American journal of pathology* **177**, 1491-1502

71. Li, Z., and Rich, J. N. (2010) Hypoxia and hypoxia inducible factors in cancer stem cell maintenance. *Current topics in microbiology and immunology* **345**, 21-30

72. Patel, P., and Chen, E. I. (2012) Cancer stem cells, tumor dormancy, and metastasis. *Frontiers in Endocrinology* **3**, 125

73. Giancotti, F. G. (2013) Mechanisms Governing Metastatic Dormancy and Reactivation. *Cell* **155**, 750-764

74. Liu, G., Yu, J., Qian, F., Huang, J., Tang, Z., Wang, Y., and Zhu, J. (2014) [Cell morphology in the dormancy and proliferation stage of colorectal

cancer stem cells]. *Zhonghua wei chang wai ke za zhi = Chinese journal of gastrointestinal surgery* **17**, 279-283

75. Lin, W.-C., Rajbhandari, N., and Wagner, K.-U. (2014) Cancer cell dormancy in novel mouse models for reversible pancreatic cancer: a lingering challenge in the development of targeted therapies. *Cancer research* **74**, 2138-2143

76. Zhou, N., Wu, X., Yang, B., Yang, X., Zhang, D., and Qing, G. (2014) Stem cell characteristics of dormant cells and cisplatininduced effects on the stemness of epithelial ovarian cancer cells. *Molecular medicine reports* **10**, 2495-2504

77. Plaks, V., Kong, N., and Werb, Z. (2015) The cancer stem cell niche: how essential is the niche in regulating stemness of tumor cells? *Cell stem cell* **16**, 225-238

78. Axelson, H., Fredlund, E., Ovenberger, M., Landberg, G., and Pahlman, S. (2005) Hypoxia-induced dedifferentiation of tumor cells--a mechanism behind heterogeneity and aggressiveness of solid tumors. *Seminars in cell & developmental biology* **16**, 554-563

79. Kleffel, S., and Schatton, T. (2013) Tumor Dormancy and Cancer Stem Cells: Two Sides of the Same Coin? in *Systems Biology of Tumor Dormancy* (Enderling, H., Almog, N., and Hlatky, L. eds.), Springer New York, New York, NY. pp 145-179

80. Bao, S., Wu, Q., Sathornsumetee, S., Hao, Y., Li, Z., Hjelmeland, A. B., Shi, Q., McLendon, R. E., Bigner, D. D., and Rich, J. N. (2006) Stem Cell–like Glioma Cells Promote Tumor Angiogenesis through Vascular Endothelial Growth Factor. *Cancer research* **66**, 7843

81. Frank, N. Y., Schatton, T., Kim, S., Zhan, Q., Wilson, B. J., Ma, J., Saab, K. R., Osherov, V., Widlund, H. R., Gasser, M., Waaga-Gasser, A.-M., Kupper, T. S., Murphy, G. F., and Frank, M. H. (2011) VEGFR-1

Expressed by Malignant Melanoma-Initiating Cells Is Required for Tumor Growth. *Cancer research* **71**, 1474-1485

82. Kondo, T., Setoguchi, T., and Taga, T. (2004) Persistence of a small subpopulation of cancer stem-like cells in the C6 glioma cell line. *Proceedings of the National Academy of Sciences of the United States of America* **101**, 781-786

83. Hirschmann-Jax, C., Foster, A. E., Wulf, G. G., Nuchtern, J. G., Jax, T. W., Gobel, U., Goodell, M. A., and Brenner, M. K. (2004) A distinct "side population" of cells with high drug efflux capacity in human tumor cells. *Proceedings of the National Academy of Sciences of the United States of America* **101**, 14228-14233

84. Dean, M., Fojo, T., and Bates, S. (2005) Tumour stem cells and drug resistance. *Nature reviews. Cancer* **5**, 275-284

85. Mizushima, N., Yoshimori, T., and Levine, B. (2010) Methods in mammalian autophagy research. *Cell* **140**, 313-326

86. Cecconi, F., and Levine, B. (2008) The role of autophagy in mammalian development: cell makeover rather than cell death. *Developmental cell* **15**, 344-357

87. Feng, Y., He, D., Yao, Z., and Klionsky, D. J. (2014) The machinery of macroautophagy. *Cell research* **24**, 24-41

88. Longatti, A., and Tooze, S. A. (2009) Vesicular trafficking and autophagosome formation. *Cell death and differentiation* **16**, 956-965

89. Mizushima, N., Yamamoto, A., Matsui, M., Yoshimori, T., and Ohsumi, Y. (2004) In vivo analysis of autophagy in response to nutrient starvation using transgenic mice expressing a fluorescent autophagosome marker. *Molecular biology of the cell* **15**, 1101-1111

90. Glick, D., Barth, S., and Macleod, K. F. (2010) Autophagy: cellular and molecular mechanisms. *The Journal of pathology* **221**, 3-12

91. Noda, T., Fujita, N., and Yoshimori, T. (2009) The late stages of autophagy: how does the end begin? *Cell death and differentiation* **16**, 984

92. Kim, I., Rodriguez-Enriquez, S., and Lemasters, J. J. (2007) Selective degradation of mitochondria by mitophagy. *Archives of Biochemistry and Biophysics* **462**, 245-253

93. Liu, S., Thomas;, S. M., Woodside;, D. G., Rose;, D. M., Kiosses;, W. B., Pfaff;, M., and Ginsberg, a. M. H. (1999) Induction of autophagy and inhibition of tumorigenesis by beclin 1. *Nature* **402**, 672-676

94. Jung, C. H., Ro, S.-H., Cao, J., Otto, N. M., and Kim, D.-H. (2010) mTOR regulation of autophagy. *FEBS letters* **584**, 1287-1295

95. Kroemer, G., and Levine, B. (2008) Autophagic cell death: the story of a misnomer. *Nat Rev Mol Cell Biol* **9**, 1004-1010

96. Degenhardt, K., Mathew, R., Beaudoin, B., Bray, K., Anderson, D., Chen, G., Mukherjee, C., Shi, Y., Gelinas, C., Fan, Y., Nelson, D. A., Jin, S., and White, E. (2006) Autophagy promotes tumor cell survival and restricts necrosis, inflammation, and tumorigenesis. *Cancer cell* **10**, 51-64

97. Lock, R., Roy, S., Kenific, C. M., Su, J. S., Salas, E., Ronen, S. M., and Debnath, J. (2011) Autophagy facilitates glycolysis during Ras-mediated oncogenic transformation. *Molecular biology of the cell* **22**, 165-178

98. Perera, R. M., Stoykova, S., Nicolay, B. N., Ross, K. N., Fitamant, J., Boukhali, M., Lengrand, J., Deshpande, V., Selig, M. K., Ferrone, C. R., Settleman, J., Stephanopoulos, G., Dyson, N. J., Zoncu, R., Ramaswamy, S., Haas, W., and Bardeesy, N. (2015) Transcriptional control of autophagy-lysosome function drives pancreatic cancer metabolism. *Nature* **524**, 361-365

99. Maycotte, P., and Thorburn, A. (2014) Autophagy and cancer therapy. *Cancer Biology & Therapy* **11**, 127-137

100. Meléndez, A., Tallóczy;, Z., Seaman;, M., Eskelinen;, E.-L., Hall, D. H., and Levine, a. B. (2003) Autophagy Genes Are Essential for Dauer Development and Life-Span Extension in C. elegans. *Science* **301**, 1387-1391

101. Lock, R., and Debnath, J. (2008) Extracellular matrix regulation of autophagy. *Current opinion in cell biology* **20**, 583-588

102. Campos, T., Ziehe, J., Fuentes-Villalobos, F., Riquelme, O., Pena, D., Troncoso, R., Lavandero, S., Morin, V., Pincheira, R., and Castro, A. F. (2016) Rapamycin requires AMPK activity and p27 expression for promoting autophagy-dependent Tsc2-null cell survival. *Biochimica et biophysica acta* **1863**, 1200-1207

103. Lu, Z., Luo, R. Z., Lu, Y., Zhang, X., Yu, Q., Khare, S., Kondo, S., Kondo, Y., Yu, Y., Mills, G. B., Liao, W. S., and Bast, R. C., Jr. (2008) The tumor suppressor gene ARHI regulates autophagy and tumor dormancy in human ovarian cancer cells. *The Journal of clinical investigation* **118**, 3917-3929

104. Sosa, M. S., Bragado, P., Debnath, J., and Aguirre-Ghiso, J. A. (2013) Regulation of tumor cell dormancy by tissue microenvironments and autophagy. *Advances in experimental medicine and biology* **734**, 73-89

105. Rigo, A., and Vinante, F. (2016) The antineoplastic agent α-bisabolol promotes cell death by inducing pores in mitochondria and lysosomes. *Apoptosis* **21**, 917-927

106. Butturini, E., Carcereri De Prati, A., Chiavegato, G., Rigo, A., Cavalieri, E., Darra, E., and Mariotto, S. (2013) *Mild oxidative stress induces S-glutathionylation of STAT3 and enhances chemosensitivity of tumoral cells to chemotherapeutic drugs*,

107. Bradford, M. M. (1976) A Rapid and Sensitive Method for the Quantitation of Microgram Quantities of Protein Utilizing the Principle of Protein-Dye Binding. *Analytical Biochemistry* **72**, 248-256

108. Butturini, E., Cavalieri, E., Carcereri de Prati, A., Darra, E., Rigo, A., Shoji, K., Murayama, N., Yamazaki, H., Watanabe, Y., Suzuki, H., and Mariotto, S. (2011) Two Naturally Occurring Terpenes, Dehydrocostuslactone and Costunolide, Decrease Intracellular GSH Content and Inhibit STAT3 Activation. *PloS one* **6**, e20174

109. Wang, F., Chang, M., Shy, Y., Jiang, I., Zhao, J., Hai, I., Sharen, G., and Du, H. (2014a) Down-reluation of hypoxia-inducible factor-1 suppresses malignant biological behaviour of triple negative breast cancer cells. *Int J Cancer Exp Med* **7**, 3933-3940

110. Koumenis, C., Naczki, C., Koritzinsky, M., Rastani, S., Diehl, A., Sonenberg, N., Koromilas, A., and Wouters, B. G. (2002) Regulation of Protein Synthesis by Hypoxia via Activation of the Endoplasmic Reticulum Kinase PERK and Phosphorylation of the Translation Initiation Factor eIF2 *Molecular and Cellular Biology* **22**, 7405-7416

111. Back, S. H., Scheuner, D., Han, J., Song, B., Ribick, M., Wang, J., Gildersleeve, R. D., Pennathur, S., and Kaufman, R. J. (2009) Translation attenuation through eIF2alpha phosphorylation prevents oxidative stress and maintains the differentiated state in beta cells. *Cell metabolism* **10**, 13-26

112. Wang, R., Lv, Q., Meng, W., Tan, Q., Zhang, S., Mo, X., and Yang, X. (2014) Comparison of mammosphere formation from breast cancer cell lines and primary breast tumors. *Journal of thoracic disease* **6**, 829-837

113. An, H., Kim, J. Y., Oh, E., Lee, N., Cho, Y., and Seo, J. H. (2015) Salinomycin Promotes Anoikis and Decreases the CD44+/CD24- Stem-Like Population via Inhibition of STAT3 Activation in MDA-MB-231 Cells. *PloS one* **10**, e0141919

114. Correa, R. J., Peart, T., Valdes, Y. R., DiMattia, G. E., and Shepherd, T. G. (2012) Modulation of AKT activity is associated with reversible dormancy in ascites-derived epithelial ovarian cancer spheroids. *Carcinogenesis* **33**, 49-58

115. Correa, R. J., Valdes, Y. R., Peart, T. M., Fazio, E. N., Bertrand, M., McGee, J., Prefontaine, M., Sugimoto, A., DiMattia, G. E., and Shepherd, T. G. (2014) Combination of AKT inhibition with autophagy blockade effectively reduces ascites-derived ovarian cancer cell viability. *Carcinogenesis* **35**, 1951-1961

116. Manning, B. D., and Cantley, L. C. (2007) AKT/PKB signaling: navigating downstream. *Cell* **129**, 1261-1274

117. Scherbakov, A. M., Lobanova, Y. S., Shatskaya, V. A., and Krasil'nikov, M. A. (2009) The breast cancer cells response to chronic hypoxia involves the opposite regulation of NF-kB and estrogen receptor signaling. *Steroids* **74**, 535-542

118. Sorokin, D. V., Scherbakov, A. M., Yakushina, I. A., Semina, S. E., Gudkova, M. V., and Krasil'nikov, M. A. (2016) The Mechanism of Adaptation of Breast Cancer Cells to Hypoxia: Role of AMPK/mTOR Signaling Pathway. *Bulletin of experimental biology and medicine* **160**, 555-559

119. Meley, D., Bauvy, C., Houben-Weerts, J. H., Dubbelhuis, P. F., Helmond, M. T., Codogno, P., and Meijer, A. J. (2006) AMP-activated protein kinase and the regulation of autophagic proteolysis. *The Journal of biological chemistry* **281**, 34870-34879

120. Matsui, Y., Takagi, H., Qu, X., Abdellatif, M., Sakoda, H., Asano, T., Levine, B., and Sadoshima, J. (2007) Distinct roles of autophagy in the heart during ischemia and reperfusion: roles of AMP-activated protein kinase and Beclin 1 in mediating autophagy. *Circulation research* **100**, 914-922

121. Scherz-Shouval, R., Shvets, E., Fass, E., Shorer, H., Gil, L., and Elazar, Z. (2007) Reactive oxygen species are essential for autophagy and specifically regulate the activity of Atg4. *Embo J* **26**, 1749-1760

122. Gao, M., Yeh, P. Y., Lu, Y. S., Hsu, C. H., Chen, K. F., Lee, W. C., Feng, W. C., Chen, C. S., Kuo, M. L., and Cheng, A. L. (2008) OSU-03012, a novel celecoxib derivative, induces reactive oxygen species-related autophagy in hepatocellular carcinoma. *Cancer research* **68**, 9348-9357

123. Li, L., Ishdorj, G., and Gibson, S. B. (2012) Reactive oxygen species regulation of autophagy in cancer: implications for cancer treatment. *Free radical biology & medicine* **53**, 1399-1410

124. Poillet-Perez, L., Despouy, G., Delage-Mourroux, R., and Boyer-Guittaut, M. (2015) Interplay between ROS and autophagy in cancer cells, from tumor initiation to cancer therapy. *Redox biology* **4**, 184-192

125. Heras-Sandoval, D., Perez-Rojas, J. M., Hernandez-Damian, J., and Pedraza-Chaverri, J. (2014) The role of PI3K/AKT/mTOR pathway in the modulation of autophagy and the clearance of protein aggregates in neurodegeneration. *Cellular signalling* **26**, 2694-2701

126. Barbone, D., Yang, T. M., Morgan, J. R., Gaudino, G., and Broaddus, V. C. (2008) Mammalian target of rapamycin contributes to the acquired apoptotic resistance of human mesothelioma multicellular spheroids. *The Journal of biological chemistry* **283**, 13021-13030

127. Sodek, K. L., Ringuette, M. J., and Brown, T. J. (2009) Compact spheroid formation by ovarian cancer cells is associated with contractile behavior and an invasive phenotype. *International journal of cancer* **124**, 2060-2070

128. Wenzel, C., Riefke, B., Grundemann, S., Krebs, A., Christian, S., Prinz, F., Osterland, M., Golfier, S., Rase, S., Ansari, N., Esner, M., Bickle, M., Pampaloni, F., Mattheyer, C., Stelzer, E. H., Parczyk, K., Prechtl, S., and

Steigemann, P. (2014) 3D high-content screening for the identification of compounds that target cells in dormant tumor spheroid regions. *Experimental cell research* **323**, 131-143

129. Kunz-Schughart, L., Doetsch, J., Mueller-Klieser, W., and Groebe, K. (2000) Proliferative activity and tumorigenic conversion: Impact on cellular metabolism in 3-D culture. *Am J Physiol Cell Physiol* **278**, C765-C780

7. ACKNOWLEDGEMNTS

Un ringraziamento particolare va alla mia tutor, prof.ssa Sofia Giovanna Mariotto, che mi ha seguito con disponibilità e professionalità durante questo mio percorso.

Grazie alle dott.sse Elena Butturini e Alessandra Carcereri de Prati, per il loro aiuto e sostegno. Grazie per i preziosi consigli, li conserverò nel cuore.

Grazie a Diana, tra un esperimento e l'altro abbiamo condiviso pensieri e timori.

Grazie a Martina, la mia futura moglie, il mio conforto, mi incoraggia sempre nei momenti difficili. Senza di lei non sarei arrivato a questo bel traguardo.

Grazie alla mamma, il papà, Elisa e Tania, sempre pronti a fare il tifo per me.

Grazie anche ad Arianna, Elia, Gianluca, Riccardo, Matteo, Mattia, Andrea, Fabio ed Edoardo, amici e compagni di viaggio, di sorrisi e di chiacchierate.

ARTICLE
Journal of Cellular Biochemistry 118:3237–3248 (2017)

Journal of Cellular Biochemistry

Metastatic Breast Cancer Cells Enter Into Dormant State and Express Cancer Stem Cells Phenotype Under Chronic Hypoxia

Alessandra Carcereri de Prati,[1] Elena Butturini,[1] Antonella Rigo,[2] Elisa Oppici,[1] Michele Rossin,[1] Diana Boriero,[1] and Sofia Mariotto [1]*

[1]*Department of Neuroscience, Biomedicine and Movement Sciences, Section of Biological Chemistry, University of Verona, Strada le Grazie 8, Verona 37134, Italy*

[2]*Department of Medicine, Section of Hematology, Cancer Research and Cell Biology Laboratory University of Verona, Piazzale Scuro, Verona 37134, Italy*

ABSTRACT

Tumor dormancy is a poorly understood stage in cancer progression characterized by mitotic cycle arrest in G0/G1 phase and low metabolism. The cells survive in a quiescent state and wait for appropriate environmental conditions to begin proliferation again giving rise to metastasis. Despite their key role in cancer development and metastasis, the knowledge about their biology and origin is still very limited due to the poorness of established in vitro models that faithfully recapitulated tumor dormancy. Using at least three cycles of 1% O_2 hypoxia and reoxygenation, we establish and characterize the hypoxia-resistant human breast cancer cell line chMDA-MB-231 that can stably survive under 1% O_2 condition by entering into dormant state characterized by arrest in G0/G1 phase and low metabolism. This dormant state is reversible since once replaced in normoxia the cells recover the proliferation rate in 2 weeks. We show that chronic hypoxia induces autophagy that may be the survival mechanism of chMDA-MB-231 cells. Furthermore, the data in this work demonstrate that cycling hypoxic/reoxygenation stress selects MDA-MB-231 population that presents the cancer stem-like phenotype characterized by $CD24^-/CD44^+/ESA^+$ expression and spheroid forming capacity. We believe that our study presents a promising approach to select dormant breast cancer cells with stem-like phenotype using the hypoxia/reoxygenation regimen that may represent an area with profound implications for therapeutic developments in oncology. J. Cell. Biochem. 118: 3237–3248, 2017.

KEY WORDS: CHRONIC HYPOXIA; DORMANCY; AUTOPHAGY; CANCER STEM CELLS; TUMORSPHERE

Breast cancer is one of the most frequent cancers among women worldwide and despite the introduction of new therapy a significant portion of patients shows diseases recurrences. Although progress has been made in treating early-stage breast cancer, there is no effective strategy to prevent or treat metastasis, which is the major cause of breast cancer-related mortality. Recent studies have described a subpopulation of cancer cells within breast cancers, termed "cancer stem cells" (CSCs) which have stem like properties and are responsible for tumor initiation, growth, metastasis and resistance to chemotherapy or radiation therapy. Despite their role as central players in cancer biology, our knowledge about their biology and origin is still very limited even if it is now clear that the tumor microenvironment provides a breeding ground for CSCs selection and evolution [Dales et al., 2005; Semenza, 2012b; Aguirre-Ghiso et al., 2013; Hensel et al., 2013]. Because of incomplete blood vessel networks and the imbalance between proliferation and angiogenesis, the microenvironment in some parts of a solid tumor can be hypoxic and poorly supplied with nutrients [Pouyssegur et al., 2006; Denko, 2008]. The hypoxia/reoxygenation cycles that occur frequently within tumor tissue, lead to a rapid tumor progression so that a hypoxic microenvironment has been recognized as a cause of malignancy or resistance to various cancer therapies [Aguirre-Ghiso, 2007]. Investigating the biology of tumor cells in hypoxic conditions might be critical for improving therapeutic efficacy and for eradication of cancer. After the discovery of hypoxia-inducible factor-1α (HIF-1α), transcriptional regulation in response to acute hypoxia has been quite well elucidated [Semenza, 2012a]. Otherwise,

Conflicts of Interest: All authors declare no competing financial interest.
Alessandra Carcereri de Prati and Elena Butturini contributed equally to this work.
Grant sponsor: Aboca, Sansepolcro (AR), Italy.
*Correspondence to: Prof. Sofia Mariotto, Department of Neuroscience, Biomedicine and Movement Sciences, Biochemistry Section, University of Verona, Strada Le Grazie, 8, Verona 37134, Italy. E-mail: sofia.mariotto@univr.it
Manuscript Received: 11 January 2017; Manuscript Accepted: 2 March 2017
Accepted manuscript online in Wiley Online Library (wileyonlinelibrary.com): 6 March 2017
DOI 10.1002/jcb.25972 • © 2017 Wiley Periodicals, Inc.

the effect of a chronic exposure to hypoxia and reoxygenation cycles remains elusive [Bristow and Hill, 2008]. Although most of the tumor cells die in chronic hypoxia, some of them, characterized by mitotic arrest in G0/G1 phase and metabolic suppression, can survive for more than several days in a quiescent state. This dormant state is reversible, with tumor cells recovering the ability to self-renew once closed vessels reopen or new vasculatures reach the hypoxic areas. Because dormant tumor cells may be the founders of metastasis, one hypothesis is that these cells, or at least a fraction of them, share stem cell-like characteristics that may be responsible for their long half-lives.

In recent years, considerable progress has been made in understanding how tumor cells circulating in the blood interact and extravasate into secondary sites and which factors might determine whether these cells survive, remain dormant, or become metastases. It has been reported that phospho-ERK/phospho-p38 ratio represents the molecular switch for induction of tumor cell dormancy. High phospho-ERK/phospho-p38 ratio promotes cells proliferation and metastasis formation. Conversely, in restrictive microenvironments, low phospho-ERK/phospho-p38 ratio induces both G0/G1 arrest and survival signals, which will in turn lead to a prolonged phase of dormancy [Adam et al., 2009]. In addition, activation of p38 signaling in these cells promotes pro-survival mechanism via the up regulation of endoplasmic reticulum stress that results in unfolded protein response. Furthermore, it has been demonstrated that suppression of AKT activity, a key molecule in cell proliferation and metabolism, is necessary for induction of dormancy and survival of the cancer cells [Endo et al., 2014]. Recent reports suggest that microenviromental stress activates autophagy, the bulk degradation of cellular material that allows cells to recycle both nutrients and energy and functions as a fitness mechanism [Jain et al., 2013].

An understanding of the regulatory machinery of tumor dormancy is essential for identifying early cancer biomarkers and could provide a rationale for the development of novel agents to target dormant tumor cells population. The lack of established in vitro models of tumor dormancy represents the major factor that hampers the understanding of dormant cells response. Indeed, the majority of in vitro hypoxia studies have been carried out exposing cell lines to acute hypoxia (3–24 h) whereas only few reports of chronic hypoxia have been published.

In the current study, we find that human breast cancer cell line MDA-MB-231 can stably survive by entering into dormant state after at least three cycles of hypoxia (1% O_2) and reoxygenation and that autophagy sustains viability of cells in hypoxic conditions. In this contest, chronic hypoxia acts as a physiological selective pressure for the expansion of CSCs that acquire sphere-forming capacity and exhibit an outstanding $CD24^-/CD44^+/ESA^+$ stem-like phenotype.

MATERIALS AND METHODS

CELL LINES AND CELL CULTURE

Human breast cancer cell lines MDA-MB-231, MDA-MB-468, T47D, and MCF-7 were purchased from American Type Culture Collection. All the cell lines were cultured in DMEM (LifeTechnologies) supplemented with 10% FBS, 100 UI/ml penicillin, 100 μg/ml streptomycin, and 40 μg/ml gentamycin (Life Technologies) in a 5% CO_2 atmosphere at 37°C. Hypoxic culture was achieved by incubating cells with 1% O_2 and 5% CO_2 in a Multigas Incubator (RUSKINN C300, RUSKINN Technology Ltd) in DMEM without sodium pyruvate and supplemented with 25 mM Hepes, 10% FBS, 100 UI/ml penicillin, 100 μg/ml streptomycin, and 40 μg/ml gentamycin.

MORPHOLOGICAL ANALYSES OF DORMANT CELLS AND TUMORSPHERES

Approximately 6×10^4 MDA-MB-231 and chMDA-MB-231 cells were seeded on a 4-chamber μslide, with 13 mm glass bottom (Ibidi GmbH). After 24 h, cells were incubated for 5 min with a staining solution made of CellMaskDeep Red (LifeTechnologies) 1:1000 in complete cell media. Before the acquisition, the medium was replaced with a special medium without phenol red (DMEM/F12 NoPhenolRED, LifeTechnologies) to avoid any interference with the fluorescence signal.

The tumospheres deriving from 60 wells of a coated 96 well-plate were gently collected by a p1000 tip with a cut extremity and seeded on a 4-chamber μslide. After 24 h, cells were incubated for 60 min with a staining solution made of CellMaskDeep Red (LifeTechnologies) 1:1000 and Hoescht 1:1000 (LifeTechnologies) in DMEM/F12 NoPhenolRED. Cell images were captured using a confocal laser-scanning fluorescence microscope Leica SP5 (Leica Microsystem) at 63× magnification and processed using Adobe Photoshop and ImageJ softwares (Rasband, W.S., ImageJ, U. S. National Institute of Health, Bethesda, Maryland, http://rsb.info.nih.gov/ij/, 1997–2008).

CELLS VIABILITY

The viability of MDA-MB-231 and chMDA-MB-231 cells were evaluated with a 0.1% Trypan Blue exclusion test using a Countess Automated Cell Counter (LifeTechnologies).

IMMUNOPHENOTYPE

Cells were harvested, washed in phosphate buffer saline (PBS) and stained with anti-human CD326/ESA-FITC, CD24-FITC (Miltenyi Biotec), CD44-PE (BD Pharmingen). After incubation at room temperature for 15 min, cells were washed in PBS, acquired on a FACScan cytometer (Becton Dickinson) and analyzed by FlowJo 9.3.3 software (Tree Star). Data were expressed as the difference of Median Fluorescence Intensity (MFI) between stained and unstained cells.

CELL CYCLE

Cells were incubated with 10 μM Vybrant DyeCycle orange stain (LifeTechnologies) for 15 min and with 1 μM Sytox Blue dead Cell stain (LifeTechnologies) for additionally 15 min to exclude dead cells from cytometric analysis.

CELL PROLIFERATION

Cells were labeled with the amine-reactive dye 5,6-carboxyfluorescein diacetate, succinimidyl ester (CFSE), as described previously [Rigo and Vinante, 2016]. This dye is incorporated into cells and divided equally into daughter cells during proliferation. Thus, cells

proliferation can be determined by measuring the MFI by flow cytometry on a FACS can flow cytometer. Briefly, they were resuspended at a final concentration of 10^7 cells/ml in PBS-5% FBS and incubated with 5 μM CFSE for 5 min at room temperature. The reaction was stopped by washing twice with PBS-5% FBS. Cells were replated at 10^6 cells/ml in complete medium in normoxic and hypoxic conditions. An aliquot of cells was harvested every 24 h for 3 days, added with TO-PRO-3 (LifeTechnologies) and subjected to flow cytometry analysis.

MEASUREMENT OF GLUCOSE, PYRUVATE, AND LACTATE CONCENTRATION

After 3–5 days of culture under normoxic or hypoxic conditions the medium of MDA-MB-231 and chMDA-MB-231 cells were harvested and cells were counted. The concentration of glucose and lactate in the media was measured by using the glucose assay kit (CaymanChemical) and the lactate assay kit (Megazyme International), respectively, according to the manufacturer's instructions. To measure the amount of pyruvate produced, 5–50 μl of medium were added to 370 mM Tris–HCl pH 8, containing 350 mM NADH and 3 μg of LDH (Sigma), to a final volume of 300 μl. The total change of the absorbance at 340 nm was measured and using the molar extinction coefficient of NADH at 340 nm (6,220 M/cm), the moles of NADH oxidized, that are equal to the moles of pyruvate produced, were calculated.

GLUTATHIONE CONTENT QUANTIFICATION

The intracellular GSH concentration was measured by endpoint spectrophotometric titration on a Jasco V/550 spectrophotometer (JASCO) using the 5,5′-dithiobis(2-nitrobenzoic acid) (DTNB, Ellman's reagent) [Butturini et al., 2013]. Briefly, MDA-MB-231 and chMDA-MB-231 cells were lysed by freezing and thawing in 100 mM sodium phosphate buffer, pH 7.5, containing 5 mM EDTA, (KPE buffer), and after centrifugation at 16,000 rpm for 10 min, total protein concentration was determined by using Bradford method [Bradford, 1976]. The supernatants were deproteinized with 5% trichloroacetic acid. For [GSH] measurement, acidified clear supernatants were neutralized and buffered at pH 7.4 with 200 mM K_2HPO_4, pH 7.5. The reaction was then started by the addition of 60 mM DTNB and the increase in absorbance at 412 nm was measured until no variation in absorbance was evident. The amount of total GSH was determined by comparison with GSH standard curve.

DETECTION OF INTRACELLULAR REACTIVE OXYGEN SPECIES

CM-H2DCFDA staining. MDA-MB-231 and chMDA-MB-231 cells were resuspended in HBSS (LifeTechnologies) at 3×10^5 cells/ml and loaded with 2.5 μM of the cell-permeant probe 5-(and-6)-chloromethyl-2'7'-dichlorodihydrofluorescein diacetate acetyl ester (CM-H_2DCFDA; Molecular Probes) for 1 h at 37°C, as previously described [Butturini et al., 2011]. ROS generation was evaluated in flow cytometry (Becton Dickinson) by measuring the green fluorescence signal (Fl-1) of CM-H_2DCFDA that occurs after removal of the acetate groups by intracellular esterases and oxidation by free radicals. Data were analyzed by FlowJo 9.3.3 software.

Mitosox staining. Approximately 6×10^4 MDA-MB-231 and chMDA-MB-231 cells were seeded on a 4-chamber μslide, with 13 mm glass bottom (Ibidi GmbH). After 24 h, cells were incubated for 30 min with a staining solution made of Mitosox 1:1000 (LifeTechnologies), Mitotracker greenFM 1:5000 (LifeTechnologies), and Hoescht 1:1000 (LifeTechnologies) in medium without FBS. Before the acquisition, the medium was replaced with a medium without phenol red (DMEM/F12 NoPhenolRED, LifeTechnologies) to avoid any interference with the fluorescence signal. Cell images were captured using a confocal laser-scanning fluorescence microscope Leica SP5 at 63× magnification and processed using Adobe Photoshop and ImageJ softwares (Rasband, W.S., ImageJ, U. S. National Institute of Health, Bethesda, Maryland, http://rsb.info.nih.gov/ij/, 1997–2008).

WESTERN BLOT

Cells were homogenized at 4°C in 20 mM Hepes, pH 7.4, containing 420 mM NaCl, 1 mM EDTA, 1 mM EGTA, 1% Nonidet-P40 (NP-40), 20% glycerol, protease cocktail inhibitors (GE Healthcare). Protein concentration was measured by Bradford reagent (GE Healthcare), using bovine serum albumin as standard. Protein extracts (50 μg/lane) were resolved by SDS–PAGE electrophoresis and transferred to PVDF membrane (Immobilon P, Millipore). Immunoblotting assays were carried out by standard procedures using anti-LC3, anti-phospho(Thr180/Tyr182)-p38, anti-p38, anti-phosphoSer-AKT, anti-AKT, anti-phosphoThr-AMPKα, anti-AMPKα and anti-P70S6 kinase antibodies (Cell Signaling Technology), anti-STAT1, anti-STAT3, anti-p53, anti-phospho(Thr202/Tyr204)-ERK, and anti-ERK antibodies (Santa Cruz Biotechnology), anti-HIF1α antibody (BD biosciences), anti-actin antibody (Millipore), anti-HIF2α antibody (Novus Biologicals). After washing, membranes were developed using anti-rabbit or anti-mouse IgG peroxidase-conjugated antibody (Cell Signaling Technology) and chemiluminescent detection system (Immun-Star WesternC Kit, Bio-Rad). Blotted proteins were detected and quantified using the ChemiDoc XRS Imaging System (Bio-Rad).

REAL-TIME PCR

Cellular RNA was extracted by PureLink Total RNA kit (Ambion) according to the manufacturer's instructions. Total RNA was quantified at 260/280 nm, and the integrity of the samples was checked by 1% agarose gel electrophoresis. Aliquots corresponding to 1 μg of total RNA were reverse transcribed by using the SuperScript Vilo cDNA synthesis kit (LifeTechnologies) following the manufacturer's protocol. Aliquots of the cDNAs (corresponding to 50 ng of the original RNA) were subjected to real-time PCR with the QuantiTect SYBR Green PCR Kit (Qiagen) following the manufacturer's instructions. Bioinformatically validated primer sets for real-time PCRs were purchased by Qiagen (QuantiTect Primer Assays: Hs_RRN18S_1_SG for 18S, Hs_PGK_1_SG for PGK, Hs_SLC2A1_1_SG for GLUT1, and Hs_GADPH_2_SG for GAPDH). The PCR was performed with an initial pre-incubation step for 15 min at 95°C, followed by 45 cycles of 94°C for 15 s, annealing at 55°C for 30 s, and extension at 72°C for 30 s. The specificity of the amplified products was monitored performing melting curves at the end of each amplification reaction. All amplicons generated a single

peak, thus reflecting the specificity of the primers. Real-time PCR was performed using the Rotor-Gene 6000 (Corbett) and data analysis was conducted using the Rotor-Gene Software. Data were normalized to 18S and sample expression levels are shown as percentages of the internal control gene.

DETECTION OF AUTOPHAGIC MARKERS

Acridine orange staining. Approximately 6×10^4 MDA-MB-231 and chMDA-MB-231 cells were seeded on a 4-chamber μslide, with 13 mm glass bottom (Ibidi GmbH). After 24 h cells were rinsed in PBS and stained with acridine orange (AO) (1:1500 in PBS). Cell images were captured immediately by using a confocal laser-scanning fluorescence microscope Leica SP5 (Leica Microsystem) at 63× magnification and processed using Adobe Photoshop and ImageJ softwares (Rasband, W.S., ImageJ, U. S. National Institute of Health, Bethesda, Maryland, http://rsb.info.nih.gov/ij/, 1997–2008).

Monodansylcadaverine staining and autolysosome formation assay. MDA-MB-231 and chMDA-MB-231 cells were incubated with the fluorescent probe monodansylcadaverine (MDC; Sigma) a selective marker for acidic vesicular organelles, such as autophagic vacuoles. Briefly, cells were seeded in 96-well plates (3×10^4 cells/well) and after 24 stained with acridine orange were incubated in culture medium containing 50 μM MDC at 37°C for 15 min. Cells were then washed with Hanks buffer (20 mM Hepes pH 7.2, 10 mM glucose, 118 mM NaCl, 4.6 mM KCl, and 1 mM $CaCl_2$) and fluorescence was measured using a multimode plate reader ($Ex_{340\,nm}$ and $Em_{535\,nm}$) (GENios Pro, Tecan). The values were normalized for cell proliferation by Crystal Violet assay.

LC3-II. The presence of lipidated LC3-II isoform was analyzed by Western Blot as described above using mouse anti-LC3I/II antibody that detects endogenous levels of LC3B isoforms I and II.

STATISTICAL ANALYSIS

Data are reported as means ± SE of four independent experiments (n = 4); statistical analyses were performed using Student's *t* test.

RESULTS

SURVIVAL OF MDA-MB-231 CELL LINE UNDER CHRONIC HYPOXIA

In order to establish an in vitro model of breast cancer hypoxia-resistant cells, we cultured MDA-MB-231, MDA-MB-468, T47D, and MCF-7 cell lines in 1% O_2 atmosphere for 1–3 days and exposed the surviving cells to reoxygenation for 1–3 weeks depending on the rescue of cells and their proliferation rate. Only MDA-MB-231 cells were able to recover their proliferation rate and grow until the confluence. The cells were then exposed to repetitive cycles of hypoxia/reoxygenation. We set up the hypoxia/reoxygenation conditions with regard to number of cycles and exposure time.

The optimized procedure included exposure of the MDA-MB-231 breast cancer cells up to 7 days to hypoxia and reoxygenation of the surviving cells for 7–10 days depending on the viability of surviving cells. After reoxygenation and growing, we exposed the cell line again to a second round of hypoxia, and found an increase in viability. After three rounds of hypoxia and oxygenation, the cells, designed as chronic hypoxia resistant MDA-MB-231 (chMDA-MB-231), were able to stably grow in hypoxia even if with a decreased proliferation rate. chMDA-MB-231 cells were cultured under hypoxia for 3 months.

Cell cycle analysis revealed that the new established hypoxia-resistant chMDA-MB-231 cells were accumulated in G0/G1 phase and the percent in G2/M phase was drastically reduced (Fig. 1A).

Analysis of CFSE dilution showed a lesser decrease of fluorescence in chMDA-MB-231 respect to MDA-MB-231 cells after 24, 48, and 72 h of culture under hypoxia or normoxia, respectively (Fig. 1B). These data indicate that chMDA-MB-231 cells have a lower proliferation capacity than parental cells.

The arrest in G0/G1 phase and the low proliferation rate were reversible since, once replaced into fresh medium and re-oxygenized the cells, designed as reverted chronic hypoxia resistant MDA-MB-231 (RchMDA-MB-231), showed a recovery of the proliferation rate in 2 weeks (Fig. 1A and B).

Furthermore, chMDA-MB-231 cells displayed apparent morphological differences as showed by live confocal microscopy experiments were the plasma membrane was stained with CellMask dye. As compared to the parental cells, dormant chMDA-MB-231 cells show a longer and tapered shape and a higher cellular volume (Fig. 1C). Differently from the parental cells, chMDA-MB-231 cells viability was less affected by doxorubicin, one of the most effective agents in the treatment of breast cancer patients (Fig. 1D).

These results indicated that chMDA-MB-231 cells reversibly entered an inactive status, dormancy, under prolonged hypoxic condition.

In order to investigate the kinetic of dormant status induction, MDA-MB-231 cells were cultured in hypoxic condition until 7 days. As shown in Figure 2, phospho-p38 increased after 3 days of culture in hypoxia reaching a high level of phosphorylation after 7 days whereas phosphorylation of ERK was almost the same at all the time points examined. The densitometric analysis shows that the ratio of phospho-ERK/phospho-p38 in MDA-MB-231 cells cultured in hypoxia was reduced as compared to MDA-MB-231 cells in normoxia starting from 7 days.

EVALUATION OF REDOX STATE UNDER CHRONIC HYPOXIA

The redox environment in chronic hypoxic condition was evaluated measuring ROS production and GSH concentration.

chMDA-MB-231 cell line loaded with CM-H_2DCFDA, a specific cell-permeant ROS indicator, exhibited a clear fluorescence increase as respect to parental cell line ($MFI_{chMDA\text{-}MB\text{-}231} = 1344 \pm 541$ vs. $MFI_{MDA\text{-}MB\text{-}231} = 331 \pm 71$, Fig. 3A). These data are consistent with an enhancement of intracellular ROS. Moreover, the intracellular GSH concentration, analyzed by DTNB staining, was lower in chMDA-MB-231 cell line compared to parental cells (10.60 ± 2.00 nmoles/mg proteins versus 20,70 ± 1,50 nmoles/mg proteins, Fig. 3B).

At the same time, confocal live microscopy analysis revealed a marked increase of mitochondrial ROS production in dormant chMDA-MB-231 cells as indicated by the appearance of a red signal, originated by the oxidation of the MitoSOX red reagent, which co-localizes with that of the mitochondrial marker (MitoTracker) (Fig. 3C).

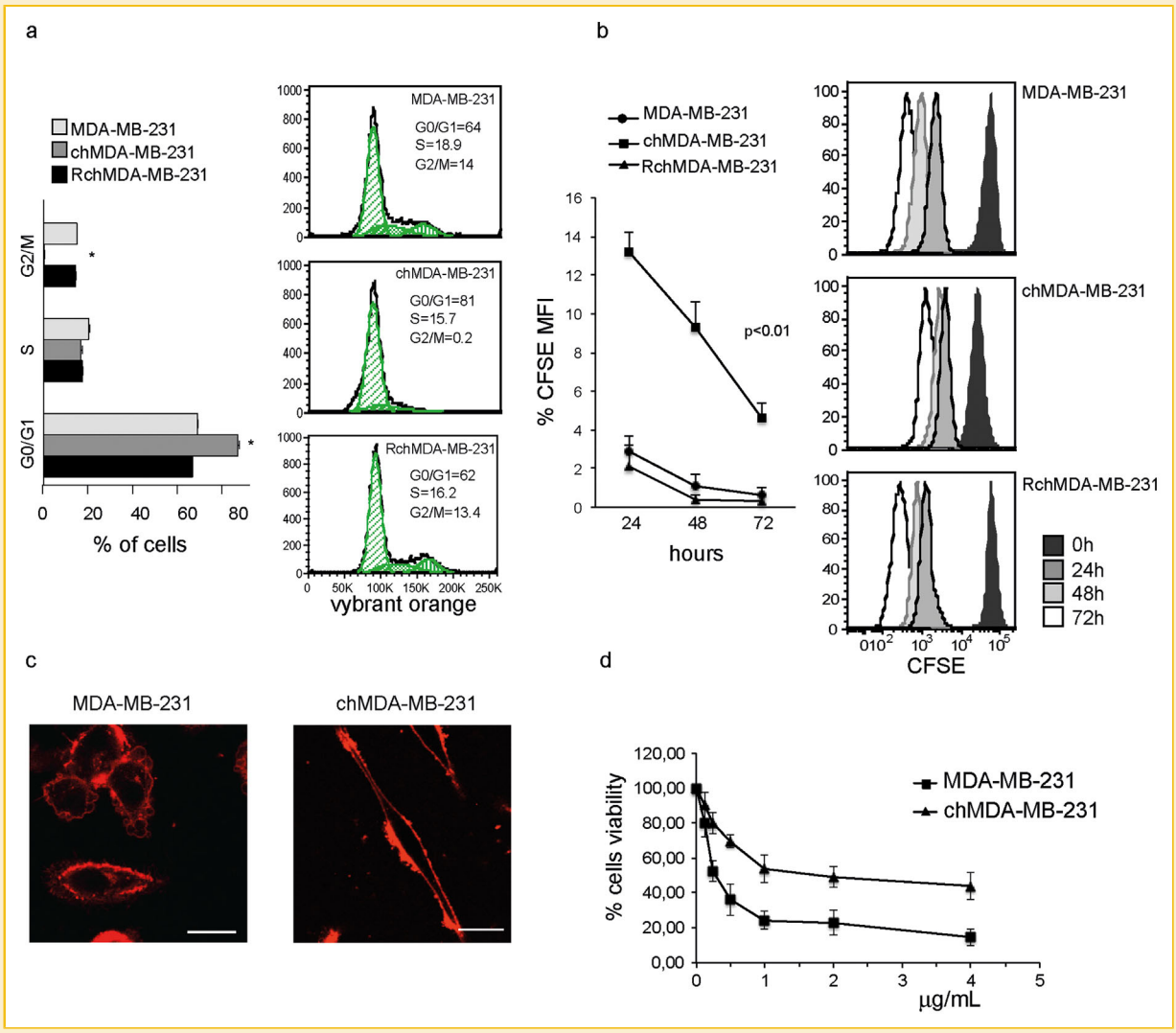

Fig. 1. MDA-MB-231 cell line can survive under chronic hypoxia entering into dormant state (a) Right. Flow cytometry analysis of cell cycle in MDA-MD-231 cells and in chMDA-MB-231. The cells were stained with 10 μM Vybrant DyeCycle orange and with 1 μM Sytox Blue (to exclude died cells from analysis). The cell cycle of chMDA-MB-231 reoxygenated in fresh medium (RchMDA-MB-231) was analyzed too. Left. Statistical analysis of the cell cycle phases. $^{*}P < 0.01$ (b) Right. Overlay histogram of the daily CFSE fluorescence intensity in the TO-PRO-3neg population. In MDA-MB-231 cells, CFSE is diluted among the daughter cells and fluorescence intensity decreases day by day. In chMDA-MB-231 cells, a lesser dilution of CFSE indicates decreased cell division. In RchMDA-MB-231 cells, the pattern of CFSE dilution is similar to that of MDA-MB-231 cells. Left. Plot of the daily percentage of CFSE fluorescence intensity as respect to time 0 in each condition (MFI ± SE, $P < 0.01$). (c) Confocal microscopy of MDA-MB-231 and chMDA-MB-231 after CellMaskDeep staining. Scale bar 10 μm. (d) Cell viability of MDA-MB-231 and chMDA-MB-231 cells after 24 h treatment with doxorubicin. ChMDA-MB-231 cells show a higher chemoresistance than the parental cell line (EC50 = 0.25 μg/ml ± 0.05, MDA-MB-231; EC50 = 2.00 μg/ml ± 0.15, chMDA-MB-231). Representative results or means ± SE of at least four experiments are depicted.

EVALUATION OF ENERGY METABOLISM UNDER CHRONIC HYPOXIA

We further assessed the status of energy metabolism of the cancer cells in the dormant state. We analyzed glucose consumption, as well as pyruvate and lactate production in the supernatants of MDA-MB-231 and chMDA-MB-231 cells. The results obtained indicated that the metabolism of dormant cells was strongly attenuated compared to MDA-MB-231 cells, as shown by the reduced levels of glucose consumed and pyruvate/lactate produced (Fig. 4A). Moreover, while under normoxic conditions the amount of lactate produced is 3.3-fold lower than that of pyruvate, under hypoxic conditions the amounts of pyruvate and lactate are similar. These data suggest that under normoxic conditions the aerobic catabolism of pyruvate prevails while under hypoxic conditions the anaerobic lactic fermentation occurs at significant extents.

Next, we examined the expression of HIF-1α, a master regulator of energy metabolism network under hypoxic condition. As a transcriptional activator, HIF-1α can induce the expression of target genes that promote angiogenesis, glycolysis, cellular proliferation,

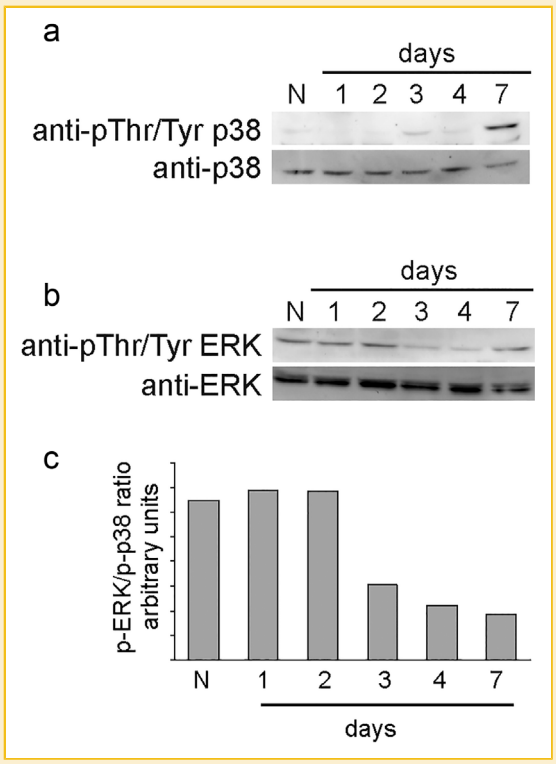

Fig. 2. Effect of chronic hypoxia on phosphorylation of ERK and p38 in MDA-MB-231. Western blot analysis shows that chronic hypoxia time-dependently triggers Thr/Tyr phosphorylation of p38 (a) whereas does not modify ERK phosphorylation state (b) in MDA-MB-231 cells cultured under 1% O_2 for the indicated time. (c) The densitometric analysis of each western blot was analyzed by QuantityOne software. The bars represent the ratio between phosphorylation of ERK, normalized on total ERK protein, and phosphorylation of p38, normalized on total p38 protein. MDA-MB-231 cells cultured under normoxic condition were used as control (N). The images are representative of four independent experiments.

and metastasis. In line with previous study [Wang et al., 2014a], MDA-MB-231 cells expressed HIF-1α under normal oxygen condition while chMDA-MB-231 cells present a lower level of HIF-1α protein (Fig. 4B). As expected the expression of GLUT1, GAPDH, and PGK genes decreased in chMDA-MB-231 (Fig. 4C).

It has been reported that a condition of energy deprivation induces phosphorylation of AMPK that inhibits energy-consuming pathway while increases energy-producing one. Western blot analysis demonstrated that threonine phosphorylation level of AMPK increased in MDA-MB-231 after 7 days under hypoxic condition (Fig. 4D).

These results confirm the lowering of energy metabolism and point out another characteristic of cancer cells in the dormant state.

CHRONIC HYPOXIA INDUCES DIFFERENT PROTEIN PROFILE IN MDA-MB-231

Western blot analysis revealed that the expression of various proteins was down-modulated in chMDA-MB-231 suggesting a different protein expression pathway between the cells cultured under normoxia or chronic hypoxia (Fig. 4B). Therefore, we analyzed the phosphorylation state of eIF2α, a key factor in the modulation of global protein synthesis [Koumenis et al., 2002]. Interestingly, the phosphorylation of eIF2α increased in chMDA-MB-231 compared to parental cells (Fig. 4E).

AUTOPHAGY SUSTAINS MDA-MB-231 SURVIVAL UNDER CHRONIC HYPOXIA

Autophagy is a cellular process that removes damaged or unwanted cellular components and recycles them to build new constituents and promotes cell survival as well as cell death. It is now recognized that induction of autophagy in tumor cells may also contribute to tumor dormancy [Degenhardt et al., 2006]. Autophagy induction was examined through the formation of autolysosomes (autophagic vesicles joined with lysosomes) using the fluorescent probe AO, which changes its fluorescence emission from green to red upon accumulation into lysosomal acidic compartments. Autophagy induction was confirmed through the detection of autolysosomes by AO staining. Live cell staining with AO revealed a significant increase of red dots in the cytosol of chMDA-MB-231 cells as compared to MDA-MB-231 cells cultured under normoxic condition where AO displayed mainly a diffuse green pattern (Fig. 5A). The induction of autophagy was supported by sixfold MDC uptake increase in chMDA-MB-231 cells (Fig. 5B). To confirm the activation of autophagy, we also examined the presence of LC3-II by Western Blot. During the activation of autophagy, LC3-I is cleaved, conjugated with phosphatidylethanolamine (LC3-II) and associated with newly formed autolysosomes [Kim et al., 2007, Noda et al., 2009]. Since the lipidated form migrates slightly fast on the gel, this can be a good marker for the activation of autophagy. As expected, under chronic hypoxic conditions western blot showed increased LC3-II accumulation (Fig. 5C).

It has been previously demonstrated that epithelial ovarian cancer cells enter a dormant state and survive through autophagy controlled in part by decreased AKT signaling [Correa et al., 2012, 2014]. Western blot analysis showed that serine phosphorylation of AKT was down-regulated in chMDA-MB-231 cells compared to MDA-MB-231 cells cultured under normoxic condition (Fig. 5C). The AKT kinase is a pivotal node in the PI3K/AKT/mTOR pathway, which phosphorylate numerous downstream targets to regulate cellular functions including growth, proliferation and survival [Manning and Cantley, 2007]. Unfortunately, we could not check the phosphorylation state of 70S6K, a downstream target of mTORC1, because the protein level of 70S6K decreased in chMDA-MB-231 cells compared to MDA-MB-231 cells cultured under normoxic condition (Fig. 4B).

CHRONIC HYPOXIA SELECTS CANCER STEM CELLS POPULATION AND INDUCES TUMORSPHERES FORMATION IN MDA-MB-231

In the last years, literature reports that hypoxia exerts a physiological pressure that promotes tumor invasion and metastasis and selects cells with stemness properties. This small subpopulation is characterized by self-renewal, anoikis, and ability to form tumorsphere.

Using the flow cytometry analysis, we found that chMDA-MB-231 cells were $CD24^{-}$ (data not shown) and displayed an up-modulation of CD44 and ESA expression in comparison with the parental cell line

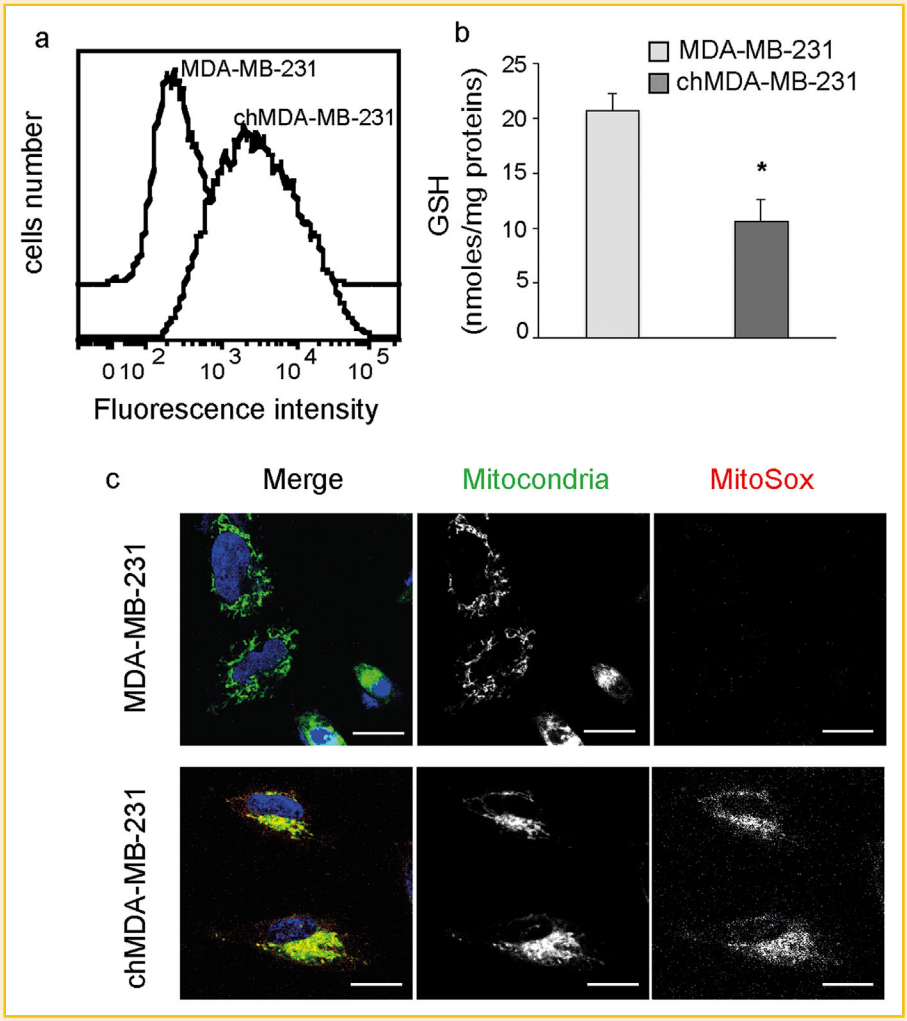

Fig. 3. Evaluation of redox state under chronic hypoxia. (a) Flow cytometry analysis of ROS production in MDA-MB-231 and chMDA-MB-231 cells loaded with CM-H2DCFDA. The fluorescence increase in chMDA-MB-231 cells indicates a higher ROS production as respect to parental cells. (b) Spectrophotometric analysis of intracellular GSH concentration in MDA-MB-231 and in chMDA-MD-231. The decrease of absorbance at 420 nm in chMDA-MB-231 cells indicates a lower GSH concentration as respect to parental cells. Bar graphs represent the mean ± SE. $^{*}P < 0.01$. (c) Confocal live microscopy of MDA-MB-231 and chMDA-MB-231 after Mitosox, Mitotracker greenFM, and Hoescht staining. Merge and single channel images come from a single zplane. Scale bar 10 μm. The appearance of red signal in chMDA-MB-231 reveals an increase of mitochondrial ROS production. Representative results of at least four experiments are depicted.

(Fig. 6A). These are characteristic markers of breast cancer stem cells [Wang et al., 2014b; An et al., 2015; Chen et al., 2015].

In order to test the ability of chronic hypoxia to induce tumorsphere formation, the floating cells in the culture medium of chMDA-MB-231 cells (F-chMDA-MB-231), were analyzed by Trypan Blue assay. These non-adherent cells were still viable, $CD24^{-}$ (data not shown) and express higher level of CD44 and ESA in comparison to parental cells (Fig. 6A). These cells were seeded at low density on coated 96 multiwell plates and cultured under hypoxic condition. Images of cells from each well were taken at days 1, 3, 5, 7, and 10 to visualize the formation of tumorspheres. After 3 days, the cells were able to form compact and asymmetrical tumorspheres of at least 80 μm that was able to proliferate reaching the diameter of 150 μm after 10 days (Fig. 6B). Live cell imaging of tumorspheres after 10 days, stained with a nuclear probe (Hoechst), and a plasma membrane marker (CellMask) are reported in Figure 6C.

Furthermore, chMDA-MB-231 tumorspheres (150 μm diameter) were able to re-differentiate into adherent cells re-acquiring epithelial morphology after 7–10 days of culturing in normoxic condition (Fig. 6B).

As expected, parental cell line MDA-MB-231 did not show any tumorsphere-forming ability under normoxic condition (data not shown).

DISCUSSION

It is known that both hypoxia and consecutive hypoxia/reoxygenation can exert a variety of effects on tumor cells biology, including a prolonged quiescent state that induce cells to enter dormancy. Some

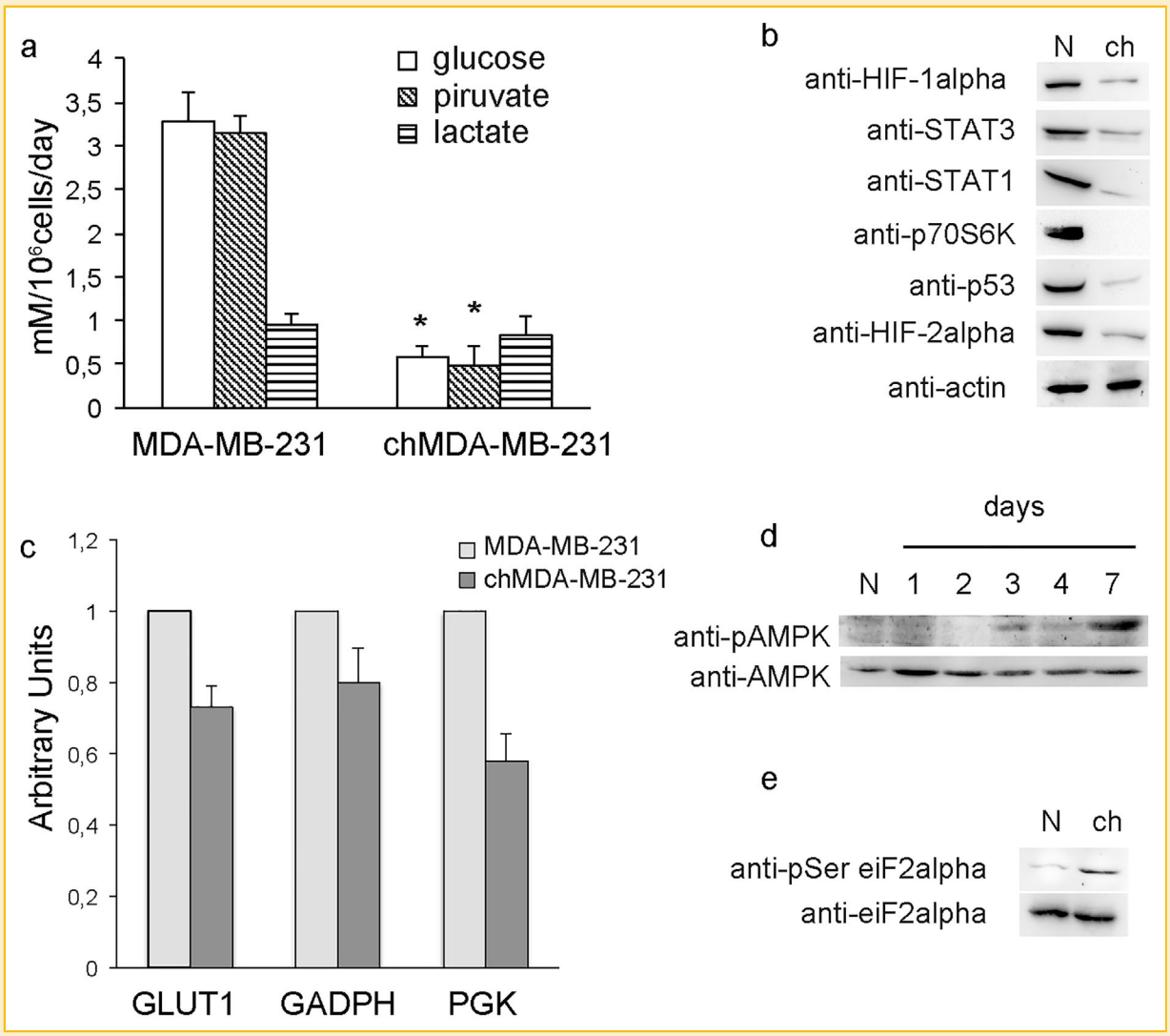

Fig. 4. Effect of chronic hypoxia on energy metabolism and protein expression in MDA-MB-231. (a) Analysis of MDA-MB-231 and chMDA-MB-231 cells metabolism. The media were analyzed to define the amount of glucose consumed (□), pyruvate produced (▨), and lactate produced (▤). Bar graphs represent the meansf glucose consumed ± SE of three independent experiments. $^{*}P < 0.01$ versus normoxic condition. (b) Western blot analysis of various proteins expression in chMDA-MB-231 (ch) compared to MDA-MB-231 (N). Actin is used as control loading. The images are representative of four independent experiments. (c) Histograms of the analysis of GLUT1, GAPDH, and PGK gene expression in MDA-MB-231 in normoxic and hypoxic conditions by RT-PCR. (d) Western blot analysis shows that chronic hypoxia up-regulated Thr phosphorylation of AMPK without affecting the total amount of AMPK in MDA-MB-231. MDA-MB-231 cells cultured under normoxic condition were used as control (N). (e) Western blot analysis shows that chronic hypoxia up-regulated Ser phosphorylation of eIF2α without affecting the total amount of eIF2 in chMDA-MB-231. MDA-MB-231 cells cultured under normoxic condition were used as control (N). The images are representative of four independent experiments.

studies have shown that hypoxia, can drive a reversible phenotype that enhances stem-like properties of cells to ensure survival of the tumor. Although dormant cancer cells do not directly contribute to tumor growth, they can be a reservoir and a source of tumorigenic cells and chemoresistance. One factor hampering improved understanding of the response of dormant cells is the lack of established in vitro models and a hypoxia-resistant cell line might be useful for the study of cancer dormancy. The results presented here demonstrate that chronic hypoxic condition, that mimics tumor microenvironment, enriches MDA-MB-231 cells for a dormant tumor cell population that is normally under-represented in the parental tumor cell line. We exposed diverse breast cancer cell lines to repetitive cycles of hypoxia/reoxygenation and most of them did not proliferate and survive after 1–2 cycles. Only MDA-MB-231 cell line was able to adapt and survive under prolonged hypoxic condition. Controversial data concerning the ability of breast cancer cell lines to resist to prolonged hypoxia are present in the literature. Although some researchers established MCF7 hypoxia-resistant cells [Scherbakov et al., 2009], in our hands, only MDA-MB-231 cells survive under the chronic hypoxia and reoxygenation cycles described. These differences may be due to the use of different culture conditions, such as different cellular density at the moment

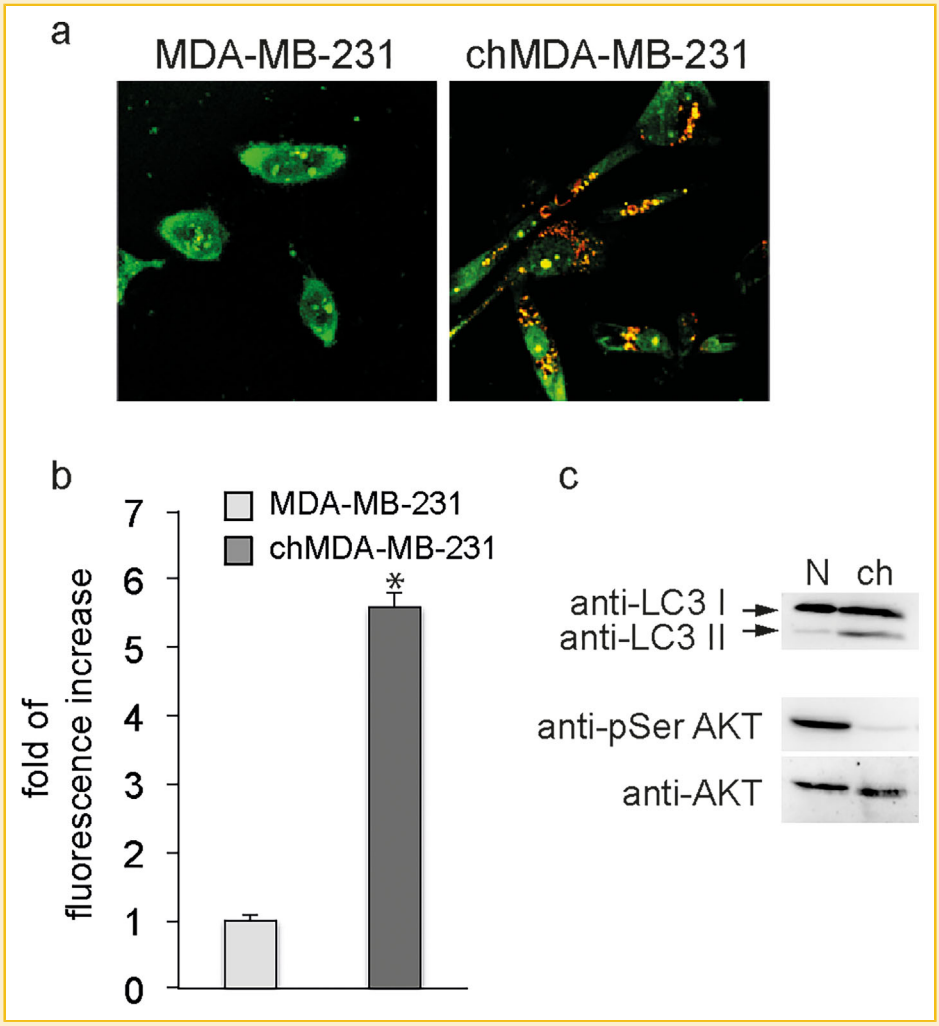

Fig. 5. Analysis of autophagy in chMDA-MB-231. (a) Confocal microscopy of MDA-MB-231 and chMDAMB-231 after Acridine Orange staining. Scale bar 10 μm. The images are representative of three biological replicates. The red dots in the cytosol of chMDA-MB-231 indicate the formation of autolysosomes. (b) MDC incorporation assay in MDA-MB-231 and chMDA-MB-231 cells. Bar graphs represent the mean ± SE of three independent biological replicates, each performed using three technical replicates. $^{*}P < 0.05$. (c) Western blot of the autophagy-related protein LC3 and of the serine phosphorylation state of AKT in MDA-MB-231 (N) and chMDA-MB-231 (ch). The induction of autophagy was confirmed by the apparance of LC3-II. The serine phosphorylation of AKT was down-regulated in chMDA-MB-231 cells compared to the parental cells. AKT expression was used as control loading. The images are representative of four independent experiments.

of seeding, different medium composition, and different type of hypoxia induction (i.e., cobalt chloride).

The chMDA-MB-231 cells established in this work are characterized by a decreased proliferation, arrest in G0/G1 phase and low metabolic rate. Previous studies from Aguirre-Ghiso laboratory discovered that HEp3, human head and neck carcinoma cell line, displays a high phospho-ERK to phospho-p38 signaling ratio that favors proliferation in vivo [Aguirre-Ghiso et al., 2001, 2003, 2004]. The reprogramming of cells into dormancy (D-HEp3 cells) results in a reversion of this ratio with p38 signaling that predominates over ERK [Aguirre-Ghiso et al., 1999, 2002; Liu et al., 2002]. Accordingly, we demonstrated that p38 phosphorylation was elevated in chMDA-MB-231 cells, resulting in a phospho-ERK/phospho-p38 ratio that favored p38 and induced a prolonged phase of dormancy.

Under conditions where metabolic activity is low, AMPK acts as a metabolic checkpoint by activating catabolic processes and inhibiting anabolic metabolism. Our study shows that AMPK was activated in MDA-MB-231 starting from 7 days of hypoxia suggesting that AMPK activation could regulate cellular energy homeostasis through the autophagic recycling of intracellular components, as recently described [Meley et al., 2006; Matsui et al., 2007].

Some reports describe that hypoxia promotes autophagy as a cells survival mechanism in the tumor core as well as in tumor cell line [Degenhardt et al., 2006]. On the other hand, lot of literatures describe that oxidative stress induced by the ROS increase and GSH depletion maybe directly correlated with autophagy activation [Scherz-Shouval et al., 2007; Gao et al., 2008; Li et al., 2012; Poillet-Perez et al., 2015]. Interestingly, we found that chMDA-MB-231 cells have a high level of autophagy, as measured by the

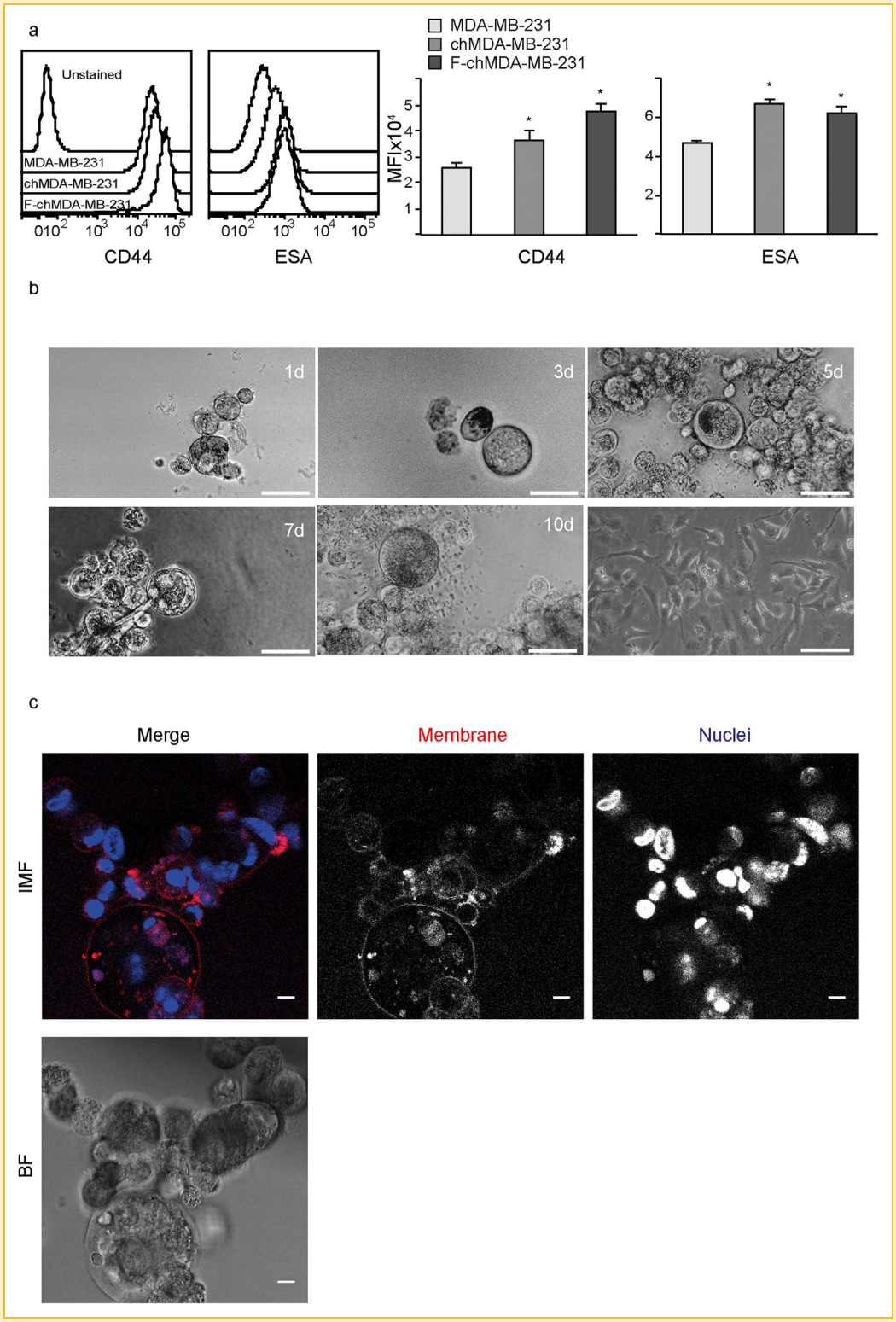

Fig. 6. Chronic hypoxia selects cancer stem cells population. (a) Cell surface expression of CD44 and ESA in MDA-MB-231 and chMDA-MB-231. Left. Flow cytometry pattern. Right. Quantitative comparison (MFI). Bar graphs represent the mean ± SE of at least four independent $^{*}P < 0.01$ versus normoxic condition. (b) Phase-contrast microscopy images of tumorospheres formation starting from the viable floating cells in the culture medium of chMDA-MB-231 on day 1, 3, 5, 7, and 10. The image of F-chMDA-MB-231 (150 μm diameter) reoxygenated in fresh medium was analyzed too. Representative images from three separate experiments are shown. Scale bar 50 μm. (c) Confocal live cell microscopy of spheroids after 10 days under chronic hypoxia stained with nuclear probe Hoechst and plasma membrane marker CellMaskDeep. Representative images from three separate experiments are shown.

detection of autophagolysome and LC3-II expression, suggesting that autophagy may be the survival mechanism of dormant chMDA-MB-231 cells. As previously described, in chronic hypoxia inhibition of AKT activity is necessary for induction of dormancy and survival of cancer cells [Endo et al., 2014]. In accordance with these data, AKT serine phosphorylation was suppressed in chMDA-MB-231 preserving the energy source by decreasing energy demand. Protein synthesis is one of the most energy-demanding metabolic processes and it has been reported that the eukaryotic initiation factor eIF2α plays a critical role in the down-regulation of protein synthesis in response to hypoxic stress [Koumenis et al., 2002]. MDA-MB-231 cells are characterized by constitutively phosphorylated eiF2α due to their increased activation of epithelial to mesenchymal transition associated with cells migration and metastasis ability [Feng et al., 2014]. Our data, consistent with these notions, show further increase in phosphorylation state of eIF2α in chMDA-MB-231 compared to parental cell line that could be correlated to the selective translation repression of proteins.

Furthermore, the data in this work demonstrate that cycling hypoxic/reoxygenation stress selected MDA-MB-231 population that presents the characteristic phenotype of CSCs, $CD24^{-}/CD44^{+}/ESA^{+}$ and is able to generate tumorspheres. The biological significance and clinical relevance of multicellular spheroids has been documented in many different tumor types [Barbone et al., 2008; Valcarcel et al., 2008; Sodek et al., 2009; Lawrenson et al., 2011; Wenzel et al., 2014] It is well accepted that spheroids more closely mimic the cell–cell, cell-matrix interactions, metabolic gradients, cellular viability, and differentiation of malignant cells within a solid tumor than do conventional monolayer cultures [Kunz-Schughart et al., 2000]. We believe that our study presents a promising approach to isolate dormant cells and stem-like breast CSCs using the hypoxia/reoxygenation regimen that may represent an area with profound implications for therapeutic developments in oncology.

REFERENCES

Adam AP, George A, Schewe D, Bragado P, Iglesias BV, Ranganathan AC, Kourtidis A, Conklin DS, Aguirre-Ghiso JA. 2009. Computational identification of a p38SAPK-regulated transcription factor network required for tumor cell quiescence. Cancer Res 69:5664–5672.

Aguirre Ghiso JA, Kovalski K, Ossowski L. 1999. Tumor dormancy induced by downregulation of urokinase receptor in human carcinoma involves integrin and MAPK signaling. J Cell Biol 147:89–104.

Aguirre-Ghiso JA, Liu D, Mignatti A, Kovalski K, Ossowski L. 2001. Urokinase receptor and fibronectin regulate the ERK(MAPK) to p38(MAPK) activity ratios that determine carcinoma cell proliferation or dormancy in vivo. Mol Biol Cell 12:863–879.

Aguirre Ghiso JA. 2002. Inhibition of FAK signaling activated by urokinase receptor induces dormancy in human carcinoma cells in vivo. Oncogene, 21:2513–2524.

Aguirre-Ghiso JA, Estrada Y, Liu D, Ossowski L. 2003. ERK(MAPK) activity as a determinant of tumor growth and dormancy; regulation by p38(SAPK). Cancer Res 63:1684–1695.

Aguirre-Ghiso JA, Ossowski L, Rosenbaum SK. 2004. Green fluorescent protein tagging of extracellular signal-regulated kinase and p38 pathways reveals novel dynamics of pathway activation during primary and metastatic growth. Cancer Res 64:7336–7345.

Aguirre-Ghiso JA, Bragado P, Sosa MS. 2013. Metastasis awakening: Targeting dormant cancer. Nat Med 19:276–277.

Aguirre-Ghiso JA. 2007. Models, mechanisms and clinical evidence for cancer dormancy. Nat Rev Cancer 7:834–846.

AN H, Kim JY, OH E, Lee N, Cho Y, Seo JH. 2015. Salinomycin promotes anoikis and decreases the CD44+/$CD24^{-}$ stem-Like population via inhibition of STAT3 activation in MDA-MB-231 cells. PLoS ONE 10:e0141919.

Barbone D, Yang TM, Morgan JR, Gaudino G, Broaddus VC. 2008. Mammalian target of rapamycin contributes to the acquired apoptotic resistance of human mesothelioma multicellular spheroids. J Biol Chem 283:13021–13030.

Bradford MM. 1976. A rapid and sensitive method for the quantitation of microgram quantities of protein utilizing the principle of protein-dye binding. Anal Biochem 72:248–254.

Bristow RG, Hill RP. 2008. Hypoxia and metabolism. Hypoxia, DNA repair and genetic instability. Nat Rev Cancer 8:180–192.

Butturini E, Cavalieri E, DE Prati AC, Darra E, Rigo A, Shoji K, Murayama N, Yamazaki H, Watanabe Y, Suzuki H, Mariotto S. 2011. Two naturally occurring terpenes, dehydrocostuslactone and costunolide, decrease intracellular GSH content and inhibit STAT3 activation. PLoS ONE 6: e20174.

Butturini E, Carcereri DE, Prati A, Chiavegato G, Rigo A, Cavalieri E, Darra E, Mariotto S. 2013. Mild oxidative stress induces S-glutathionylation of STAT3 and enhances chemosensitivity of tumoural cells to chemotherapeutic drugs. Free Radic Biol Med 65:1322––330.

Chen Y, Song J, Jiang Y, YU C, MA Z. 2015. Predictive value of CD44 and CD24 for prognosis and chemotherapy response in invasive breast ductal carcinoma. Int J Clin Exp Pathol 8:11287–11295.

Correa RJ, Peart T, Valdes YR, Dimattia GE, Shepherd TG. 2012. Modulation of AKT activity is associated with reversible dormancy in ascites-derived epithelial ovarian cancer spheroids. Carcinogenesis 33:49–58.

Correa RJ, Valdes YR, Peart TM, Fazio EN, Bertrand M, Mcgee J, Prefontaine M, Sugimoto A, Dimattia GE, Shepherd TG. 2014. Combination of AKT inhibition with autophagy blockade effectively reduces ascites-derived ovarian cancer cell viability. Carcinogenesis 35:1951–1961.

Dales JP, Garcia S, Meunier-Carpentier S, Andrac-Meyer L, Haddad O, Lavaut MN, Allasia C, Bonnier P, Charpin C. 2005. Overexpression of hypoxia-inducible factor HIF-1alpha predicts early relapse in breast cancer: Retrospective study in a series of 745 patients. Int J Cancer 116:734–739.

Degenhardt K, Mathew R, Beaudoin B, Bray K, Anderson D, Chen G, Mukherjee C, Shi Y, Gelinas C, Fan Y, Nelson DA, Jin S, White E. 2006. Autophagy promotes tumor cell survival and restricts necrosis, inflammation, and tumorigenesis. Cancer Cell 10:51–64.

Denko NC. 2008. Hypoxia, HIF1 and glucose metabolism in the solid tumour. Nat Rev Cancer 8:705–713.

Endo H, Okuyama H, Ohue M, Inoue M. 2014. Dormancy of cancer cells with suppression of AKT activity contributes to survival in chronic hypoxia. PLoS ONE 9:e98858.

Feng YX, Sokol ES, Del Vecchio CA, Sanduja S, Claessen JH, Proia TA, Jin DX, Reinhardt F, Ploegh HL, Wang Q, Gupta PB. 2014. Epithelial-to-mesenchymal transition activates PERK-eIF2alpha and sensitizes cells to endoplasmic reticulum stress. Cancer Discov 4:702–715.

Gao M, Yeh PY, LU YS, Hsu CH, Chen KF, Lee WC, Feng WC, Chen CS, Kuo ML, Cheng AL. 2008. OSU-03012, a novel celecoxib derivative, induces reactive oxygen species-related autophagy in hepatocellular carcinoma. Cancer Res 68:9348–9357.

Hensel JA, Flaig TW, Theodorescu D. 2013. Clinical opportunities and challenges in targeting tumour dormancy. Nat Rev Clin Oncol 10:41–51.

Jain K, Paranandi KS, Sridharan S, Basu A. 2013. Autophagy in breast cancer and its implications for therapy. Am J Cancer Res 3:251–265.

Kim I, Rodriguez-Enriquez S, Lemasters JJ. 2007. Selective degradation of mitochondria by mitophagy. Arch Biochem Biophys 462:245–253.

Koumenis C, Naczki C, Koritzinsky M, Rastani S, Diehl A, Sonenberg N, Koromilas A, Wouters BG. 2002. Regulation of protein synthesis by hypoxia via activation of the endoplasmic reticulum kinase PERK and phosphorylation of the translation initiation factor eIF2alpha. Mol Cell Biol 22:7405–7416.

Kunz-Schughart LA, Doetsch J, Mueller-Klieser W, Groebe K. 2000. Proliferative activity and tumorigenic conversion: Impact on cellular metabolism in 3-D culture. Am J Physiol Cell Physiol 278:C765–C780.

Lawrenson K, Sproul D, Grun B, Notaridou M, Benjamin E, Jacobs IJ, Dafou D, Sims AH, Gayther SA. 2011. Modelling genetic and clinical heterogeneity in epithelial ovarian cancers. Carcinogenesis 32:1540–1549.

Li L, Ishdorj G, Gibson SB. 2012. Reactive oxygen species regulation of autophagy in cancer: Implications for cancer treatment. Free Radic Biol Med 53:1399–1410.

Liu D, Aguirre Ghiso J, Estrada Y, Ossowski L. 2002. EGFR is a transducer of the urokinase receptor initiated signal that is required for in vivo growth of a human carcinoma. Cancer Cell 1:445–457.

Manning BD, Cantley LC. 2007. AKT/PKB signaling: Navigating downstream. Cell 129:1261–1274.

Matsui Y, Takagi H, QU X, Abdellatif M, Sakoda H, Asano T, Levine B, Sadoshima J. 2007. Distinct roles of autophagy in the heart during ischemia and reperfusion: Roles of AMP-activated protein kinase and Beclin 1 in mediating autophagy. Circ Res 100:914–922.

Meley D, Bauvy C, Houben-Weerts JH, Dubbelhuis PF, Helmond MT, Codogno P, Meijer AJ. 2006. AMP-activated protein kinase and the regulation of autophagic proteolysis. J Biol Chem 281:34870–34879.

Noda T, Fujita N, Yoshimori T. 2009. The late stages of autophagy: How does the end begin?. Cell Death Differ 16:984–990.

Poillet-Perez L, Despouy G, Delage-Mourroux R, Boyer-Guittaut M. 2015. Interplay between ROS and autophagy in cancer cells, from tumor initiation to cancer therapy. Redox Biol 4:184–192.

Pouyssegur J, Dayan F, Mazure NM. 2006. Hypoxia signalling in cancer and approaches to enforce tumour regression. Nature 441:437–443.

Rigo A, Vinante F. 2016. The antineoplastic agent alpha-bisabolol promotes cell death by inducing pores in mitochondria and lysosomes. Apoptosis 21:917–927.

Scherbakov AM, Lobanova YS, Shatskaya VA, KRASIL'nikov MA. 2009. The breast cancer cells response to chronic hypoxia involves the opposite regulation of NF-kB and estrogen receptor signaling. Steroids 74:535–542.

Scherz-Shouval R, Shvets E, Fass E, Shorer H, Gil L, Elazar Z. 2007. Reactive oxygen species are essential for autophagy and specifically regulate the activity of Atg4. Embo J 26:1749–1760.

Semenza GL. 2012a. Hypoxia-inducible factors in physiology and medicine. Cell 148:399–408.

Semenza GL. 2012b. Molecular mechanisms mediating metastasis of hypoxic breast cancer cells. Trends Mol Med 534–543.

Sodek KL, Ringuette MJ, Brown TJ. 2009. Compact spheroid formation by ovarian cancer cells is associated with contractile behavior and an invasive phenotype. Int J Cancer 124:2060–2070.

Valcarcel M, Arteta B, Jaureguibeitia A, Lopategi A, Martinez I, Mendoza L, Muruzabal FJ, Salado C, Vidal-Vanaclocha F. 2008. Three-dimensional growth as multicellular spheroid activates the proangiogenic phenotype of colorectal carcinoma cells via LFA-1-dependent VEGF: implications on hepatic micrometastasis. J Transl Med 6:57.

Wang F, Chang M, Shi Y, Jiang L, Zhao J, Hai L, Sharen G, Du H. 2014a. Down-regulation of hypoxia-inducible factor-1 suppresses malignant biological behavior of triple-negative breast cancer cells. Int J Clin Exp Med 7:3933–3940.

Wang R, Lv Q, Meng W, Tan Q, Zhang S, Mo X, Yang X. 2014b. Comparison of mammosphere formation from breast cancer cell lines and primary breast tumors. J Thorac Dis 6:829–837.

Wenzel C, Riefke B, Grundemann S, Krebs A, Christian S, Prinz F, Osterland M, Golfier S, Rase S, Ansari N, Esner M, Bickle M, Pampaloni F, Mattheyer C, Stelzer EH, Parczyk K, Prechtl S, Steigemann P. 2014. 3D high-content screening for the identification of compounds that target cells in dormant tumor spheroid regions. Exp Cell Res 323,131–143.